Topology and Deformation Theory of Singularities

Chenglong Yu

Spring 2026

Contents

Preface

These lecture notes accompany the graduate course *Topology and Deformation Theory of Singularities*, taught at SIMIS and Fudan University in Spring 2026. They cover the local topology, Hodge theory, and deformation theory of isolated hypersurface singularities and, more generally, isolated complete intersection singularities (ICIS).

Logical Structure and Dependencies

The notes are organized into four thematic parts, reflecting the natural progression from local topology to global algebraic geometry.

Part I: Local Topology of Singularities (§§1–8). We begin with the foundational definitions (§1) and generalize to ICIS (§2). The Curve Selection Lemma (§3) provides the key technical tool for local topology, leading to the theory of good representatives (§4). The central result of Part I is the Milnor Fibration Theorem (§5), established via Ehresmann's fibration theorem, which equips each isolated hypersurface singularity with a canonical fiber bundle structure. The homotopy type of the Milnor fiber (§6) and the geometric monodromy (§7) are then studied, culminating in the local Picard-Lefschetz theory (§8) that describes how vanishing cycles generate the topology of the fiber.

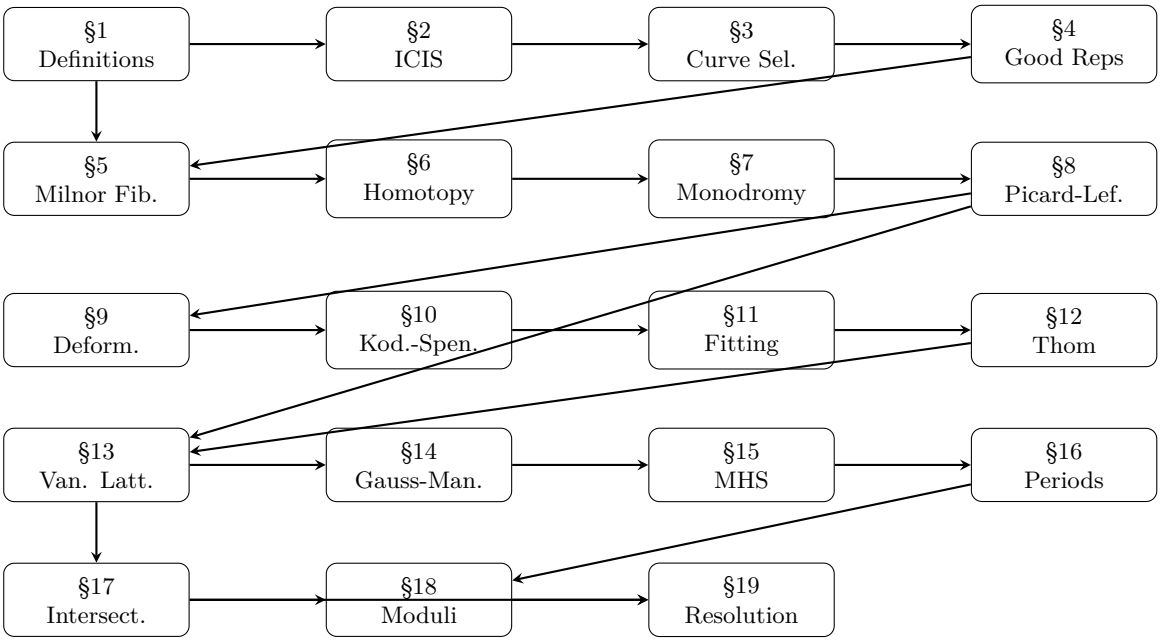

Part II: Deformation Theory (§§9–12). Part II shifts focus from the topology of a fixed singularity to families of singularities. We begin with the foundations of deformation theory (§9), including flatness and versality, and the Tjurina number τ. The Kodaira-Spencer map (§10) provides the infinitesimal criterion for versality. Fitting ideals and critical spaces (§11) give coordinate-free descriptions of singularity loci, which are applied to study discriminants and Thom-Boardman strata (§12). The primary references for Part II are Greuel-Lossen-Shustin [GLS07] and Looijenga [Loo84].

Part III: Vanishing Cycles, Monodromy, and Hodge Theory (§§13–16). This is the analytic heart of the course. Vanishing lattices and monodromy groups (§13) connect deformation theory back to topology via Morsification. The Monodromy Theorem and Gauss-Manin connection (§14) — the key construction of Brieskorn [Bri70] — lift the topological monodromy to an algebraic differential equation (the Picard-Fuchs equation), proving that monodromy eigenvalues are roots of unity. This algebraic framework is further developed via the Brieskorn lattice hierarchy $H_0' \subset H_0''$ and the V-filtration (Kashiwara-Malgrange). Mixed Hodge structures on the Milnor fiber (§15), following the foundational work of Steenbrink [Ste77] and Varchenko [Var81], introduce the spectrum as a refinement of the Milnor number. Newton polygon methods (Kouchnirenko, Danilov-Khovanskii) provide powerful computational tools. Period mappings and the Torelli problem (§16) encode the variation of Hodge structure across the moduli space of singularities. The primary reference for this part is Kulikov [Kul98].

Part IV: Classification and Resolution (§§17–19). The course concludes with a synthesis of the preceding theory. Intersection forms and Dynkin diagrams (§17) classify simple singularities via the positive definiteness of the intersection form (Gabrielov's theorem), connecting singularity theory to Lie algebra combinatorics. Moduli spaces and unimodal singularities (§18) apply Arnold's classification. Finally, resolution of singularities (§19) replaces singular points with exceptional divisors, and the dual resolution graph recovers the Dynkin diagram (Du Val's theorem). A'Campo's formula computes the monodromy zeta function from the resolution data.

Computational Tools and Algorithms

Throughout the notes, we emphasize explicit computability. The principal computational methods include:

- **Milnor number via the Jacobian ideal** (§6): $\mu = \dim_{\mathbb{C}} \mathcal{O}/J_f$, computable by standard basis algorithms in computer algebra systems such as SINGULAR or MACAULAY2;
- **Newton polygon methods** (§15): Kouchnirenko's formula computes μ from the Newton polyhedron volume, and Varchenko's formula computes the spectrum from lattice point counts;
- **Picard-Fuchs equations** (§14): explicit ODE computation via the Gauss-Manin connection on the Brieskorn lattice;
- **Resolution and A'Campo's formula** (§19): the monodromy zeta function from iterated blow-up data;
- **Bernstein-Sato polynomial** (§15): the b-function, computable by $\mathcal{D}$-module algorithms, encodes spectral numbers.

References and Sources

The following table summarizes the principal references for each section.

Section	Topic	Primary Reference(s)
§1	Definitions & ADE	Milnor [Mil68] Ch. 2; Greuel et al. [GLS07] Ch. 1
§2	ICIS	Looijenga [Loo84] Ch. 1–2; Hamm (1971)
§3	Curve Selection	Milnor [Mil68] Ch. 3
§4	Good Representatives	Looijenga [Loo84] Ch. 2
§5	Milnor Fibration	Milnor [Mil68] Ch. 4–5
§6	Homotopy & μ	Milnor [Mil68] Ch. 6–7
§7	Monodromy & Alexander	Milnor [Mil68] Ch. 8–10
§8	Picard-Lefschetz	Arnold et al. [AGV85]; Looijenga [Loo84] Ch. 3
§9–10	Deformation theory	Greuel et al. [GLS07]; Looijenga [Loo84] Ch. 5–6
§11–12	Fitting, Thom	Looijenga [Loo84] Ch. 6–7
§13	Vanishing lattices	Arnold et al. [AGV85]; Looijenga [Loo84] Ch. 7
§14	Gauss-Manin	Brieskorn [Bri70]; Kulikov [Kul98] Ch. I
§15	MHS & spectrum	Steenbrink [Ste77]; Kulikov [Kul98] Ch. II
§16	Period maps	Kulikov [Kul98] Ch. III; Hertling [Her02]
§17	Intersection forms	Arnold et al. [AGV85]; Ebeling [Ebe87]
§18	Moduli, unimodal	Arnold et al. [AGV85]
§19	Resolution	Wall [Wal04]; Dimca [Dim92] Ch. 4

Prerequisites

We assume familiarity with commutative algebra (local rings, Noetherian properties), differential topology (transversality, Morse theory), algebraic topology (homology, fibrations, covering spaces), and basic algebraic geometry (schemes, sheaves, coherent sheaves). Some acquaintance with Hodge theory is helpful for Parts III–IV but is developed from scratch in the text.

Acknowledgments

These notes draw extensively on the books of Milnor [Mil68], Arnold-Gusein-Zade-Varchenko [AGV85], Looijenga [Loo84], Greuel-Lossen-Shustin [GLS07], and Kulikov [Kul98], as well as the foundational papers of Brieskorn [Bri70] and Steenbrink [Ste77]. The author thanks all students for their feedback during the course.

Introduction: Topology and Deformation Theory Through Examples

Singularity theory begins with a deceptively simple question: what does the zero-set of a holomorphic function look like near a point where the implicit function theorem fails? There are two complementary answers. The *topological* answer replaces the singular fiber by a nearby smooth fiber and studies its homotopy type, its boundary link, and its monodromy. The *deformation-theoretic* answer perturbs the equation itself and studies how the singular point splits, smooths, or persists inside a miniversal family. The central theme of these notes is that these two answers are governed by computable algebra: Jacobian rings, Tjurina algebras, resolution graphs, Brieskorn lattices, and Bernstein–Sato polynomials.

What makes the subject irresistible is that the first examples are already surprising. A quadratic singularity produces a tangent bundle of a sphere; a cusp produces the trefoil knot and a punctured torus; a carefully chosen high-dimensional diagonal singularity produces an exotic sphere. Thus singularity theory is not merely a taxonomy of bad points. It is a machine that converts a local equation into topology, knot theory, Lie theory, and deformation theory.

For a beginner, the basic dictionary to keep in mind is the following.

- The singular fiber $f^{-1}(0)$ is usually hard to understand directly, but a nearby smooth fiber $f^{-1}(t)$ carries the essential topology.
- The link $K = f^{-1}(0) \cap S^{2n+1}_{\epsilon}$ records how the singularity sits inside the ambient space; in dimension one this is a knot or link in S^3.
- The Jacobian ring computes the number of vanishing cycles, while the Tjurina algebra computes the first-order deformation parameters.
- The monodromy and the Bernstein–Sato polynomial refine these numerical invariants and begin to detect subtle geometry invisible in the equation alone.

The examples in this introduction may be summarized in one page as follows.

Example	Equation	μ	Milnor fiber	Topological / deformation avatar
Curve node A_1	$x^2 + y^2 = 0$	1	annulus	boundary is the Hopf link
Cusp A_2	$y^2 - x^3 = 0$	2	punctured torus	trefoil knot; cusp discriminant
Surface node A_1	$x^2 + y^2 + z^2 = 0$	1	TS^2	one vanishing 2-sphere
E_8 surface	$x^2 + y^3 + z^5 = 0$	8	$\bigvee_8 S^2$	E_8 Dynkin resolution graph
Brieskorn link	$z_0^2 + \cdots + z_4^2 + z_5^3 = 0$	2	$\bigvee_2 S^5$	exotic homotopy 9-sphere link

The Ordinary Double Point: the First Topological Model

The basic local model is the Morse singularity

$$q_n(z_0, \ldots, z_n) = z_0^2 + \cdots + z_n^2.$$

This is the A_1 singularity in complex dimension n. Its Milnor fiber at a small real value $t > 0$ is

$$F_t(q_n) = \{z \in \mathbb{C}^{n+1} : q_n(z) = t\} \cap B_\epsilon.$$

Writing $z = u + iv$ with $u, v \in \mathbb{R}^{n+1}$, the defining equation becomes

$$|u|^2 - |v|^2 = t, \qquad u \cdot v = 0.$$

Hence $u \neq 0$, and the map

$$(u, v) \longmapsto \left(\frac{u}{|u|}, v\right)$$

identifies the affine quadric $q_n^{-1}(t)$ with the tangent bundle TS^n: the vector v is tangent to the sphere because $u \cdot v = 0$, and conversely one reconstructs u from $|u|^2 = t + |v|^2$. Thus the smooth fiber of the simplest singularity is already a cotangent-bundle-type object.

Two low-dimensional cases are especially important.

- For $n = 1$, the node $x^2 + y^2 = 0$ has Milnor fiber diffeomorphic to a bounded piece of $TS^1 \cong S^1 \times \mathbb{R}$, hence to an annulus, i.e. a cylinder. Equivalently, after the linear change of coordinates $u = x + iy$, $v = x - iy$, the fiber becomes $uv = t$, and projection to u identifies it with an annulus in the punctured disk.
- For $n = 2$, the surface node $x^2 + y^2 + z^2 = 0$ has Milnor fiber diffeomorphic to TS^2. In particular it deformation retracts to the zero section S^2, so its middle homology is generated by one vanishing 2-sphere.

This is the first instance of Milnor's general picture: for an isolated hypersurface singularity in $\mathbb{C}^{n+1}$, the Milnor fiber has the homotopy type of a bouquet of n-spheres,

$$F_t \simeq \bigvee_{\mu} S^n,$$

where the number of spheres is the Milnor number μ. For the ordinary double point, $\mu = 1$, so the vanishing topology is exactly one sphere.

The Cusp: Knotting, Monodromy, and Deformation

The next example is qualitatively richer:

$$f(x, y) = y^2 - x^3.$$

Its Jacobian ideal is $(\partial f/\partial x, \partial f/\partial y) = (-3x^2, 2y)$, so the Jacobian ring is

$$\mathrm{Jac}_f = \mathbb{C}\{x, y\}/(x^2, y), \qquad \mu(f) = \dim_{\mathbb{C}} \mathrm{Jac}_f = 2.$$

Milnor's bouquet theorem therefore predicts that the Milnor fiber has the homotopy type of a wedge of two circles. Since the boundary has one component, the fiber is in fact a punctured torus. In this example the boundary itself is already nontrivial: the link

$$K = f^{-1}(0) \cap S^3_\epsilon$$

is the $(2, 3)$-torus knot, i.e. the trefoil knot. Thus the simplest non-Morse plane curve singularity already produces a nontrivial knot in S^3, a nontrivial Seifert surface, and a nontrivial monodromy action on $H_1(F; \mathbb{Z})$.

The characteristic polynomial of the monodromy is computable from the Brieskorn–Pham formula:

$$\det(tI - h_*) = \frac{(t^6-1)(t-1)}{(t^3-1)(t^2-1)} = t^2 - t + 1.$$

Milnor's theorem identifies this polynomial with the Alexander polynomial of the trefoil. In other words, the topology of the knot complement and the topology of the Milnor fibration are encoded by the same characteristic polynomial. For isolated plane curve singularities with one branch, this is the bridge between singularity theory and classical knot theory.

The cusp is equally fundamental from the viewpoint of deformation theory. Its Tjurina algebra is again two-dimensional, so a miniversal deformation has two parameters:

$$F(x, y; a, b) = y^2 - x^3 - ax - b.$$

The discriminant is the semicubical cusp

$$4a^3 + 27b^2 = 0.$$

Away from this curve, the fiber is smooth. On the discriminant but away from the origin, the fiber has a single node. Thus the cusp deforms to the node: one singularity with Milnor number 2 splits into a nearby singular fiber with Milnor number 1. This is the local prototype for adjacency, morsification, and the stratification of the base of a miniversal deformation.

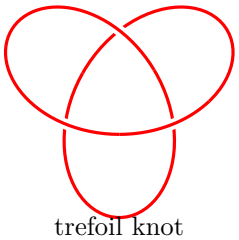

(a) The link of $y^2 = x^3$.

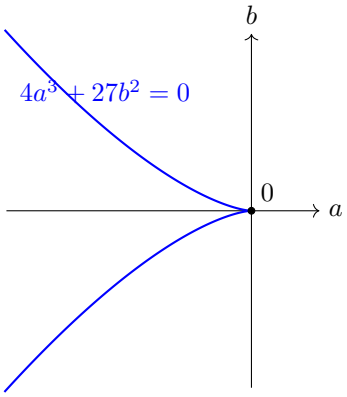

(b) The discriminant of the miniversal deformation.

Figure 1: The cusp singularity simultaneously produces a nontrivial knot and a nontrivial deformation discriminant.

ADE Singularities: Vanishing Spheres and Dynkin Diagrams

Higher-dimensional singularities add new topology without losing computability. For the surface singularity

$$E_8: \qquad f(x, y, z) = x^2 + y^3 + z^5,$$

the Jacobian ideal is $(2x, 3y^2, 5z^4)$, so

$$\mathrm{Jac}_f \cong \mathbb{C}\{x, y, z\}/(x, y^2, z^4)$$

has basis

$$1,\ y,\ z,\ yz,\ z^2,\ yz^2,\ z^3,\ yz^3.$$

Hence $\mu(E_8) = 8$. Milnor's theorem then implies that the Milnor fiber has the homotopy type of a bouquet of eight 2-spheres. At the same time, the minimal resolution replaces the singular point by a configuration of (-2)-curves arranged in the E_8 Dynkin diagram. The same singularity is therefore visible in three different languages:

- as a hypersurface equation in analytic geometry;
- as a bouquet of vanishing spheres in topology;
- as a Dynkin diagram of exceptional curves in birational geometry.

This ADE trinity is one of the guiding principles of the subject.

High-Dimensional Links and Exotic Spheres

The knot-theoretic picture does not stop in dimension three. For a Brieskorn–Pham polynomial

$$f(z_0, \dots, z_n) = z_0^{a_0} + \cdots + z_n^{a_n},$$

the link

$$\Sigma(a_0, \dots, a_n) = f^{-1}(0) \cap S_\epsilon^{2n+1}$$

is a smooth manifold of dimension $2n-1$. In dimension one this gives torus knots and links. In higher dimensions, the same construction can produce homotopy spheres. Even more strikingly, some of these homotopy spheres are not diffeomorphic to the standard sphere.

One classical example is the Brieskorn link of

$$z_0^2 + z_1^2 + z_2^2 + z_3^2 + z_4^2 + z_5^3 = 0.$$

Its link is a homotopy 9-sphere, and Brieskorn showed that it realizes a Kervaire exotic sphere. So a single isolated hypersurface singularity knows about a smooth manifold which is topologically a sphere but carries a nonstandard differentiable structure. From a beginner's point of view this is one of the most compelling reasons to study singularities: local holomorphic equations can detect global smooth-topological phenomena that are invisible to ordinary homology.

This high-dimensional story is governed by the same ideas as in the trefoil example. One computes the monodromy, studies the characteristic polynomial $\Delta(t)$, and uses the Wang sequence together with Alexander duality to determine when the link is a homology sphere. In low dimension this recovers classical knot invariants; in high dimension it reaches the frontier of differential topology.

The Key Theorems Behind These Examples

The general theory developed later in the notes explains the preceding examples in a remarkably uniform way.

- **Milnor fibration.** For a sufficiently small sphere, the map

  $$\Phi = \frac{f}{|f|} : S_\epsilon^{2n+1} \setminus K \to S^1$$

  is a smooth fiber bundle. This turns the ambient sphere into an open book with binding K and pages the Milnor fiber. For the cusp, the page is a punctured torus; for the node, it is an annulus; and for higher-dimensional singularities, the page becomes the basic carrier of the vanishing topology.

- **Milnor's bouquet theorem.** The Milnor fiber of an isolated hypersurface singularity has the homotopy type of a bouquet of n-spheres. This is why the Jacobian ring is so powerful: once μ is computed, one already knows the number of vanishing spheres in the fiber.
- **Morsification and Picard–Lefschetz theory.** A generic perturbation of an isolated hypersurface singularity splits it into exactly μ Morse points. Each Morse point contributes one vanishing cycle, and the total monodromy is obtained by composing the corresponding Picard–Lefschetz transformations. In this sense, the complicated topology of a cusp or an E_8 singularity is built by assembling many copies of the ordinary double point.
- **Gauss–Manin connection and Brieskorn lattice.** Period integrals of holomorphic forms over vanishing cycles vary holomorphically and satisfy a linear differential equation. Brieskorn's regular-singularity theorem and the V-filtration then constrain the monodromy eigenvalues and connect them to the Bernstein–Sato polynomial. Thus the same singularity can be studied topologically by vanishing cycles and analytically by differential equations.
- **Miniversal deformation and discriminant.** The Tjurina algebra determines the dimension and first-order directions of the miniversal deformation. The discriminant inside the base space marks precisely where the topology of the fiber changes. For the cusp, this discriminant is again a cusp; for simple singularities it organizes adjacencies and eventually leads to ADE classification.

From the standpoint of the course, these five theorems form the backbone of the subject: §§3–6 build the Milnor fibration and bouquet theorem, §§7–8 and 13 explain monodromy and vanishing cycles, §§9–12 study versal deformations and discriminants, and §§14–15 reinterpret the same topology through Gauss–Manin connections, Hodge theory, and Bernstein–Sato polynomials.

From Computation to Topology

These examples illustrate the computational philosophy of the course.

- The Jacobian ring
$$\mathrm{Jac}_f = \mathcal{O}_{\mathbb{C}^{n+1},0}/\left(\frac{\partial f}{\partial z_0},\dots,\frac{\partial f}{\partial z_n}\right)$$
is finite-dimensional exactly in the isolated case, and its dimension is the Milnor number. In practice this is computed by Gröbner-basis methods.
- The Tjurina algebra
$$T_f = \mathcal{O}_{\mathbb{C}^{n+1},0}/\left(f,\frac{\partial f}{\partial z_0},\dots,\frac{\partial f}{\partial z_n}\right)$$
controls first-order deformations and the dimension of the miniversal base. For the cusp it explains why the parameters a, b are the correct deformation coordinates.
- The Bernstein–Sato polynomial $b_f(s)$, computable by $\mathcal{D}$-module algorithms, refines the Jacobian-ring information. For the cusp one has
$$b_f(s) = (s+1)\left(s+\frac{5}{6}\right)\left(s+\frac{7}{6}\right).$$
Its roots recover the spectrum, hence the monodromy eigenvalues $e^{\pm i\pi/3}$, and therefore the characteristic polynomial t^2-t+1. In dimension one this is simultaneously the Alexander polynomial of the trefoil knot.

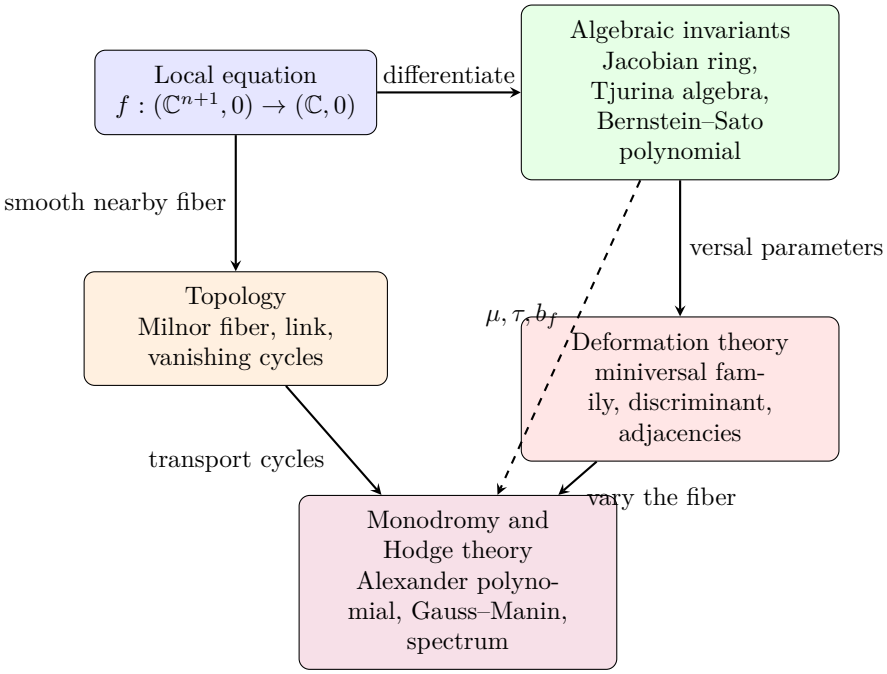

Figure 2: A road map for the course: local equations feed algebraic invariants, topology of the Milnor fiber, and deformation theory, which meet again in monodromy and Hodge theory.

Bernstein–Sato Polynomials, Resolution, and the Monodromy Conjecture

The Bernstein–Sato polynomial is one of the clearest places where analysis, algebra, and birational geometry meet. For a nonzero holomorphic germ f, the *b-function* is the monic polynomial $b_f(s) \in \mathbb{C}[s]$ of smallest degree for which there exists a differential operator $P(s, z, \partial_z) \in \mathcal{D}[s]$ satisfying

$$b_f(s) f^s = P(s, z, \partial_z) f^{s+1}.$$

Already this definition is suggestive: it says that the apparently multivalued object f^s is constrained by a finite-dimensional algebraic relation inside the ring of differential operators.

For Brieskorn–Pham plane curves one can write the answer explicitly. If

$$f(x, y) = x^p + y^q, \qquad \gcd(p, q) = 1,$$

then

$$b_f(s) = (s+1) \prod_{i=1}^{p-1} \prod_{j=1}^{q-1} \left(s + \frac{i}{p} + \frac{j}{q} \right).$$

For the cusp $f(x, y) = x^2 + y^3$, this becomes

$$b_f(s) = (s+1) \left(s + \frac{5}{6} \right) \left(s + \frac{7}{6} \right).$$

Thus one reads off three distinguished rational numbers: the universal root -1, and the two finer roots $-5/6$ and $-7/6$. The reduced polynomial $\widetilde{b}_f(s) = b_f(s)/(s+1)$ already determines the spectral numbers of the cusp and hence its monodromy eigenvalues $e^{\pm i\pi/3}$.

Resolution of singularities gives a complementary explanation for why such rational numbers appear. If

$$\pi : \widetilde{X} \to (\mathbb{C}^{n+1}, 0)$$

is an embedded resolution and

$$\pi^* f = u \prod_i E_i^{N_i}, \qquad K_{\widetilde{X}/\mathbb{C}^{n+1}} = \sum_i (\nu_i - 1) E_i,$$

then the pairs (N_i, ν_i) control the local zeta functions attached to f. The Denef–Loeser topological zeta function is built entirely from this resolution data:

$$Z_f^{\mathrm{top}}(s) = \sum_{\emptyset \neq I} \chi(E_I^\circ \cap \pi^{-1}(0)) \prod_{i \in I} \frac{1}{\nu_i + N_i s}.$$

Its candidate poles are therefore the rational numbers $-\nu_i/N_i$. For the cusp, the actual poles are -1 and $-5/6$. They are visible in the resolution, and they are also roots of $b_f(s)$. The extra root $-7/6$ shows that the Bernstein–Sato polynomial usually contains strictly finer information than the zeta function alone.

This is the entry point to the *Igusa monodromy conjecture*. Very roughly, the conjecture predicts that every pole of a local zeta function coming from f should force a monodromy eigenvalue of the Milnor fibration; the stronger form predicts that every such pole should in fact be a root of the Bernstein–Sato polynomial. So the philosophy is:

$$\text{resolution data} \Longrightarrow \text{zeta poles} \Longrightarrow \text{monodromy eigenvalues},$$

with the Bernstein–Sato polynomial serving as the algebraic intermediary between birational geometry and topology. The cusp is the first example where one can see this entire circle of ideas explicitly by hand.

Quasi-Homogeneity, Newton Polygons, and Computability

Not every useful computation in singularity theory requires a full resolution or a full $\mathcal{D}$-module calculation. There are two large classes of singularities for which the main invariants are often visible almost immediately: weighted homogeneous singularities and Newton non-degenerate singularities. They form the basic laboratory in which the general theorems become concrete.

Suppose first that $f(z_0, \ldots, z_n)$ is weighted homogeneous of degree 1 with positive weights $w_0, \ldots, w_n$. Then the Milnor algebra

$$M_f = \mathbb{C}[z_0, \ldots, z_n] / \left(\partial_{z_0} f, \ldots, \partial_{z_n} f\right)$$

has a monomial basis, and Steenbrink's formula says that the spectral numbers are read directly from the weighted degrees

$$\alpha(z^K) = \sum_{i=0}^{n} w_i (k_i + 1)$$

of those basis monomials [Ste77]. For the cusp $x^2 + y^3$, the weights are $(1/2, 1/3)$ and the Milnor algebra basis is $\{1, y\}$, so the spectrum is immediately

$$\left\{ \frac{5}{6}, \frac{7}{6} \right\}.$$

That single calculation already recovers the monodromy eigenvalues $e^{\pm i\pi/3}$ and matches the roots of the reduced Bernstein–Sato polynomial. In the weighted homogeneous world, topology, Hodge theory, and local algebra become almost transparent.

The next layer of computability is provided by Newton polygons. If a plane curve germ is non-degenerate with respect to its Newton boundary, then Kouchnirenko's formula computes the Milnor number purely from the area under the boundary. For example,

$$f(x, y) = x^5 + y^5 + x^2y^2$$

is not quasi-homogeneous, but its Newton boundary still controls the topology. The boundary cuts the coordinate axes at $(5, 0)$ and $(0, 5)$ and encloses area $S_- = 10$, so

$$\mu = 2S_- - 5 - 5 + 1 = 11.$$

Thus a local topological invariant of the singular fiber is recovered from elementary convex geometry rather than from a direct Jacobian-algebra computation.

What makes this especially powerful is that Newton data does not stop at μ. Varchenko's theory extracts the spectrum from lattice points in the Newton polyhedron, and his semicontinuity theorem then turns those spectral numbers into deformation-theoretic obstructions [Var81]. In practice, this means that a well-chosen Newton diagram can already predict not only how many vanishing cycles the Milnor fiber carries, but also which adjacencies are impossible because the spectrum would have to move in a forbidden direction.

For a beginner, these examples are important because they show that singularity theory is not merely abstract structure. In favorable classes, one really can read topology off weights, off lattice points, and off the convex hull of exponents. The general theory later in the notes explains why these miracle computations work and how far they extend beyond the quasi-homogeneous and Newton non-degenerate settings.

Distinguished Bases, Braid Groups, and ADE Geometry

There is one more mechanism behind the ubiquity of ADE singularities that is worth seeing already in the introduction. A generic morsification of an isolated hypersurface singularity produces exactly μ Morse critical points. Choosing nonintersecting paths from a base value to these critical values gives a *distinguished basis of vanishing cycles*

$$(\delta_1, \dots, \delta_\mu) \subset H_n(F; \mathbb{Z}).$$

Their intersection pairing records how the vanishing spheres are attached inside the Milnor fiber. In favorable cases, drawing one vertex for each δ_i and connecting vertices according to their intersection numbers produces a graph that is already the right combinatorial shadow of the singularity.

For the cusp A_2, a morsification has two Morse points, hence two vanishing cycles δ_1, δ_2 with intersection number $\langle \delta_1, \delta_2 \rangle = 1$. In a suitable basis, the Picard–Lefschetz operators can be written as

$$T_1 = \begin{pmatrix} 1 & -1 \\ 0 & 1 \end{pmatrix}, \qquad T_2 = \begin{pmatrix} 1 & 0 \\ 1 & 1 \end{pmatrix}.$$

Their product is

$$T = T_2T_1 = \begin{pmatrix} 1 & -1 \\ 1 & 0 \end{pmatrix}, \qquad \chi_T(t) = t^2 - t + 1.$$

So the same cusp produces, at once, a trefoil knot, an A_2 Dynkin diagram, and a Coxeter-type monodromy operator with characteristic polynomial $t^2 - t + 1$. This is the first place where one

sees that the ADE labels are not an arbitrary naming convention: they arise from the actual intersection geometry of vanishing cycles.

The deformation side explains why braid groups appear. For the one-variable singularity A_k, the miniversal family may be written as

$$x^{k+1} + s_{k-1}x^{k-1} + \cdots + s_1 x + s_0.$$

Away from the discriminant, this polynomial has $k+1$ distinct roots, so the discriminant complement identifies with the configuration space of $k+1$ unordered points in $\mathbb{C}$. Its fundamental group is therefore the braid group B_{k+1}. Moving around in the discriminant complement braids the critical values, and on the level of vanishing cycles this becomes the *Hurwitz action* on distinguished bases. Thus braid groups enter singularity theory not by analogy, but because the parameter space of a morsification literally remembers how critical values can be exchanged.

For the simple hypersurface singularities, one can choose distinguished bases whose intersection graphs are precisely the Dynkin diagrams A_k, D_k, E_6, E_7, and E_8 [AGV85; Loo84]. The total monodromy is then represented by the corresponding Coxeter element. This gives a conceptual route from local equations to Lie-theoretic combinatorics:

$$\text{morsification} \Longrightarrow \text{vanishing cycles} \Longrightarrow \text{intersection graph} \Longrightarrow \text{ADE diagram}.$$

From the viewpoint of these notes, this is one of the deepest organizing principles in the subject: topology, deformation theory, reflection groups, and classification are all encoded in the same finite collection of vanishing cycles.

This perspective also clarifies adjacency. When one moves in the base of a miniversal deformation toward a boundary stratum, only some vanishing cycles collapse. For the cusp A_2, allowing just one vanishing cycle to shrink produces the adjacent node A_1. More generally, many basic adjacencies of simple singularities are reflected by passing to appropriate subconfigurations of vanishing cycles, or heuristically, by passing to suitable subdiagrams. The topology of the Milnor fiber therefore does not merely count how many singular points appear after perturbation; it organizes which simpler singularities can appear and how they sit inside the deformation space.

In short, singularity theory turns local equations into global topology. A quadratic form already knows about tangent bundles of spheres; a cusp already knows about trefoil knots, punctured tori, and cusp discriminants; an ADE equation already knows about bouquets of vanishing spheres and Dynkin diagrams. The later sections will build the general theory explaining why these coincidences are in fact the main structure the subject is trying to reveal.

1 Singularities: Definitions and Examples

Singularity theory studies the spaces that locally look like Euclidean spaces, except at certain *bad* points called singularities. In this chapter, we will introduce the basic definitions of singular points in both algebraic and analytic settings. We will emphasize hypersurface singularities, especially plane curve singularities and surface singularities, which provide the most intuitive and computationally accessible examples. We will conclude with the famous ADE classification of simple singularities and their relation to quotient singularities.

1.1 Algebraic and Analytic Varieties

Let K be an algebraically closed field. For most of this course, we will heavily rely on the case $K = \mathbb{C}$, as topology plays a crucial role.

Definition 1.1 (Affine Algebraic Variety)**.** *An **affine algebraic variety** $X \subset \mathbb{C}^n$ is the zero locus of a collection of polynomials $f_1, \ldots, f_k \in \mathbb{C}[x_1, \ldots, x_n]$:*

$$X = V(f_1, \ldots, f_k) = \{z \in \mathbb{C}^n \mid f_1(z) = \cdots = f_k(z) = 0\}.$$

*The **ideal** of X is $I(X) = \{f \in \mathbb{C}[x_1, \ldots, x_n] \mid f(z) = 0 \text{ for all } z \in X\}$. The **coordinate ring** of X is $\mathbb{C}[X] = \mathbb{C}[x_1, \ldots, x_n]/I(X)$.*

When studying the local behavior of X at a point $p \in X$, we can translate p to the origin $0 \in \mathbb{C}^n$. The local geometry is governed by the **local ring** $\mathcal{O}_{X,p}$, which is the localization of $\mathbb{C}[X]$ at the maximal ideal $\mathfrak{m}_p$.

In the analytic setting, we work locally.

Definition 1.2 (Analytic Germ)**.** *An **analytic germ** $(X, 0)$ at the origin in $\mathbb{C}^n$ is defined by the common zero locus of a finite set of convergent power series $f_1, \ldots, f_k \in \mathbb{C}\{x_1, \ldots, x_n\}$ in a small neighborhood of the origin. Here $\mathbb{C}\{x_1, \ldots, x_n\}$ denotes the ring of convergent power series at the origin. The local ring of the germ is $\mathcal{O}_{X,0} = \mathbb{C}\{x_1, \ldots, x_n\}/I$, where I is the ideal generated by $f_1, \ldots, f_k$.*

The modern viewpoint elegantly unifies these concepts using the language of schemes or complex spaces, where a space is determined by its structure sheaf. Locally, it is entirely captured by the local ring $\mathcal{O}_{X,p}$.

1.2 Singular Points and the Jacobian Criterion

Intuitively, a point on a variety is smooth if the variety looks like a manifold near that point; it is singular if it is *pinched*, has self-intersections, or sharp corners. We can formalize this using the tangent space.

Definition 1.3 (Zariski Tangent Space)**.** *Let (X, p) be a germ of a variety with local ring $(\mathcal{O}_{X,p}, \mathfrak{m})$. The **Zariski tangent space** of X at p is defined as the dual vector space of $\mathfrak{m}/\mathfrak{m}^2$:*

$$T_pX = (\mathfrak{m}/\mathfrak{m}^2)^\vee = \mathrm{Hom}_{\mathbb{C}}(\mathfrak{m}/\mathfrak{m}^2, \mathbb{C}).$$

Definition 1.4 (Regular and Singular Points)**.** *Let X be an irreducible variety of dimension d. A point $p \in X$ is called a **regular (or smooth) point** if $\dim_{\mathbb{C}} T_pX = d$. In this case, $\mathcal{O}_{X,p}$ is a regular local ring. If $\dim_{\mathbb{C}} T_pX > d$, the point p is called a **singular point** of X. The set of singular points of X is denoted by $\mathrm{Sing}(X)$.*

For practical computations, we use the Jacobian matrix.

Theorem 1.1 (Jacobian Criterion)**.** *Let $X \subset \mathbb{C}^n$ be defined by polynomials (or convergent power series) $f_1, \ldots, f_k$, and assume X is purely d-dimensional at $p \in X$. Let $\mathrm{Jac}(f)(p)$ be the Jacobian matrix evaluated at p:*

$$\mathrm{Jac}(f)(p) = \left(\frac{\partial f_i}{\partial x_j}(p) \right)_{1 \le i \le k, 1 \le j \le n}.$$

Then p is a smooth point of X if and only if $\operatorname{rank} \mathrm{Jac}(f)(p) = n - d$. Equivalently, p is a singular point if and only if $\operatorname{rank} \mathrm{Jac}(f)(p) < n - d$.

1.3 Hypersurface Singularities and Isolated Singularities

A highly important class of singularities is hypersurface singularities, defined by a single equation.

Definition 1.5 (Hypersurface Singularity)**.** *A variety (or germ) $X \subset \mathbb{C}^{n+1}$ is a **hypersurface** if it is defined by a single non-zero function $f(x_0, \dots, x_n) = 0$. In this case, the dimension of X is n. By the Jacobian criterion, $p \in X$ is singular if and only if*

$$f(p) = 0 \quad \text{and} \quad \frac{\partial f}{\partial x_0}(p) = \frac{\partial f}{\partial x_1}(p) = \cdots = \frac{\partial f}{\partial x_n}(p) = 0.$$

Definition 1.6 (Isolated Singularity)**.** *A point $p \in X$ is an **isolated singular point** if there exists a neighborhood U of p such that p is the only singular point of $X \cap U$. In other words,* $\operatorname{Sing}(X) \cap U = \{p\}$.

For a hypersurface defined by f, p is an isolated singularity if and only if p is an isolated common zero of the partial derivatives $\partial f/\partial x_0, \dots, \partial f/\partial x_n$.

Proposition 1.1 (Equivalent Criteria for an Isolated Hypersurface Singularity)**.** *Let $(X, 0) = V(f) \subset (\mathbb{C}^{n+1}, 0)$ be a hypersurface germ, where $f \in \mathcal{O}_{\mathbb{C}^{n+1},0}$ generates the ideal of X, and let $\mathfrak{m}$ be the maximal ideal of $\mathcal{O}_{\mathbb{C}^{n+1},0}$. Then the following are equivalent:*

1. *0 is an isolated singular point of X.*
2. *The Jacobian ideal*
$$J_f = \left(\frac{\partial f}{\partial x_0}, \dots, \frac{\partial f}{\partial x_n} \right)$$
contains a power of $\mathfrak{m}$.
3. *The Tjurina ideal*
$$(f) + J_f$$
contains a power of $\mathfrak{m}$.
4. *The Jacobian algebra*
$$\mathcal{O}_{\mathbb{C}^{n+1},0}/J_f$$
is finite-dimensional over $\mathbb{C}$.
5. *The Tjurina algebra*
$$\mathcal{O}_{\mathbb{C}^{n+1},0}/((f) + J_f)$$
is finite-dimensional over $\mathbb{C}$.

Proof sketch. This is the local analytic characterization emphasized by Looijenga [Loo84, Ch. 1, §A]. The implications (2) $\Rightarrow$ (4) and (3) $\Rightarrow$ (5) are immediate. Conversely, if a quotient of a regular local ring is finite-dimensional over $\mathbb{C}$, then some power of the maximal ideal annihilates it by Nakayama's lemma, so (4) $\Rightarrow$ (2) and (5) $\Rightarrow$ (3).

The subtle point is the comparison between J_f and $(f) + J_f$. Let $Y = V(J_f)$ be the germ cut out by the partial derivatives alone. If $(Y, 0)$ were not contained in $(X, 0)$, then there would exist an analytic arc $\gamma : (\mathbb{C}, 0) \to (Y, 0)$ such that $f(\gamma(t)) \neq 0$ for $t \neq 0$. But along such an arc,

$$\frac{d}{dt}(f \circ \gamma) = \sum_{i=0}^{n} \left(\frac{\partial f}{\partial x_i} \circ \gamma \right) \gamma_i'(t) = 0,$$

so $f \circ \gamma$ must be constant, hence equal to $f(\gamma(0)) = 0$, a contradiction. Therefore Y and $V(f, J_f)$ define the same germ at the origin. The analytic Nullstellensatz then identifies conditions (1), (2), and (3). $\square$

Definition 1.7 (Milnor and Tjurina Numbers for Hypersurfaces)**.** *If the equivalent conditions of proposition 1.1 are satisfied, we define*

$$\mu(X,0) = \dim_{\mathbb{C}} \mathcal{O}_{\mathbb{C}^{n+1},0}/J_f, \qquad \tau(X,0) = \dim_{\mathbb{C}} \mathcal{O}_{\mathbb{C}^{n+1},0}/((f) + J_f).$$

The number μ will later reappear as the number of vanishing n-spheres in the Milnor fiber, while τ measures the dimension of the miniversal deformation space.

Proposition 1.2 (The ring model does not affect μ or τ for polynomials)**.** *Let $f \in \mathbb{C}[z_0, \ldots, z_n]$ be a polynomial defining an isolated hypersurface singularity at the origin. Set*

$$A_{\text{alg}} = \mathbb{C}[z_0, \ldots, z_n]_{(z_0,\ldots,z_n)}, \qquad A_{\text{an}} = \mathbb{C}\{z_0, \ldots, z_n\}, \qquad A_{\text{for}} = \mathbb{C}[[z_0, \ldots, z_n]],$$

and let

$$I_\mu = (\frac{\partial f}{\partial z_0}, \ldots, \frac{\partial f}{\partial z_n}), \qquad I_\tau = (f, \frac{\partial f}{\partial z_0}, \ldots, \frac{\partial f}{\partial z_n}).$$

Then

$$\dim_{\mathbb{C}} A_{\text{alg}}/I_\mu = \dim_{\mathbb{C}} A_{\text{an}}/I_\mu A_{\text{an}} = \dim_{\mathbb{C}} A_{\text{for}}/I_\mu A_{\text{for}},$$

and likewise

$$\dim_{\mathbb{C}} A_{\text{alg}}/I_\tau = \dim_{\mathbb{C}} A_{\text{an}}/I_\tau A_{\text{an}} = \dim_{\mathbb{C}} A_{\text{for}}/I_\tau A_{\text{for}}.$$

In particular, for a polynomial germ one gets the same Milnor number and Tjurina number whether one works in the localized polynomial ring, the convergent power series ring, or the formal power series ring.

Proof. Because the singularity is isolated, both I_μ and I_τ are $\mathfrak{m}$-primary in the analytic local ring, where $\mathfrak{m} = (z_0, \ldots, z_n)$. Hence there exists $N \gg 0$ such that

$$\mathfrak{m}^N \subset I_\mu, \qquad \mathfrak{m}^N \subset I_\tau.$$

Therefore each quotient above is annihilated by $\mathfrak{m}^N$, so every class is determined by its $(N-1)$-jet. Equivalently, each quotient is represented by polynomials of degree $< N$ modulo the same linear relations among those monomials.

Now the three local rings have the same truncated quotients:

$$A_{\text{alg}}/\mathfrak{m}^N \cong A_{\text{an}}/\mathfrak{m}^N \cong A_{\text{for}}/\mathfrak{m}^N,$$

because all three are just the ring of $(N-1)$-jets at the origin. Since I_μ and I_τ already contain $\mathfrak{m}^N$, passing to the quotient by either ideal only depends on this finite jet ring. Hence the resulting $\mathbb{C}$-dimensions are identical in all three settings.

One may summarize the argument by saying that analytification and completion do not change finite-length modules: once the Jacobian or Tjurina algebra is Artinian, it is already completely captured by a sufficiently high finite jet. □

Remark 1.1 (Weighted Homogeneity and the Relation $\tau \leq \mu$)**.** *If f is weighted homogeneous of weighted degree N with positive weights $d_0, \ldots, d_n$, then Euler's weighted identity gives*

$$f = \sum_{i=0}^{n} \frac{d_i}{N} x_i \frac{\partial f}{\partial x_i}.$$

Hence $f \in J_f$, so $\tau(X,0) = \mu(X,0)$. Later we will return to Saito's converse: for isolated hypersurface singularities, the equality $\tau = \mu$ is in fact a rigid indication of quasihomogeneity.

Example 1.1 (Node and Cusp)**.** *Let us consider curves in* $\mathbb{C}^2$ *(*$n = 1$*).*

1. ***Node*** *(Ordinary double point):* $X = \{y^2 - x^2(x+1) = 0\}$*. The partial derivatives are* $-2x(x+1) - x^2 = -x(3x+2)$ *and* $2y$*. The singularity is at* $(0,0)$*. This is a curve crossing itself.*
2. ***Cusp****:* $X = \{y^2 - x^3 = 0\}$*. The partial derivatives are* $-3x^2$ *and* $2y$*. The singularity is at* $(0,0)$*. The curve has a sharp point.*

1.4 Plane Curve Singularities and Surface Singularities

Plane Curve Singularities ($n = 1$**):** These are given by $f(x,y) = 0$. For reduced plane curves, isolated singularities are automatic.

Proposition 1.3 (Reduced Plane Curves Have Isolated Singularities)**.** *Let* $(C,0) \subset (\mathbb{C}^2,0)$ *be the germ defined by a reduced holomorphic function* $f(x,y) \in \mathbb{C}\{x,y\}$*. Then*

$$\mathrm{Sing}(C) = V\left(f, \frac{\partial f}{\partial x}, \frac{\partial f}{\partial y}\right)$$

is zero-dimensional. In particular, every singular point of a reduced plane curve germ is isolated.

Proof. Assume that $\mathrm{Sing}(C)$ had dimension 1. Then some irreducible factor g of f would divide both $\dfrac{\partial f}{\partial x}$ and $\dfrac{\partial f}{\partial y}$. Write $f = gh$ with $\gcd(g,h) = 1$. Reducing

$$\frac{\partial f}{\partial x} = \frac{\partial g}{\partial x}h + g\frac{\partial h}{\partial x}, \qquad \frac{\partial f}{\partial y} = \frac{\partial g}{\partial y}h + g\frac{\partial h}{\partial y}$$

modulo g, we obtain $g \mid \dfrac{\partial g}{\partial x}h$ and $g \mid \dfrac{\partial g}{\partial y}h$. Since g and h are coprime, it follows that $g \mid \dfrac{\partial g}{\partial x}$ and $g \mid \dfrac{\partial g}{\partial y}$. This is impossible: in characteristic 0, at least one partial derivative of a nonconstant holomorphic germ is nonzero, and any nonzero partial derivative has strictly smaller order than the germ itself. Hence $\mathrm{Sing}(C)$ is zero-dimensional. □

This is the one-dimensional case of the general fact that the smooth locus of a reduced complex variety is a dense open subset; equivalently, for any reduced complex variety X one has $\dim \mathrm{Sing}(X) < \dim X$; see [GLS07, Ch. 1]. For curves this forces singularities to be isolated, but in higher dimension a positive-dimensional singular locus may still occur.

Example 1.2 (Why Reducedness Matters)**.** *The doubled line* $\{y^2 = 0\} \subset \mathbb{C}^2$ *is not reduced, and its singular locus is the whole line* $\{y = 0\}$*. Thus non-reduced curve germs need not have isolated singularities.*

Example 1.3 (Reduced Plane Curve Examples)**.**

1. ***Node****:* $C = \{xy = 0\}$ *is reduced, and* $\mathrm{Sing}(C) = \{0\}$*.*
2. ***Cusp****:* $C = \{y^2 - x^3 = 0\}$ *is reduced and irreducible, and* $\mathrm{Sing}(C) = \{0\}$*.*
3. ***Torus curves****:* $C_{p,q} = \{x^p - y^q = 0\}$ *is reduced in characteristic* 0*; if* $\gcd(p,q) = 1$*, it is an irreducible branch. In all cases the singular locus is still* $\{0\}$*. For* $\gcd(p,q) = 1$*, the link is the* (p,q)*-torus knot; for general* p, q*, it is the* (p,q)*-torus link.*

The topology of a plane curve singularity at the origin is completely determined by its combinatorial data: how the curve branches and how the branches intersect. Equivalently, one may encode the topological type by the Puiseux characteristic or by the embedded resolution graph; see [Wal04, Ch. 1].

Surface Singularities ($n = 2$): These are given by $f(x, y, z) = 0$. The study of isolated surface singularities leads to rich geometry, as resolving the singularity requires blowing up points, replacing the singular point with a configuration of curves.

Example 1.4 (A cone over a smooth rational curve)**.** *Let $X \subset \mathbb{C}^3$ be defined by $x^2+y^2+z^2 = 0$. The gradient is $(2x, 2y, 2z)$, which vanishes only at $(0, 0, 0)$. Thus, the origin is an isolated surface singularity. This surface X is naturally equivalent to the cone over the smooth projective curve* $\mathrm{Proj}(\mathbb{C}[x, y, z]/(x^2 + y^2 + z^2)) \cong \mathbb{P}^1$.

Example 1.5 (Whitney Umbrella)**.** *Consider $X = \{x^2 - y^2z = 0\} \subset \mathbb{C}^3$. The singular locus is defined by $2x = 0, -2yz = 0, -y^2 = 0$, which yields the entire z-axis $(0, 0, z)$. Since $x^2 - y^2z$ is square-free, X is reduced. Thus this is a reduced variety with a* ***non-isolated*** *singular locus.*

1.5 ADE Singularities

A particularly beautiful and ubiquitous class of singularities are the simple (or ADE) singularities. Under the right local coordinate changes (analytic or formal), they can be classified into discrete types.

Definition 1.8 (ADE Singularities)**.** *A hypersurface germ $(X, 0) \subset (\mathbb{C}^3, 0)$ has an* ***ADE singularity*** *(or is a* ***Du Val singularity****, or* ***Kleinian singularity****) if it is locally analytically isomorphic to one of the following germs:*

$$\begin{aligned}
A_k \quad & (k \geq 1): && x^2 + y^2 + z^{k+1} = 0 \\
D_k \quad & (k \geq 4): && x^2 + y^2z + z^{k-1} = 0 \\
E_6 \quad & : && x^2 + y^3 + z^4 = 0 \\
E_7 \quad & : && x^2 + y^3 + yz^3 = 0 \\
E_8 \quad & : && x^2 + y^3 + z^5 = 0
\end{aligned}$$

These singularities are called *simple* because they do not have moduli (they are rigid up to Right-equivalence). The subscripts k correspond to the Milnor number (which we will define in later chapters), and remarkably, the intersection matrix of the irreducible components of the exceptional divisor in their minimal resolution corresponds precisely to the negative of the Cartan matrix of the corresponding simple Lie algebra of A-D-E type.

1.6 ADE Singularities as Quotient Singularities

The connection between the ADE equations and Dynkin diagrams becomes even more magical when we realize they arise as quotient singularities.

Let $G \subset \mathrm{SL}(2, \mathbb{C})$ be a finite subgroup. It acts naturally on $\mathbb{C}^2$ and therefore on the polynomial ring $\mathbb{C}[x, y]$. The invariant ring $\mathbb{C}[x, y]^G$ is finitely generated. It turns out that $\mathbb{C}[x, y]^G$ is always generated by 3 polynomials X, Y, Z subject to a single relation $f(X, Y, Z) = 0$.

Therefore, the quotient space $\mathbb{C}^2/G \cong \mathrm{Spec}\,\mathbb{C}[x, y]^G$ can be embedded as a hypersurface in $\mathbb{C}^3$. The remarkable theorem of Felix Klein is that the singularities appearing this way are exactly the ADE singularities!

Theorem 1.2 (Klein's Theorem)**.** *There is a one-to-one correspondence between finite subgroups of* $\mathrm{SL}(2,\mathbb{C})$ *(up to conjugation) and ADE singularities* $\mathbb{C}^2/G$*:*

- *Cyclic groups* C_{k+1} *correspond to* A_k*.*
- *Binary dihedral groups* BD_{k-2} *correspond to* D_k*.*
- *Binary tetrahedral group corresponds to* E_6*.*
- *Binary octahedral group corresponds to* E_7*.*
- *Binary icosahedral group corresponds to* E_8*.*

This deep property initiates the McKay correspondence, linking finite subgroups of $\mathrm{SL}(2,\mathbb{C})$, Dynkin diagrams, representations of groups, and the geometry of singularities.

1.7 Exercises

Exercise 1.1. *Show that the curve* $x^3 - y^3 = 0$ *in* $\mathbb{C}^2$ *has an isolated singularity at the origin. Find its decomposition into irreducible components.*

Exercise 1.2. *Compute the singular locus of the affine variety corresponding to the matrix rank conditions: let* M *be a generic* 2×3 *matrix with coordinate entries* x_{ij}*. Let* X *be the locus where* $\operatorname{rank} M \leq 1$*. Determine* $\mathrm{Sing}(X)$ *and its dimension.*

Exercise 1.3. *Consider the cyclic group* $G = \mathbb{Z}/k\mathbb{Z}$ *acting on* $\mathbb{C}^2$ *by* $\zeta \cdot (x, y) = (\zeta x, \zeta^{-1} y)$*, where* $\zeta = \exp(2\pi i/k)$*. Show that the invariant ring* $\mathbb{C}[x,y]^G$ *is generated by* $u = x^k, v = y^k, w = xy$*. Deduce that the quotient space* $\mathbb{C}^2/G$ *satisfies the equation* $uv = w^k$*. Show that this equation is isomorphic to the* A_{k-1} *singularity germ* $X^2 + Y^2 + Z^k = 0$*.*

Exercise 1.4. *Compute the Jacobian matrix and determine the singular point(s) of the* E_6 *singularity* $x^2 + y^3 + z^4 = 0$*. Prove that the origin is an isolated singularity.*

Exercise 1.5. *Let* $f(x, y, z) = x^a + y^b + z^c = 0$ *restrict to an isolated singularity at the origin. For which triples of integers* (a, b, c) *with* $a, b, c \geq 2$ *does the variety define an ADE singularity?*

2 Isolated Complete Intersection Singularities (ICIS)

While hypersurface singularities are defined by a single equation, many natural geometric objects are defined by multiple equations. A particularly well-behaved generalization is the class of isolated complete intersection singularities (ICIS). This forms a foundational class of singularities developed extensively by Looijenga and others.

2.1 Definition of ICIS

Definition 2.1 (Complete Intersection)**.** *A germ of an analytic space* $(X, 0) \subset (\mathbb{C}^n, 0)$ *is a* ***complete intersection*** *of dimension* d *if its ideal* $I_{X,0} \subset \mathcal{O}_{\mathbb{C}^n,0}$ *can be generated by* $k = n - d$ *elements* $f_1, \ldots, f_k$*, which form a regular sequence in* $\mathcal{O}_{\mathbb{C}^n,0}$*. Equivalently, the local codimension of* X *matches the number of defining equations.*

Definition 2.2 (Isolated Complete Intersection Singularity)**.** *We say* $(X, 0)$ *is an* ***isolated complete intersection singularity*** *(often abbreviated as* ***ICIS****) if it is a complete intersection, and* 0 *is an isolated singular point. By the Jacobian criterion, this means that the* $k \times n$ *Jacobian matrix* $\mathrm{Jac}(f) = (\partial f_i/\partial x_j)$ *has rank strictly less than* k *at* 0*, but has maximal rank* k *at all points in* $X \setminus \{0\}$ *sufficiently close to the origin.*

This generalizes isolated hypersurface singularities ($k = 1$). Many theorems for hypersurfaces extend to ICIS, though the proofs often require more sophisticated algebraic machinery such as local cohomology and projective dimension techniques.

2.2 Regular Sequences, Embedding Dimension, and Local Complete Intersections

Looijenga's point of view is that complete intersections are best understood as a local algebra condition, not merely as a convenient way of writing down equations.

Proposition 2.1 (Regular Sequence Criterion for Complete Intersections)**.** *Let $I = (f_1, \dots, f_k) \subset \mathcal{O}_{\mathbb{C}^N,0}$ and assume that the germ $V(I)$ has dimension $d = N - k$. Then the following are equivalent:*

1. *$V(I)$ is a complete intersection of dimension d.*
2. *$f_1, \dots, f_k$ form a regular sequence in $\mathcal{O}_{\mathbb{C}^N,0}$.*

If these conditions hold, then $\mathcal{O}_{\mathbb{C}^N,0}/I$ is a Cohen–Macaulay local ring of dimension d.

Idea of proof. The point is that a regular sequence cuts the ambient space by codimension one at each step without producing embedded components. Conversely, for a geometric complete intersection of codimension k, the defining equations must have exactly this non-zero-divisor property. See [Loo84, Ch. 1, §B] or Matsumura for the commutative algebra behind this equivalence. □

Definition 2.3 (Embedding Dimension and Embedding Codimension)**.** *For a local analytic algebra $(A, \mathfrak{m}_A)$, the **embedding dimension** and **embedding codimension** are defined by*

$$\operatorname{embdim}(A) = \dim_{\mathbb{C}} \mathfrak{m}_A/\mathfrak{m}_A^2, \qquad \operatorname{embcodim}(A) = \operatorname{embdim}(A) - \dim A.$$

The number $\operatorname{embdim}(A)$ is the minimal ambient dimension in which the germ can be embedded, and a local analytic algebra is a complete intersection precisely when, in such a minimal embedding, its defining ideal can be generated by $\operatorname{embcodim}(A)$ elements forming a regular sequence.

Remark 2.1 (Complete Intersections Are Special)**.** *Not every isolated singularity is a complete intersection. Standard nonexamples include the union of two coordinate planes in $\mathbb{C}^4$ and the cone over the twisted cubic. Looijenga stresses this point early: complete intersections are broad enough to include hypersurfaces, ADE singularities, and many quasihomogeneous examples, but restrictive enough that homological algebra and deformation theory remain especially effective.*

Proposition 2.2 (Positive-dimensional ICIS are Reduced)**.** *If $(X, 0)$ is an ICIS of positive dimension, then its defining ideal is radical; equivalently, X is reduced.*

Proof. By proposition 2.1, the local ring $\mathcal{O}_{X,0}$ of an ICIS is Cohen–Macaulay. Let I_{red} be the radical of the defining ideal I. Then the quotient I_{red}/I is a finite-length submodule of $\mathcal{O}_{\mathbb{C}^N,0}/I$, because the nonreducedness would be supported at the isolated singular point. But a positive-dimensional Cohen–Macaulay local ring has no nonzero finite-length submodules. Therefore $I_{\text{red}} = I$. □

2.3 Milnor and Tjurina Numbers for ICIS

For a hypersurface defined by $f = 0$, the Milnor number μ is the dimension of the Jacobian algebra $\mathcal{O}_{\mathbb{C}^n,0}/(\partial f/\partial x_1, \ldots, \partial f/\partial x_n)$, and the Tjurina number τ is the dimension of $\mathcal{O}_{\mathbb{C}^n,0}/(f, \partial f/\partial x_1, \ldots, \partial f/\partial x_n)$. These invariants can be elegantly generalized.

For an ICIS defined by $f = (f_1, \ldots, f_k) : (\mathbb{C}^n, 0) \to (\mathbb{C}^k, 0)$, we consider the $\mathcal{O}_{X,0}$-module spanned by the $k \times k$ minors of the Jacobian matrix, denoted by $J(f)$. The Tjurina number τ is intimately related to the module of relative differentials and deformation theory. Geometrically, $\mu(X, 0)$ can still be defined topologically as the middle Betti number of the Milnor fiber (which we will define in later chapters). One deeply algebraic definition for the Tjurina number is $\tau(X, 0) = \dim_{\mathbb{C}} \operatorname{Ext}^1_{\mathcal{O}_{X,0}}(\Omega^1_{X,0}, \mathcal{O}_{X,0})$. It measures the dimension of the base space of the miniversal deformation of $(X, 0)$.

2.4 Examples: Quasi-conical and Cusp Singularities

Example 2.1 (Quasi-conical Singularities)**.** *A normal surface singularity $(X, 0)$ with a good $\mathbb{C}^*$-action is called a quasi-conical singularity. These are algebraic surfaces that can be viewed as cones over projective curves equipped with ample line bundles. Simple elliptic singularities (which we will classify later, such as $\tilde{E}_6, \tilde{E}_7, \tilde{E}_8$) provide canonical examples of such structure. Some of these can be realized directly as ICIS.*

Example 2.2 (Cusp Singularities)**.** *Cusp singularities arise naturally in the context of Hilbert modular surfaces, constructed by compactifying quotient spaces using orbit space techniques. For instance, the triangle singularities $D_{p,q,r}$ associated to Fuchsian groups can often be realized as ICIS.*

Example 2.3 (Space Curve ICIS)**.** *Consider the map germ $f = (f_1, f_2) : (\mathbb{C}^3, 0) \to (\mathbb{C}^2, 0)$ with*

$$f_1(x, y, z) = x^2 + y^2, \quad f_2(x, y, z) = y^2 + z^3.$$

The zero locus $(X, 0) = V(f_1, f_2) \subset (\mathbb{C}^3, 0)$ is a space curve (dimension 1). To verify it is ICIS, we compute the Jacobian matrix:

$$\operatorname{Jac}(f) = \begin{pmatrix} 2x & 2y & 0 \\ 0 & 2y & 3z^2 \end{pmatrix}.$$

The matrix has rank < 2 precisely when both 2×2 minors vanish: $4xy = 0$, $6xz^2 = 0$, and $4y^2 - 0 = 4y^2$. On $X \setminus \{0\}$, at least one of these is nonzero (since $x^2 = -y^2$ and $y^2 = -z^3$ force $x = y = z = 0$ for simultaneous vanishing). Hence $(X, 0)$ is an ICIS.

2.5 The Lê–Greuel Formula

For an isolated hypersurface singularity $f : (\mathbb{C}^{n+1}, 0) \to (\mathbb{C}, 0)$, the Milnor number $\mu(f) = \dim_{\mathbb{C}} \mathcal{O}_{\mathbb{C}^{n+1},0}/(\dfrac{\partial f}{\partial z_0}, \ldots, \dfrac{\partial f}{\partial z_n})$ is purely algebraic. For an ICIS defined by a map germ $f = (f_1, \ldots, f_k) : (\mathbb{C}^n, 0) \to (\mathbb{C}^k, 0)$, the topological Milnor number $\mu(X, 0)$ (defined as the middle Betti number of the Milnor fiber) is harder to compute directly. The Lê–Greuel formula provides an elegant inductive method.

Theorem 2.1 (Lê–Greuel Formula)**.** *Let $f = (f_1, \ldots, f_k) : (\mathbb{C}^n, 0) \to (\mathbb{C}^k, 0)$ define an ICIS $(X, 0)$ of dimension $d = n - k$. Let $(X', 0)$ be the ICIS defined by $f' = (f_1, \ldots, f_{k-1})$, so*

$\dim X' = d+1$. *Then:*

$$\mu(X,0) + \mu(X',0) = \dim_{\mathbb{C}} \frac{\mathcal{O}_{X',0}}{(\frac{\partial f_k}{\partial z_1}|_{X'}, \ldots, \frac{\partial f_k}{\partial z_n}|_{X'})}$$

where the right-hand side denotes the dimension of the local algebra of the restriction of f_k to X' modulo its Jacobian ideal on X'.

When $k = 1$ (hypersurface case), we recover the classical Milnor number since $X' = \mathbb{C}^n$ is smooth with $\mu(X', 0) = 0$, and the right-hand side reduces to the Jacobian algebra.

Proof Sketch. The formula arises from comparing the Euler characteristics of the Milnor fibers of f and f'. Let F be the Milnor fiber of f and F' the Milnor fiber of f'. The function $f_k|_{X'} : X' \to \mathbb{C}$ has an isolated singularity at the origin (ensured by the ICIS condition). By Milnor's fibration theorem applied to $f_k|_{F'}$, the Euler characteristic satisfies

$$\chi(F') = \chi(F) \cdot \chi(\text{generic fiber of } f_k|_{F'}) - (\text{critical contribution}).$$

A careful topological analysis using the relative Milnor fiber and the Picard-Lefschetz theory of the function f_k restricted to F' yields the stated formula. The right-hand side is exactly the **intersection multiplicity** of the gradient of f_k with the variety X' at the origin. □

Example 2.4 (Computing μ for a Space Curve)**.** *Consider again $f_1 = x^2 + y^2, f_2 = y^2 + z^3$ in $\mathbb{C}^3$. Here $k = 2$, $n = 3$, $d = 1$.*

- *$X' = V(f_1) = \{x^2 + y^2 = 0\}$ is a surface with an A_1 singularity: $\mu(X', 0) = 1$.*
- *The partials of f_2 restricted to X' are $\frac{\partial f_2}{\partial x}|_{X'} = 0$, $\frac{\partial f_2}{\partial y}|_{X'} = 2y$, $\frac{\partial f_2}{\partial z}|_{X'} = 3z^2$.*
- *The right side is $\dim_{\mathbb{C}} \mathcal{O}_{X',0}/(2y, 3z^2) = \dim_{\mathbb{C}} \mathbb{C}\{x, y, z\}/(x^2 + y^2, 2y, 3z^2)$.*
- *Setting $y = 0$: we get $\mathbb{C}\{x, z\}/(x^2, z^2)$ which has basis $\{1, x, z, xz\}$, so dimension $= 4$.*
- *Therefore $\mu(X, 0) = 4 - 1 = 3$.*

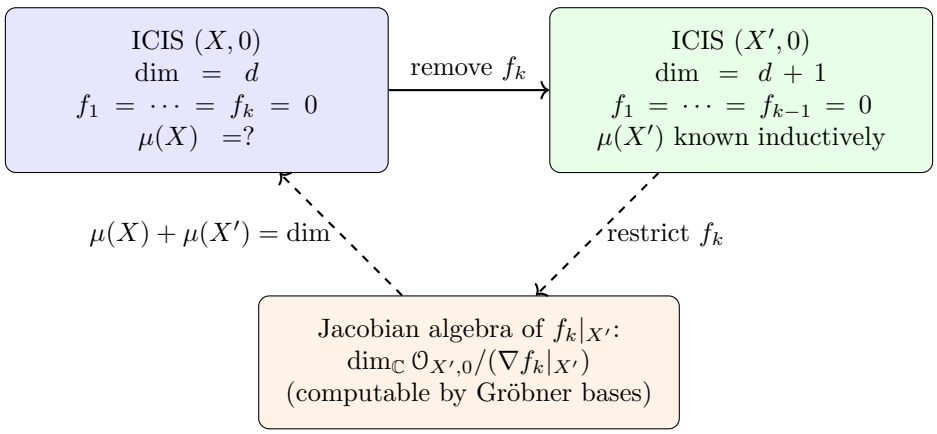

Figure 3: The Lê–Greuel formula inductively reduces the Milnor number computation for an ICIS to the hypersurface case via a chain of intermediate complete intersections.

2.6 The Milnor Fiber of an ICIS

We briefly describe the Milnor fibration in the ICIS setting, following Looijenga and Hamm.

Theorem 2.2 (Hamm, 1971)**.** *Let $f = (f_1, \dots, f_k) : (\mathbb{C}^n, 0) \to (\mathbb{C}^k, 0)$ define an ICIS $(X, 0)$ of dimension $d = n - k \geq 1$. Then for sufficiently small $\epsilon > 0$ and $0 < \delta \ll \epsilon$, the map*

$$f : B_\epsilon \cap f^{-1}(D^k_\delta \setminus \{0\}) \to D^k_\delta \setminus \{0\}$$

*is a smooth fiber bundle (where D^k_δ is a small polydisk in $\mathbb{C}^k$). The fiber $F = f^{-1}(s) \cap B_\epsilon$ for generic s is called the **Milnor fiber of the ICIS**. It satisfies:*

1. *F is a Stein manifold of complex dimension d, hence has the homotopy type of a CW-complex of real dimension $\leq d$.*
2. *F has the homotopy type of a bouquet of d-dimensional spheres: $F \simeq \bigvee^\mu S^d$, where $\mu = \mu(X, 0)$.*
3. *The homology is concentrated in the middle dimension: $\tilde{H}_j(F; \mathbb{Z}) = 0$ for $j \neq d$, and $H_d(F; \mathbb{Z}) \cong \mathbb{Z}^\mu$.*

Proof Sketch. The proof parallels Milnor's argument for hypersurfaces but requires more delicate transversality arguments. First, Hamm establishes the local fibration using the Ehresmann fibration theorem applied to the map f restricted to a suitable Milnor tube $B_\epsilon \cap f^{-1}(\partial D^k_\delta)$. The homotopy type follows from the Lefschetz hyperplane theorem: since F is the Milnor fiber of a function on a Stein space, it is obtained from a point by attaching cells of dimension $\leq d$. To show it is actually a bouquet, one uses the high connectivity of F (analogous to Milnor's argument) combined with the Hurewicz theorem. □

Remark 2.2. *Unlike hypersurface singularities, where the Milnor fiber always has one boundary component, the ICIS Milnor fiber may have a more complicated boundary structure. The boundary ∂F is the link of the ICIS, and its topology can itself be highly nontrivial.*

2.7 Exercises

Exercise 2.1. *Show that the cone over the twisted cubic curve, which is the image of the map $\mathbb{C}^2 \to \mathbb{C}^3$ given by $(s, t) \mapsto (s^3, s^2t, st^2, t^3)$, is NOT a complete intersection at the origin. (Hint: Determine the number of generators of its ideal in $\mathbb{C}[x, y, z, w]$ and its local dimension).*

Exercise 2.2. *Verify that the zero locus of $f_1 = z_1^2 + z_2^2 + z_3^2$ and $f_2 = z_1^2 + 2z_2^2 + 3z_3^2$ in $\mathbb{C}^3$ is an ICIS at the origin of dimension 1.*

Exercise 2.3. *Let $(X, 0)$ be a complete intersection of dimension d defined by $f_1, \dots, f_{n-d} = 0$. Prove using the Jacobian criterion that if the origin is an isolated singularity, then the singular locus of the affine variety defined by the same polynomials is a discrete set.*

3 The Curve Selection Lemma and its Corollaries

To understand the topological structure of a variety near an isolated singularity, a standard technique is to intersect the variety with a small ball centered at the singular point. However, to rigorously show that the local topology is well-behaved (e.g., to prove it is a topological cone), we need to analyze how the variety approaches the singular point. The fundamental tool for this is the Curve Selection Lemma, which allows us to *select* an analytic path approaching the singularity along any given semi-algebraic set.

3.1 Real Semi-algebraic Sets

While we study complex algebraic varieties, regarding them as real varieties in $\mathbb{R}^{2n}$ is often technically advantageous for topological purposes (e.g., when taking the distance function $d(x) = \|x\|^2$).

Definition 3.1 (Semi-algebraic Set)**.** *A subset $X \subset \mathbb{R}^n$ is called **semi-algebraic** if it can be constructed by finite unions, intersections, and complements of sets of the form*

$$\{x \in \mathbb{R}^n \mid f(x) > 0\} \quad \text{and} \quad \{x \in \mathbb{R}^n \mid g(x) = 0\}$$

where $f, g \in \mathbb{R}[x_1, \ldots, x_n]$ are real polynomials.

Semi-algebraic sets form a boolean algebra. A deep theorem due to Tarski and Seidenberg states that the image of a semi-algebraic set under a polynomial mapping (or even projection) is again semi-algebraic. This ensures that most sets defined by geometric conditions (like the set of critical values of a polynomial map restricting to a semi-algebraic set) remain semi-algebraic.

3.2 The Curve Selection Lemma

The Curve Selection Lemma bridges the gap between the purely set-theoretic notion of the closure of a semi-algebraic (or semi-analytic) set and the existence of geometric paths. We present John Milnor's version. Looijenga uses a slightly more general real-analytic formulation, which is the version actually needed in the proofs that follow.

Theorem 3.1 (Curve Selection Lemma (Milnor, 1968; Looijenga))**.** *Let $V \subset \mathbb{R}^n$ be a semi-algebraic set. Suppose that the origin 0 lies in the closure $\overline{V}$, but $0 \notin V$. Then there exists a real analytic path $p : [0, \epsilon) \to \mathbb{R}^n$ such that:*

1. *$p(0) = 0$,*
2. *$p(t) \in V$ for all $t \in (0, \epsilon)$.*

More generally (following Looijenga [Loo84, Ch. 2, §A]), the same conclusion holds when V is a semi-analytic *set, i.e., defined near 0 by conditions of the form $f_\kappa(y) = 0$ ($\kappa = 1, \ldots, k$) and $g_\lambda(y) > 0$ ($\lambda = 1, \ldots, \ell$) with real-analytic functions f_κ, g_λ. This real-analytic version is what underpins the arguments about defining functions, transversality, and good representatives in the sections below.*

By real analytic path, we mean that the components of $p(t)$ can be expanded as convergent power series in t (or a fractional power $t^{1/k}$ depending on the parameterization). This is a highly nontrivial statement: while finding a continuous path is easy in nicely stratified spaces, finding a real analytic one requires the semi-algebraic geometry of the set.

Proof Sketch. The rigorous proof often relies on either **Cylindrical Algebraic Decomposition** or algebraic properties of the real spectrum and **Puiseux series**. The conceptual steps are:

1. **Reduction to a 1-dimensional case**: Since $0 \in \overline{V}$, one can intersect V with small spheres S_r. By considering the minima of suitable generic polynomial functions restricted to $V \cap S_r$ and taking the locus of these minima as $r \to 0$, one can find a 1-dimensional semi-algebraic subset $C \subset V$ such that $0 \in \overline{C}$.

2. **Puiseux parameterization**: A geometric theorem in real algebraic geometry asserts that any 1-dimensional semi-algebraic set near a point consists of a finite number of branches. Algebraically, these branches can be parameterized by real Puiseux series, i.e., $x_i(s) = a_i s^{q_i} + \dots$ where q_i are positive rational numbers.

3. **Analytic reparameterization**: By substituting $s = t^k$, where k is the least common multiple of the denominators of the rational exponents q_i appearing in the series, all fractional powers vanish. The components $x_i(t)$ become convergent power series in integers powers of t, providing the desired real analytic path.

□

3.3 Defining Functions and Regular Levels

The Euclidean distance-squared function is the most convenient choice in practice, but Looijenga emphasizes that the local link and conical structure do not depend on this special choice.

Definition 3.2 (Defining Function for the Singular Point)**.** *Let $(X, 0)$ be an analytic germ with isolated singular point at the origin. A real-analytic function*

$$r : X \to [0, \infty)$$

is said to ***define the point*** 0 ***in*** X *if* $r^{-1}(0) = \{0\}$.

Lemma 3.1 (Critical Values Do Not Accumulate at the Origin)**.** *Let $(X, 0)$ be an analytic germ such that $X \setminus \{0\}$ is smooth of pure dimension, and let $r : X \to [0, \infty)$ be a real-analytic function defining the point 0. Then 0 is not an accumulation point of the critical values of $r|_{X\setminus\{0\}}$.*

Proof sketch. This is the invariant form of the transversality lemma in [Loo84, Ch. 2, §A]. The critical set of $r|_{X\setminus\{0\}}$ is a real-analytic subset of X. If critical values accumulated at 0, then by the Curve Selection Lemma there would exist an analytic arc $\gamma(t)$ in the critical set approaching the origin. But along such an arc one has

$$\frac{d}{dt}(r \circ \gamma) = 0,$$

so $r \circ \gamma$ would be constant, contradicting the fact that $r^{-1}(0) = \{0\}$. □

3.4 Transversality and the Milnor Sphere

A key question when studying the local topology of a complex hypersurface singularity $(X, 0) \subset (\mathbb{C}^{n+1}, 0)$ defined by $f = 0$ is how X intersects small spheres $S_r = \{z \in \mathbb{C}^{n+1} \mid \|z\| = r\}$.

Let $\rho(z) = \|z\|^2 = \sum_{i=0}^{n} |z_i|^2$ be the square distance function. The intersections $X \cap S_r$ behave smoothly only if X is transversal to S_r, which is equivalent to saying that the restriction of ρ to $X \setminus \{0\}$ has no critical points near the origin.

Proposition 3.1. *Let $(X, 0)$ be a germ of an algebraic variety in $\mathbb{C}^{n+1}$. For $r > 0$ sufficiently small, the sphere S_r intersects $X \setminus \{0\}$ transversally.*

Proof Sketch using Curve Selection. Suppose the contrary. Then there is a sequence of points $z_k \to 0$ in $X \setminus \{0\}$ where X is not transversal to the distances spheres. The condition of non-transversality is semi-algebraic (it means the gradient of f and the gradient of ρ are linearly dependent over $\mathbb{C}$). Let V be the semi-algebraic set of all points $z \in X \setminus \{0\}$ where $S_{\|z\|}$ is not

transversal to X. By assumption, $0 \in \overline{V}$. By the Curve Selection Lemma, there is an analytic path $p : [0, \epsilon) \to \mathbb{C}^{n+1}$ with $p(0) = 0$ and $p(t) \in V$. We can expand $p(t) = at^k + bt^{k+1} + \dots$ with $a \neq 0$. Taking the derivative of the norm along the path, $\frac{d}{dt}\|p(t)\|^2 = \frac{d}{dt}(|a|^2 t^{2k} + \dots) = 2k|a|^2 t^{2k-1} + \dots > 0$ for small $t > 0$. However, since $p(t)$ consists of critical points of the distance function on X, the tangent vector $p'(t) \in T_{p(t)}X$ should be annihilated by the differential of the distance function, which forces $\frac{d}{dt}\|p(t)\|^2 = 0$. This gives a contradiction. □

This fundamental result allows us to define the **Link** of the singularity:

$$K = X \cap S_\epsilon \subset S_\epsilon$$

for any sufficiently small $\epsilon > 0$. The topological type of the link K is independent of ϵ, providing a robust topological invariant.

3.5 Local Cone Structure

The existence of a smooth intersection with small spheres directly implies one of the most foundational theorems in singularity theory.

Theorem 3.2 (Local Cone Structure)**.** *Let $(X, 0) \subset (\mathbb{C}^{n+1}, 0)$ be a complex analytic singularity, and let B_ϵ be the closed ball of radius ϵ. For sufficiently small $\epsilon > 0$, the pair $(B_\epsilon, X \cap B_\epsilon)$ is homeomorphic to the cone over the boundary pair (S_ϵ, K), i.e.,*

$$(B_\epsilon, X \cap B_\epsilon) \cong Cone(S_\epsilon, X \cap S_\epsilon).$$

Proof. Choose ϵ small enough so that the punctured disk $D_\epsilon \setminus \{0\}$ contains no singular points of X and no critical points of the distance-squared function $r(\mathbf{z}) = \|\mathbf{z}\|^2$ restricted to $X \setminus \mathrm{Sing}(X)$.

Step 1: Constructing a radial vector field. We construct a smooth vector field $\mathbf{v}(\mathbf{z})$ on $D_\epsilon \setminus \{0\}$ with two properties: (i) the inner product $\langle \mathbf{v}(\mathbf{z}), \mathbf{z} \rangle > 0$ for all $\mathbf{z}$ (i.e., $\mathbf{v}$ points away from the origin), and (ii) $\mathbf{v}(\mathbf{z})$ is tangent to X whenever $\mathbf{z} \in X \setminus \mathrm{Sing}(X)$.

At any point $\mathbf{z}^\alpha$ not on X, we simply set $\mathbf{v}^\alpha(\mathbf{z}) = \mathbf{z}$. At a point $\mathbf{z}^\alpha \in X \setminus \{0\}$, since $\mathbf{z}^\alpha$ is not a critical point of $r|_X$, at least one tangential derivative $\partial r / \partial u_h \neq 0$ (where u_h is a local coordinate along X). We set $\mathbf{v}^\alpha$ equal to $\pm \partial \mathbf{z} / \partial u_h$, choosing the sign so that $\langle \mathbf{v}^\alpha, \mathbf{z} \rangle > 0$. The global field $\mathbf{v} = \sum \lambda^\alpha \mathbf{v}^\alpha$ is obtained via a smooth partition of unity.

Step 2: Normalizing and integrating. Normalize the vector field by setting $\mathbf{w}(\mathbf{z}) = \mathbf{v}(\mathbf{z}) / \langle 2\mathbf{z}, \mathbf{v}(\mathbf{z}) \rangle$, so that the trajectories $\mathbf{p}(t)$ of $d\mathbf{p}/dt = \mathbf{w}(\mathbf{p}(t))$ satisfy $\|\mathbf{p}(t)\|^2 = t + \text{const}$. After reparametrizing so that $r(\mathbf{p}(t)) = t$, each trajectory can be extended to the full interval $(0, \epsilon^2]$ by a compactness argument using local existence and uniqueness of ODE solutions.

Step 3: Building the homeomorphism. For each $\mathbf{a} \in S_\epsilon$, let $\mathbf{p}(t) = P(\mathbf{a}, t)$ be the unique trajectory with $P(\mathbf{a}, \epsilon^2) = \mathbf{a}$. Then P maps $S_\epsilon \times (0, \epsilon^2]$ diffeomorphically onto $D_\epsilon \setminus \{0\}$. Since $\mathbf{v}$ is tangent to X, the map P also carries $K \times (0, \epsilon^2]$ diffeomorphically onto $(X \cap D_\epsilon) \setminus \{0\}$. Since $P(\mathbf{a}, t) \to 0$ uniformly as $t \to 0$, the assignment $t\mathbf{a} + (1 - t) \cdot 0 \mapsto P(\mathbf{a}, t\epsilon^2)$ extends to a homeomorphism $\mathrm{Cone}(S_\epsilon) \xrightarrow{\cong} D_\epsilon$ that carries $\mathrm{Cone}(K)$ onto $X \cap D_\epsilon$. □

Proposition 3.2 (Invariant Form of the Link)**.** *Let $(X, 0)$ be an analytic germ with isolated singular point, and let $r : X \to [0, \infty)$ be a real-analytic function defining 0. If $\epsilon > 0$ is chosen so that $X_{r \leq \epsilon}$ is compact and $r|_{X \setminus \{0\}}$ has no critical value in $(0, \epsilon]$, then:*

1. *$X_{r=\epsilon}$ is a compact smooth manifold, called a **link** of the germ;*
2. *$X_{r \leq \epsilon}$ is homeomorphic to* $\mathrm{Cone}(X_{r=\epsilon})$*;*

3. *the diffeomorphism type of $X_{r=\epsilon}$ depends only on the analytic germ $(X, 0)$, not on the particular defining function r or the chosen regular value ϵ.*

Proof sketch. The first two assertions follow from the same vector-field argument used in the proof of the local cone theorem, replacing the Euclidean norm by the general defining function r. For the invariance statement, one compares two defining functions r and r' and studies the region where both are small. Looijenga shows that there is a vector field tangent to X for which both r and r' decrease, and integrating this vector field produces a diffeomorphism between the corresponding level manifolds; see [Loo84, Ch. 2, §A]. □

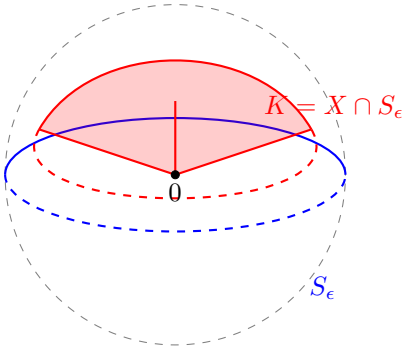

Figure 4: Local cone structure: The variety $X \cap B_\epsilon$ is topologically the geometric cone over the link K.

In particular, the singularity $X \cap B_\epsilon$ is topologically just the cone over its link K. Since the cone over any space is contractible, the local topological space of a singularity is always contractible! (The interesting topology lies in the embedding of $K \subset S_\epsilon$).

3.6 The Regular Point Case

To motivate the study of singularities, it is important to understand what happens at a *regular* point, where the topology is completely trivial. The following two results, due to Milnor, show that at a non-singular point, neither the link nor the Milnor fiber carry any interesting topology.

Lemma 3.2 (Unknotted Sphere at a Regular Point)**.** *If $\mathbf{z}^0$ is a non-singular point of a complex variety $V \subset \mathbb{C}^m$, then the intersection $K = V \cap S_\epsilon$ is an **unknotted** sphere in S_ϵ, for all sufficiently small ϵ.*

Proof. The smooth function $r(\mathbf{z}) = \|\mathbf{z} - \mathbf{z}^0\|^2$ restricted to the smooth manifold $V \setminus \mathrm{Sing}(V)$ has a non-degenerate critical point at $\mathbf{z}^0$. By the Morse Lemma, there exist local coordinates $u_1, \ldots, u_k$ for V near $\mathbf{z}^0$ such that $r(\mathbf{z}) = u_1^2 + \cdots + u_k^2$, so $K = V \cap S_\epsilon$ is diffeomorphic to a standard sphere S^{k-1}. Moreover, by a sharpened form of the Morse Lemma applied to the pair of manifolds $V \subset \mathbb{C}^m$, one can find local coordinates $u_1, \ldots, u_{2m}$ for $\mathbb{C}^m$ near $\mathbf{z}^0$ such that $r = u_1^2 + \cdots + u_{2m}^2$ and V corresponds to the locus $u_{k+1} = \cdots = u_{2m} = 0$. Thus the pair (S_ϵ, K) is diffeomorphic to a sphere with a great sub-sphere, which is unknotted. □

Lemma 3.3 (Fiber at a Regular Point)**.** *If $\mathbf{z}^0$ is a non-singular point of the complex hypersurface $V = f^{-1}(0) \subset \mathbb{C}^{n+1}$, then the fiber $F_0 = \{\mathbf{z} \in S_\epsilon \mid f(\mathbf{z})/|f(\mathbf{z})| = 1\}$ is diffeomorphic to an open $2n$-disk. In particular, F_0 is contractible.*

Proof Sketch. Since $\mathbf{z}^0$ is a regular point, the gradient $\operatorname{grad} f(\mathbf{z}^0) \neq 0$. By the implicit function theorem, V is a smooth complex manifold near $\mathbf{z}^0$, and the level sets $f^{-1}(c)$ foliate a neighborhood of $\mathbf{z}^0$. The intersection of the half-line $\{f > 0\}$ with S_ϵ yields a fiber diffeomorphic to a real $2n$-dimensional ball. □

These two results serve as a baseline: at regular points, K is an unknotted sphere and the Milnor fiber is contractible. All of the rich topology we will encounter (knotting of K, nontrivial homology of F, monodromy) is a direct consequence of the singularity.

3.7 A Key Example: The Cusp Singularity

Let us apply these geometric consequences to a plane curve. Consider the cusp $(X, 0) \subset (\mathbb{C}^2, 0)$ defined by $f(x, y) = x^3 - y^2 = 0$.

1. Real Link computation: To visualize, let's look at the real points of the cusp in $\mathbb{R}^2$. It is transversal to real circles $x^2 + y^2 = r^2$ for any $r > 0$. If we set $x^3 = y^2$, traversing the curve outwards from $(0, 0)$, the distance monotonically increases. Thus the intersection with a small circle S^1 is just two points. The local cone over two points is an arc, confirming the real cusp is a topological 1-manifold.

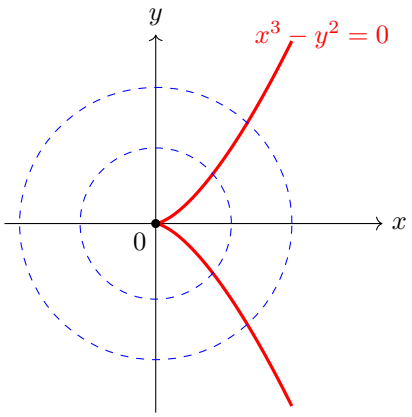

Figure 5: The real cusp singularity intersecting distance circles transversally.

2. Complex Link computation: Now consider $X \subset \mathbb{C}^2$. The link $K = X \cap S^3_\epsilon$. We can parameterize X globally by $t \mapsto (t^2, t^3)$. Then the sphere intersection condition is $|x|^2 + |y|^2 = |t|^4 + |t|^6 = \epsilon^2$. For any $\epsilon > 0$, the equation $r^4 + r^6 = \epsilon^2$ has exactly one positive real root r_0. Thus t must satisfy $|t| = r_0$. The set of such $t \in \mathbb{C}$ is a circle $S^1 \subset \mathbb{C}$. The map $t \mapsto (t^2, t^3)$ maps this circle to K. This mapping is clearly injective since $(t^2)^3 = (t^3)^2$, but $t^3/t^2 = t$ recovers the phase uniquely. Thus, the link K of a cusp is homeomorphic to S^1, a knotted circle in S^3. Since x wraps twice around the origin while y wraps three times, K is precisely the **Trefoil Knot** $(2, 3)$-torus knot in S^3_ϵ.

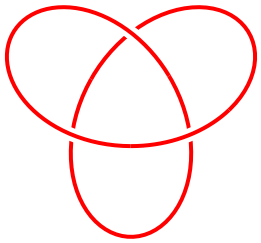

(Standard projection of the trefoil knot from S^3 to $\mathbb{R}^2$)

Figure 6: The complex link of the cusp $x^3 - y^2 = 0$ is the trefoil knot.

The topological cone over S^1 is a 2-disk. Thus, X is homeomorphic (though not diffeomorphic) to a plane!

3.8 Exercises

Exercise 3.1. *Consider the node singularity $f(x, y) = x^2 - y^2 + x^3 = 0$. Find a parametrization of the two branches passing through the origin. Compute the link $K = X \cap S^3_\epsilon$. Show that K consists of two unlinked circles in S^3 (the Hopf link).*

Exercise 3.2. *Explain why the set $V = \{(x, y) \in \mathbb{R}^2 \mid y > 0, y = e^{-1/x} \text{ for } x > 0\}$ is not a semi-algebraic set. Show that although 0 is in the closure $\overline{V}$, no analytic curve can approach 0 entirely within V.*

Exercise 3.3. *Let $X \subset \mathbb{C}^3$ be the cone singularity given by $x^2 + y^2 + z^2 = 0$. By intersecting this variety with the real unit sphere in $\mathbb{C}^3 \cong \mathbb{R}^6$, determine the topological type of the link K. (Hint: K has the structure of the unit tangent bundle of S^2, which is isomorphic to $\mathbb{R}P^3$).*

Exercise 3.4. *Compute the local distance function squared $\rho(x, y) = |x|^2 + |y|^2$ restricted to the plane curve given by $x = t^p, y = t^q$ $(p < q)$. Show that ρ is strictly increasing as t moves away from 0, verifying transversality explicitly.*

4 Good Representatives of Analytic Germs

When analyzing local properties of analytic germs $f : (\mathbb{C}^{n+1}, x) \to (\mathbb{C}, 0)$, statements strictly hold only on "sufficiently small" neighborhoods. However, to rigorously study geometric objects such as Milnor fibrations, monodromy, and global deformations, we need actual spaces and actual maps which are well-behaved up to their boundaries. This necessitates the introduction of a distinguished class of representatives whose members are mutually topologically equivalent: the **good representatives**.

4.1 Definition of a Good Representative

By the Curve Selection Lemma, for any isolated singularity f, there exists $\epsilon_0 > 0$ such that for all $0 < \epsilon \leq \epsilon_0$, the sphere S_ϵ intersects the zero fiber $f^{-1}(0)$ transversally.

Definition 4.1 (Good Representative)**.** *Let $f_x : (X, x) \to (S, s)$ be a germ of an analytic map. A **good representative** of f_x is a proper analytic map $f : X \to S$ between suitable neighborhoods of x and s, usually constructed as follows: Choose a Milnor ball $B \subset \mathbb{C}^{n+1}$ of radius $\epsilon \leq \epsilon_0$*

and a sufficiently small disk $\Delta \subset \mathbb{C}$ of radius $\delta \ll \epsilon$. Let $X = B \cap f^{-1}(\Delta)$ and $S = \Delta$. Then $f : X \to S$ is a good representative if:

1. *f is a proper map.*
2. *The critical locus of f intersects the boundary ∂X trivially; i.e., f restricts to a topological submersion on $X \setminus \mathrm{Sing}(X)$ and locally around ∂X.*
3. *Within this specific representative, the boundary ∂X consists of elements mapping transversally to S, meaning that the restriction $f|_{\partial X} : \partial X \to S$ is a smooth fiber bundle.*

The fundamental advantage of a good representative is that any two good representatives of the same analytic germ are (stratum-preserving) homeomorphic over the base. Thus, properties defined using a good representative intrinsically belong to the germ itself.

Definition 4.2 (Critical Locus and Discriminant of a Good Representative)**.** *Let $f : X \to S$ be a good representative. Its **critical locus** $C_f \subset X$ is the set of points where either X is singular or f fails to be a submersion. The image*

$$D_f = f(C_f) \subset S$$

*is called the **discriminant** of f.*

4.2 Construction of Good Representatives

The existence of good representatives is subtle and requires careful control of the interplay between the Milnor ball and the critical locus. The key construction, following Looijenga (Ch. 2), proceeds as follows.

Proposition 4.1 (Existence of Good Representatives)**.** *Let $f : (\mathbb{C}^{n+1}, 0) \to (\mathbb{C}, 0)$ be a holomorphic germ with an isolated singularity at the origin. Then there exist $\epsilon_0 > 0$ and a continuous function $\delta : (0, \epsilon_0] \to \mathbb{R}_{>0}$ with $\delta(\epsilon) \ll \epsilon$ such that for every $0 < \epsilon \leq \epsilon_0$ and $0 < \eta \leq \delta(\epsilon)$, the map*

$$f : B_\epsilon \cap f^{-1}(D_\eta) \to D_\eta$$

is a good representative of the germ f.

Proof Sketch. **Step 1 (Transversality of the sphere):** By the Curve Selection Lemma applied to the semi-algebraic set $\{z \in X \setminus \{0\} : \mathrm{grad}\, f(z) = \lambda z \text{ for some } \lambda \in \mathbb{C}\}$, there exists ϵ_0 such that S_ϵ is transverse to $f^{-1}(0)$ for all $0 < \epsilon \leq \epsilon_0$.

Step 2 (Properness): Since $f^{-1}(D_\eta) \cap B_\epsilon$ is a closed subset of the compact set $\overline{B}_\epsilon$, the restriction of f is proper.

Step 3 (No critical points on the boundary): The critical values of $f|_{S_\epsilon}$ form a finite set (by analyticity). Choosing η smaller than the minimum modulus of these critical values ensures no critical points of $f|_{X \cap S_\epsilon}$ lie above D_η. This makes $f|_{\partial X} : \partial X \to D_\eta$ a submersion.

Step 4 (Fiber bundle structure on boundary): Applying the Ehresmann fibration theorem (which we will state precisely in the next section) to the proper submersion $f|_{\partial X} \to D_\eta$ yields the desired fiber bundle structure on the boundary. □

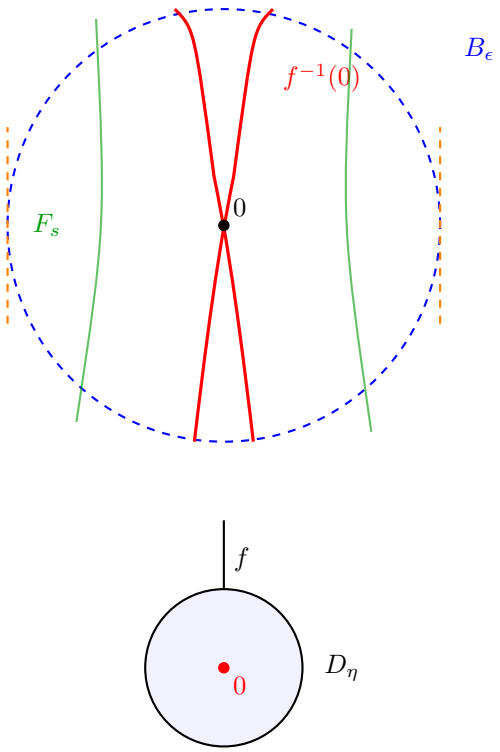

Figure 7: A good representative: the map $f : B_\epsilon \cap f^{-1}(D_\eta) \to D_\eta$ is proper, the critical locus (the origin) stays in the interior, and the boundary fibers are smooth.

4.3 Basic Properties of Good Representatives

Theorem 4.1 (Structure Theorem for Good Representatives)**.** *Let $f : \overline{X} \to S$ be a good proper representative of a germ defining an isolated complete intersection singularity of dimension n, where S is a sufficiently small contractible neighborhood in $\mathbb{C}^k$. Then:*

1. *$f|_{\partial\overline{X}} : \partial\overline{X} \to S$ is a smooth trivial fiber bundle.*
2. *The critical locus C_f is an analytic subset of X which is closed in $\overline{X}$, and the restriction $f|_{C_f} : C_f \to S$ is finite.*
3. *The singular locus X_{sing} has dimension at most k, and $C_f - X_{\text{sing}}$ is of pure dimension $k-1$ (so the discriminant $D_f = f(C_f)$ is an analytic subset of S, which is a hypersurface in S if non-empty).*
4. *Over the complement of the discriminant, the map*
$$f : (\overline{X}_{S\setminus D_f}, \partial\overline{X}_{S\setminus D_f}) \to S \setminus D_f$$
is a smooth fiber bundle pair.
5. *Each fiber over $S \setminus D_f$ is a smooth complex n-manifold with boundary.*
6. *At every point $y \in X_{\text{reg}}$ (where X is smooth and f is a submersion), f defines an isolated complete intersection singularity; in particular, any smooth fiber X_s ($s \notin D_f$) is itself nonsingular.*

Proof sketch. These are the basic consequences of Looijenga's theorem on good representatives [Loo84, Ch. 2, §B]. Properness is built into the construction, and the boundary map is a proper submersion, so Ehresmann's theorem gives the smooth fiber-bundle statement on $\partial\overline{X}$. The critical locus is analytic because it is defined by the rank-drop conditions on the Jacobian matrix together with the singular locus of X. Since the critical locus stays away from the boundary, its image is proper over the base, hence finite. The analyticity of D_f then follows from the finite mapping theorem. Finally, after removing D_f, the map becomes a proper submersion between manifolds with boundary, so Ehresmann again yields a smooth locally trivial fibration. □

Proposition 4.2 (Uniqueness of Good Proper Representatives)**.** *Any two good proper representatives of the same analytic germ become fiberwise diffeomorphic after shrinking the base. In particular, the Milnor fiber and the geometric monodromy are well-defined up to diffeomorphism and isotopy.*

Idea of proof. One takes a third good representative contained in the intersection of the first two and applies Ehresmann's theorem to the collar regions between them. Looijenga's argument produces a diffeomorphism which is the identity near the critical locus and commutes with the projection to a smaller base neighborhood; see [Loo84, Ch. 2, §B]. □

4.4 Excellent Representatives in Parameter Spaces

For a single Milnor fiber, a good representative is already enough. But Looijenga emphasizes in [Loo84, Ch. 2, §D] that the full local topology of a map-germ involves all nearby fibers and the way they fit together over the base. In particular, two good representatives need not be topologically equivalent as maps, even though their individual Milnor fibers are diffeomorphic. This motivates a stricter notion: **excellent representatives**.

Definition 4.3 (Excellent Proper Representative)**.** *Let $f_x : (X, x) \to (S, 0)$ be an analytic map-germ with isolated singularity, and let $f : \overline{X} \to S$ be a good proper representative with critical locus C_f and discriminant D_f. Following Looijenga, an **excellent proper representative** is obtained by shrinking f to a sublevel set*

$$f : \overline{X}_{u<\eta} \to S_{u<\eta}$$

for a real-analytic defining function $u : S \to [0, \infty)$ of the origin, in such a way that:

1. *the total space $\overline{X}$ and the base S carry compatible Whitney stratifications refining the natural strata $S \setminus D_f$, D_f, $X_{S\setminus D_f}$, and the pieces of C_f over the strata of D_f;*
2. *the function u has no critical values on any stratum for $0 < u \leq \eta$;*
3. *the restriction over $S_{u<\eta}$ admits the stratified conical structure described by Looijenga, so that the whole map, not merely one fiber, is topologically controlled by the boundary data.*

The point is that excellence is a property of the *map* near the singular point, not just of one convenient Milnor tube. In particular, once an excellent representative is chosen, the whole family over a small neighborhood of the origin acquires a canonical conical model.

Theorem 4.2 (Excellent Representatives and Conical Structure)**.** *After shrinking the source and target, every analytic map-germ with isolated singularity admits excellent proper representatives. For such a representative:*

1. *the total space over a sufficiently small sublevel set of u is topologically a cone over the boundary fibration;*

2. *any two excellent proper representatives of the same germ are topologically equivalent as map-germs;*

3. *consequently, constructions that involve the full nearby fibration, such as geometric monodromy, depend only on the germ.*

Proof sketch. This is the content of Looijenga's discussion in [Loo84, Ch. 2, §D]. The first step is stratificational: starting from a good proper representative, one chooses Whitney stratifications on D_f and on $\overline{X}$ compatible with the critical locus and with the smooth part over $S \setminus D_f$. Next one picks a real-analytic defining function u on the base with no small positive critical values on any stratum. Thom–Mather theory then produces an integrable vector field v' on the base, tangent to the strata and moving points monotonically toward the origin.

The second step is to lift v' to a stratified vector field v on the total space. Away from the critical locus one first constructs a smooth retraction to the central fiber minus the singular point, and then chooses the lift so that it preserves this retraction near the central fiber while remaining tangent to all strata. Integrating v' and v gives the homeomorphisms that identify the base and the total space with mapping cones. This is the source of the conical structure.

Finally, the same collar-trivialization argument used for uniqueness of good representatives can be repeated in the stratified setting. Because the conical models on two excellent representatives can be matched on the boundary and near the central fiber, one obtains a topological equivalence of the maps themselves, not only of the individual fibers. □

This is essential for:

- **Well-defined relative monodromy:** When comparing the Milnor fibers of f_0 and f_t, the boundary trivialization provides a canonical identification of the boundary topology throughout the deformation.
- **Adjacency computations:** The discriminant locus $\Delta \subset S$ can be studied intrinsically as the set of singular values of F_t, without boundary artifacts contaminating the picture.
- **Gluing constructions:** When building the period mapping (§16), the boundary triviality permits coherent integration of differential forms across fibers.

4.5 The ICIS Case: Multiple Good Representatives

For an ICIS defined by $f = (f_1, \ldots, f_k) : (\mathbb{C}^n, 0) \to (\mathbb{C}^k, 0)$, the construction of a good representative requires additional care. Instead of a single ball-disk pair (B_ϵ, D_η), one uses a *Milnor tube*: the preimage of a sufficiently small polydisk $D^k_\delta \subset \mathbb{C}^k$ intersected with B_ϵ.

Because the Milnor fiber $F = f^{-1}(s) \cap B_\epsilon$ for generic s is a Stein manifold (it inherits the Stein structure from $\mathbb{C}^n$), it has the homotopy type of a CW complex of real dimension at most $d = n - k$. The homotopy type is independent of the choice of good representative, which justifies defining topological invariants (such as the Milnor number, monodromy, and intersection form) via any particular good representative.

Remark 4.1. *The existence of good representatives underpins virtually every major theorem in these notes. Without this foundational tool, statements about "the Milnor fiber" or "the monodromy of a singularity" would be poorly defined, as they could potentially depend on the specific neighborhood chosen.*

4.6 Exercises

Exercise 4.1. *Prove that for the simple fold singularity $f(x, y) = x^2 + y^2$, picking any $\epsilon > 0$ and subsequently any $0 < \delta < \epsilon^2$ yields a valid good representative. What fails if $\delta > \epsilon^2$?*

Exercise 4.2. *Let $f(x, y) = x^3 + y^2$ (the cusp). The critical values of $f|_{S_\epsilon}$ are non-zero for small ϵ. Estimate the minimum modulus of these critical values in terms of ϵ, and hence show that choosing $\delta = \epsilon^3$ works for a good representative when ϵ is small.*

Exercise 4.3. *Explain why the condition $\delta \ll \epsilon$ in the construction of good representatives is essential by constructing a counter-example: Find a map f and values ϵ, δ with $\delta \sim \epsilon$ such that $f|_{\partial X}$ has a critical point over D_δ.*

5 Milnor Fibration and Links of Singularities

In the previous chapter, we saw that the local topology of an isolated hypersurface singularity $(X, 0) \subset (\mathbb{C}^{n+1}, 0)$ defined by $f = 0$ is completely captured by its link $K = X \cap S_\epsilon \subset S_\epsilon^{2n+1}$. But looking solely at K forgets the ambient space and the deformation class of the singularity. John Milnor discovered that the map f itself carries incredibly rich topological information near the singularity via what is now classically called the **Milnor Fibration**.

5.1 Ehresmann's Fibration Theorem

Before proving the Milnor fibration theorem, we state a fundamental tool from differential topology that converts analytic properties (properness and submersivity) into topological structure (local triviality).

Theorem 5.1 (Ehresmann's Fibration Theorem, 1950)**.** *Let $f : M \to N$ be a smooth map between smooth manifolds. If f is:*

1. *a **proper** map (preimages of compact sets are compact), and*
2. *a **submersion** ($df_x : T_xM \to T_{f(x)}N$ is surjective at every point $x \in M$),*

then f is a locally trivial smooth fiber bundle. That is, for every point $y_0 \in N$, there exist a neighborhood $U \ni y_0$ and a diffeomorphism $\Psi : f^{-1}(U) \xrightarrow{\cong} U \times f^{-1}(y_0)$ such that the diagram

$$\begin{array}{ccc} f^{-1}(U) & \xrightarrow[\cong]{\Psi} & U \times f^{-1}(y_0) \\ & {\scriptstyle f} \searrow \quad \swarrow {\scriptstyle \mathrm{pr}_1} & \\ & U & \end{array}$$

commutes.

Proof Sketch. The proof constructs a horizontal distribution that trivializes the fibers.

Step 1 (Horizontal lifts): Since f is a submersion, for each $x \in M$, we can decompose $T_xM = \ker(df_x) \oplus H_x$ where H_x is a complementary subspace (a horizontal distribution). For any smooth vector field v on N, define the **horizontal lift** $\tilde{v}$ as the unique vector field on M satisfying $\tilde{v}(x) \in H_x$ and $df_x(\tilde{v}(x)) = v(f(x))$.

Step 2 (Integration): Since f is proper, the lifted flow of $\tilde{v}$ is complete (trajectories exist for all time), by the escape lemma. A vector field v on a small ball $U \subset N$ centered at y_0 generates

flows that connect any $y \in U$ to y_0 along a straight ray. Lifting this flow gives a diffeomorphism $\phi_y : f^{-1}(y_0) \to f^{-1}(y)$ for each $y \in U$.

Step 3 (Trivialization): Define $\Psi : f^{-1}(U) \to U \times f^{-1}(y_0)$ by $\Psi(x) = (f(x), \phi^{-1}_{f(x)}(x))$. The smoothness of Ψ follows from the smooth dependence of ODE solutions on initial conditions. The commutative diagram property holds by construction. □

Remark 5.1. *Ehresmann's theorem is the engine behind every fibration result in singularity theory: the Milnor fibration (this section), the existence of good representatives (previous section), the triviality of the boundary in deformations, and the local triviality of the cohomology bundle underlying the Gauss-Manin connection. Without properness, the conclusion can fail: the punctured complex line $\mathbb{C}^* \xrightarrow{z \mapsto z} \mathbb{C}^*$ is a trivial bundle, but the non-proper inclusion $\mathbb{C}^* \hookrightarrow \mathbb{C}$ does not extend trivially.*

5.2 The Milnor Fibration Theorem

Let $f : (\mathbb{C}^{n+1}, 0) \to (\mathbb{C}, 0)$ be a holomorphic germ with an isolated singularity at the origin. Recall that the link corresponds to $f = 0$ intersecting S_ϵ. What about the values of f in a small punctured neighborhood of 0?

Remark 5.2. *Unless explicitly stated otherwise, the hypersurface results in this and the next three sections are statements about* isolated *hypersurface singularities. The existence of the Milnor fibration, the bouquet theorem, the finiteness of μ, and the classical Picard–Lefschetz formula all use the isolated-critical-point hypothesis in an essential way.*

Theorem 5.2 (Milnor Fibration Theorem, 1968)**.** *Let f have an isolated critical point at 0. For $\epsilon > 0$ sufficiently small, the map*

$$\Phi = \frac{f}{|f|} : S_\epsilon \setminus K \to S^1 \subset \mathbb{C}$$

is a smooth, locally trivial fiber bundle.

Proof (Milnor, Chapters 4–5). The proof proceeds in three stages.

Stage 1: The key non-degeneracy condition. We claim that for ϵ sufficiently small, every point $z \in S_\epsilon \setminus K$ satisfies the **Milnor condition**:

$$z \text{ and } \overline{\operatorname{grad} f}(z) \text{ are linearly independent over } \mathbb{R}, \tag{1}$$

where $\overline{\operatorname{grad} f}(z) = (\overline{\frac{\partial f}{\partial z_0}}, \ldots, \overline{\frac{\partial f}{\partial z_n}})$ is the conjugate gradient vector.

Suppose not. Then there exist sequences $z_k \to 0$ with $z_k \notin V = f^{-1}(0)$ and $\overline{\operatorname{grad} f}(z_k) = \lambda_k z_k$ for some $\lambda_k \in \mathbb{C}$. The set $W = \{z \in \mathbb{C}^{n+1} \setminus V : \overline{\operatorname{grad} f}(z) = \lambda z, \text{ some } \lambda \in \mathbb{C}\}$ is semi-algebraic (after identifying $\mathbb{C}^{n+1}$ with $\mathbb{R}^{2n+2}$). By the Curve Selection Lemma, there exists a real analytic path $p : [0, \delta) \to \mathbb{C}^{n+1}$ with $p(0) = 0$ and $p(t) \in W$ for $t > 0$. Along such a path, write $p(t) = at^m + \ldots$ and compute:

$$\frac{d}{dt} f(p(t)) = \langle p'(t), \overline{\operatorname{grad} f}(p(t)) \rangle = \lambda(t) \langle p'(t), p(t) \rangle = \frac{\lambda(t)}{2} \frac{d}{dt} \|p(t)\|^2.$$

Since $p(t) \notin V$, $f(p(t)) \neq 0$, but one can show using a careful leading-term analysis that the argument $\arg(f(p(t)))$ is asymptotically constant. This forces $\frac{d}{dt} \arg(f(p(t))) = 0$, contradicting the fact that $\frac{d}{dt} \|p(t)\|^2 > 0$ and the oscillation properties of the gradient.

Stage 2: Construction of the gradient-like vector field. Define the normalized vector field on $S_\epsilon \setminus K$ as follows. At each point z, let $v(z) = iz - \mathrm{Re}\langle iz, w(z)\rangle \cdot w(z)$, where $w(z) = \overline{\mathrm{grad}} f(z)/\|\overline{\mathrm{grad}} f(z)\|$. Then $v(z)$ is tangent to S_ϵ (since $\mathrm{Re}\langle v(z), z\rangle = 0$) and satisfies

$$\mathrm{Re}\left\langle v(z), \frac{\overline{\mathrm{grad}} f(z)}{f(z)} \right\rangle > 0,$$

which means v rotates the argument of f in the positive direction. The existence of such v at every point of $S_\epsilon \setminus K$ follows from condition (1).

Stage 3: Integration and local triviality. Normalizing v so that $\frac{d}{dt}\arg(f(\phi_t(z))) = 1$ (where ϕ_t is the flow of v), each trajectory rotates the argument of f at unit speed. The flow is complete because S_ϵ is compact. For any angle θ_0, the map

$$\Psi_\theta : \Phi^{-1}(e^{i\theta_0}) \to \Phi^{-1}(e^{i(\theta_0+\theta)}), \quad z \mapsto \phi_\theta(z)$$

is a diffeomorphism. This yields the local (in fact, global) trivialization of Φ as a fiber bundle. □

There is an equivalent formulation using a small ball instead of the sphere, which is technically more convenient for many applications.

Theorem 5.3 (Interior Milnor Fibration)**.** *For the same holomorphic germ $f : (\mathbb{C}^{n+1}, 0) \to (\mathbb{C}, 0)$ with isolated critical point at the origin, and for $0 < \delta \ll \epsilon$ sufficiently small, the map*

$$f : B_\epsilon \cap f^{-1}(\partial D_\delta) \to \partial D_\delta \cong S^1$$

is a smooth, locally trivial fiber bundle, with fiber diffeomorphic to the Milnor fiber $F = f^{-1}(\delta) \cap B_\epsilon$.

Proof. By the construction of good representatives (Section 4), for suitable ϵ, δ, the map $f : B_\epsilon \cap f^{-1}(D_\delta) \to D_\delta$ has no critical points in the preimage of ∂D_δ. Since f restricted to $B_\epsilon \cap f^{-1}(\partial D_\delta)$ is a proper submersion (properness follows from compactness of $\overline{B}_\epsilon$; submersivity follows from the absence of critical points), Ehresmann's fibration theorem directly yields the fiber bundle structure. □

A standard deformation-retraction argument shows that the two definitions of the Milnor fiber (the sphere version $\Phi^{-1}(e^{i\theta}) \subset S_\epsilon$ and the interior version $f^{-1}(\delta) \cap B_\epsilon$) produce diffeomorphic fibers.

The fiber of this bundle is called the **Milnor Fiber**, denoted by F. Since the base space is S^1, the bundle is completely determined by two pieces of data:

1. The topological and differentiable structure of the fiber F.
2. The monodromy homeomorphism $h : F \to F$, induced by traveling once around the base space S^1.

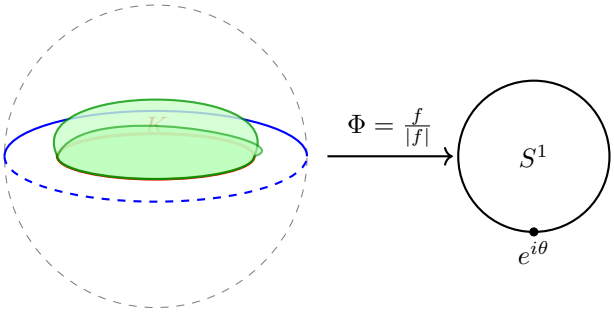

Figure 8: The Milnor Fibration realizes the sphere S_ϵ as an open book decomposition whose binding is the link K, and pages are the Milnor fibers F.

This tells us that S_ϵ^{2n+1} has a specific structure called an **open book decomposition** with binding K. The pages of this open book are the sheets of the Milnor fibers!

The following lemma makes the open book structure precise, showing that each page has K as its smooth boundary.

Lemma 5.1 (Fiber Closure as Manifold with Boundary)**.** *For the Milnor fibration of an isolated hypersurface singularity, and for ϵ sufficiently small, the closure $\overline{F}_\theta$ of each fiber $F_\theta = \Phi^{-1}(e^{i\theta})$ in S_ϵ is a smooth $2n$-dimensional manifold with boundary. The interior of $\overline{F}_\theta$ is F_θ itself, and the boundary is precisely the link K.*

Proof. It suffices to show that $f|_{S_\epsilon}$ has no critical points on K (i.e., 0 is a regular value of $f|_{S_\epsilon}$). Suppose for contradiction that critical points $\mathbf{z}_k \in K$ with $\operatorname{grad} f(\mathbf{z}_k) = \lambda_k \mathbf{z}_k$ (for some $\lambda_k \in \mathbb{C}$) accumulate at the origin. By the Curve Selection Lemma, there is an analytic path $\mathbf{p}(t) \to 0$ with $f(\mathbf{p}(t)) \equiv 0$ and $\operatorname{grad} f(\mathbf{p}(t)) = \lambda(t)\mathbf{p}(t)$. Then

$$\frac{d}{dt} f(\mathbf{p}(t)) = \langle \mathbf{p}'(t), \operatorname{grad} f(\mathbf{p}(t)) \rangle = \lambda(t) \langle \mathbf{p}'(t), \mathbf{p}(t) \rangle = \frac{\lambda(t)}{2} \frac{d}{dt} \|\mathbf{p}(t)\|^2.$$

Since $f(\mathbf{p}(t)) \equiv 0$, the left side is 0. But $\|\mathbf{p}(t)\|^2$ is strictly increasing (as in the transversality proof), giving a contradiction.

Now, at any $\mathbf{z}^0 \in K$, choose real local coordinates $u_1, \ldots, u_{2n+1}$ for S_ϵ near $\mathbf{z}^0$ so that $f(\mathbf{z}) = u_1(\mathbf{z}) + iu_2(\mathbf{z})$. The fiber $F_0 = \Phi^{-1}(1)$ is locally characterized by $u_1 > 0, u_2 = 0$. Its closure $\overline{F}_0$ is $\{u_1 \geq 0, u_2 = 0\}$, which is a smooth manifold with boundary $\{u_1 = 0, u_2 = 0\} = K$ locally. The argument for other fibers F_θ is identical. □

5.3 Topology of the Link K

The link $K = f^{-1}(0) \cap S_\epsilon^{2n+1}$ is a smooth, closed, orientable manifold of real dimension $2n - 1$. Because K acts as the binding of the open book decomposition of the highly connected sphere S^{2n+1}, its own topology is remarkably simple.

Theorem 5.4 (Milnor)**.** *If f has an isolated critical point at the origin, then the link K is $(n-2)$-connected.*

Proof. The proof uses Morse theory on the complement $S_\epsilon \setminus K$. Consider the smooth function $a(\mathbf{z}) = \log |f(\mathbf{z})|$ on $S_\epsilon \setminus K$. By Milnor's analysis of the Hessian, every critical point of a has Morse index $\geq n$. The key step is:

Morse index $\geq n$: At a critical point $\mathbf{z}$ of $a|_{F_\theta}$, we have $\operatorname{grad} \log f(\mathbf{z}) = \lambda \mathbf{z}$ for some $\lambda \in \mathbb{C}$, and the Hessian takes the form $H(\mathbf{v}) = \operatorname{Re}(\sum b_{jk} v_j v_k) - c\|\mathbf{v}\|^2$ where $c > 0$. The crucial observation is: if $H(\mathbf{v}) \geq 0$ for some tangent vector $\mathbf{v}$, then $H(i\mathbf{v}) < 0$, since the first term changes sign while $-c\|i\mathbf{v}\|^2 = -c\|\mathbf{v}\|^2$ remains negative. Since the tangent space of F_θ at a critical point is a complex vector space (of real dimension $2n$), splitting it as $T_0 \oplus T_1$ where $H < 0$ on T_0 and $H \geq 0$ on T_1, we get $\dim T_0 \geq \dim(iT_1) = \dim T_1 = 2n - \dim T_0$, hence the Morse index $\dim T_0 \geq n$.

Connectivity argument: Let $N_\eta(K)$ be a closed tubular neighborhood of K in S_ϵ (which retracts onto K). After a generic perturbation, we may assume all critical points of a are non-degenerate and lie outside $N_\eta(K)$. By Morse theory, S_ϵ is obtained from $N_\eta(K)$ by attaching handles of index $\geq n$. Attaching a handle of index I does not change π_i for $i \leq I - 2$. Since all handles have index $\geq n$, the inclusion $N_\eta(K) \hookrightarrow S_\epsilon$ induces isomorphisms on π_i for $i \leq n-2$. But $N_\eta(K)$ deformation retracts onto K and $S_\epsilon \cong S^{2n+1}$ is $(2n)$-connected, so $\pi_i(K) \cong \pi_i(S^{2n+1}) = 0$ for $i \leq n - 2$. □

This means that the lower homotopy groups $\pi_i(K)$ are trivial for $i \leq n - 2$. For instance, if $n = 2$ (a surface singularity in $\mathbb{C}^3$), the link K is a 3-manifold that is 0-connected (connected). For $n \geq 3$, K is simply connected. Consequently, the only non-trivial homology groups of K (besides H_0 and H_{2n-1}) can occur in the middle dimension $n - 1$.

In fact, whether K is a topological sphere is of great historical importance. Brieskorn showed that for certain diagonal polynomials $f(z) = z_0^{a_0} + \cdots + z_n^{a_n}$, the link K can be a *homotopy sphere* that is not diffeomorphic to the standard sphere (an exotic sphere), providing a profound connection between singularity theory and differential topology.

The Wang Sequence and Sphere Criterion

To determine whether K is a topological sphere, one uses the **Wang exact sequence** associated to the Milnor fibration $\Phi : S_\epsilon \setminus K \to S^1$.

Lemma 5.2 (Wang Exact Sequence)**.** *For any fiber bundle $E \to S^1$ with fiber F_0 and monodromy $h : F_0 \to F_0$, there is a long exact sequence:*

$$\cdots \longrightarrow H_{j+1}(E) \longrightarrow H_j(F_0) \xrightarrow{h_* - \mathrm{I}_*} H_j(F_0) \longrightarrow H_j(E) \longrightarrow \cdots$$

Proof Sketch. The covering homotopy $\{h_t : F_0 \to F_t\}_{0 \leq t \leq 2\pi}$ with $h_0 = \mathrm{I}$, $h_{2\pi} = h$ induces a map $F_0 \times [0, 2\pi] \to E$. The resulting isomorphism $H_j(F_0 \times [0, 2\pi], F_0 \times \partial) \cong H_j(E, F_0) \cong H_{j-1}(F_0)$ substituted into the exact sequence of the pair (E, F_0) yields the Wang sequence. □

Let $\Delta(t) = \det(tI_* - h_*)$ be the **characteristic polynomial** of the monodromy action $h_* : H_n(F_0) \to H_n(F_0)$. This is a polynomial of degree μ with integer coefficients.

Theorem 5.5 (Sphere Criterion)**.** *For $n \neq 2$, the link K is homeomorphic to the sphere S^{2n-1} if and only if $\Delta(1) = \det(\mathrm{I}_* - h_*) = \pm 1$.*

Proof. Applying the Wang sequence to the Milnor fibration $S_\epsilon \setminus K \to S^1$ in degree n:

$$H_n(F_0) \xrightarrow{h_* - \mathrm{I}_*} H_n(F_0) \longrightarrow H_n(S_\epsilon \setminus K) \longrightarrow 0.$$

By Alexander duality, $H_n(S_\epsilon \setminus K) \cong H^n(K) \cong H_{n-1}(K)$ (using Poincaré duality on the $(2n-1)$-manifold K). So $H_{n-1}(K) \cong \operatorname{coker}(h_* - \mathrm{I}_*)$. Since K is $(n-2)$-connected, K is a homology sphere if and only if $\tilde{H}_{n-1}(K) = 0$, which happens if and only if $h_* - \mathrm{I}_*$ is an isomorphism, i.e., $\det(\mathrm{I}_* - h_*) = \pm 1$. For $n \neq 2$, K being a homology sphere implies it is a topological sphere (by the Generalized Poincaré Conjecture, proved by Smale for $\dim \geq 5$). □

Remark 5.3. *The polynomial $\Delta(t)$ is an n-dimensional generalization of the* ***Alexander polynomial*** *of a knot. When $n = 1$ and K is a knot in S^3, the classical Alexander polynomial of K is precisely $\Delta(t)$. For the Brieskorn–Pham singularity $f = z_0^{a_0} + \cdots + z_n^{a_n}$, the roots of $\Delta(t)$ are the products $\omega_0 \cdots \omega_n$ where each ω_j ranges over all a_j-th roots of unity other than 1.*

5.4 The Local Milnor Fiber

There is an equivalent, more analytic definition of the Milnor fiber which is often easier to compute. Instead of intersecting the fibers with the sphere S_ϵ, we consider the intersection of the nearby *smooth* fibers of f with the small ball B_ϵ.

Let $D_\delta = \{s \in \mathbb{C} \mid |s| \leq \delta\}$ be a small disk. We can define a relative version:

$$f : B_\epsilon \cap f^{-1}(D_\delta \setminus \{0\}) \to D_\delta \setminus \{0\}.$$

For $0 < \delta \ll \epsilon$, this is also a smooth locally trivial fiber bundle over the punctured disk (which retracts to S^1). The fiber of this bundle is

$$F_s = f^{-1}(s) \cap B_\epsilon \quad \text{for } s \neq 0.$$

In singularity theory, one often writes F for the Milnor fiber defined in this interior way. By Ehresmann's fibration theorem, F_s is diffeomorphic to the sphere definition of the fiber $\Phi^{-1}(e^{i\theta})$.

5.5 Examples: Curves and Torus Knots

Let us evaluate the Milnor fiber for the simple isolated singularities.

Example 5.1 (Node singularity and the Annulus)**.** *Let $f(x, y) = x^2 + y^2$. The Milnor fiber is $F_s = \{(x, y) \in \mathbb{C}^2 \mid |x|^2 + |y|^2 \leq \epsilon^2, x^2 + y^2 = s\}$. If we assume s is entirely real and positive, we can write $x = u + iv, y = z + iw$. Substituting $x^2 + y^2 = s$, we find $u^2 + z^2 - v^2 - w^2 = s$ and $uv + zw = 0$. The Milnor fiber is thus topologically equivalent to the tangent bundle of S^1, bounded by the intersection with the sphere. Since $TS^1 \cong S^1 \times \mathbb{R}$, the bounded piece is exactly an annulus (a cylinder $S^1 \times [0, 1]$).*

Let us generalize this to any Brieskorn-Pham curve singularity.

Theorem 5.6 (Brieskorn)**.** *Consider the singularity given by $f(x, y) = x^p + y^q = 0$ with $\gcd(p, q) = 1$. The link K in S^3 is exactly the (p, q)-torus knot. The Milnor fiber F is a Seifert surface of the knot K. The genus g of F (and thus of the knot) can be computed as:*

$$2g = \mu = (p - 1)(q - 1)$$

where μ is the Milnor number (dimension of the middle homology).

For the cusp $x^3 - y^2 = 0$, $p = 3, q = 2$. The link is the $(3, 2)$-trefoil knot. The Milnor fiber is a surface spanning this knot. Its genus is $g = \frac{1}{2}(2)(1) = 1$. The Milnor fiber is a punctured torus!

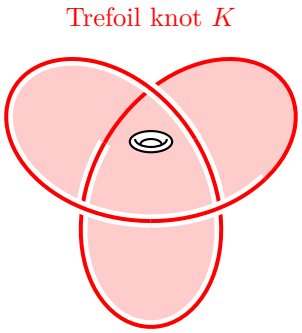

Figure 9: The Milnor fiber for the A_2 cusp singularity spans the link (trefoil knot) and is a real 2-manifold with one boundary component and genus 1.

5.6 Plane Curve Singularities and Legendrian Knots

For a plane curve singularity $f(x, y) = 0$ at the origin, its link $K = \{f = 0\} \cap S^3_\epsilon$ is not merely a smooth knot or link in S^3; it naturally interacts with the standard **contact structure** on S^3.

Recall that the 3-sphere $S^3 \subset \mathbb{C}^2$ carries a natural contact structure ξ defined as the field of complex tangencies: $\xi_p = T_pS^3 \cap iT_pS^3$. A knot $\Lambda \subset (S^3, \xi)$ is called **Legendrian** if its tangent spaces lie everywhere within the contact planes, i.e., $T_p\Lambda \subset \xi_p$ for all $p \in \Lambda$.

The link of any isolated plane curve singularity is naturally a *transverse* knot to the contact structure rather than a Legendrian one. After stereographic projection, one identifies $(S^3 \setminus \{\infty\}, \xi)$ with the standard contact space $(\mathbb{R}^3, \ker(dz - y\,dx))$, and then studies either Legendrian approximations of the transverse link or the more canonical Legendrian conormal attached to K. In this model, a generic front projection to the xz-plane has only transverse crossings and semi-cubical cusps, and the basic contact invariants are read directly from the picture:

$$\mathrm{tb}(\Lambda) = \mathrm{wr}(F) - \frac{1}{2}\#\{\text{cusps}\}, \qquad \mathrm{rot}(\Lambda) = \frac{1}{2}\big(\#\{\text{down cusps}\} - \#\{\text{up cusps}\}\big).$$

Thus front diagrams convert contact topology into a combinatorial calculus.

For algebraic links the front is highly constrained. Puiseux expansions realize the link as the closure of a positive braid, hence as a quasipositive transverse link. Because the Milnor fiber is a complex Seifert surface, the canonical transverse representative satisfies the Bennequin equality

$$\mathrm{sl}(K) = -\chi(F) = 2\delta - r = \mu - 1,$$

where r is the number of branches and we used Milnor's formula $\mu = 2\delta - r + 1$. For the cusp $y^2 = x^3$, the link is the right-handed trefoil, and a standard Legendrian representative has $(\mathrm{tb}, \mathrm{rot}) = (1, 0)$, which is exactly the extremal value predicted by the Milnor fiber.

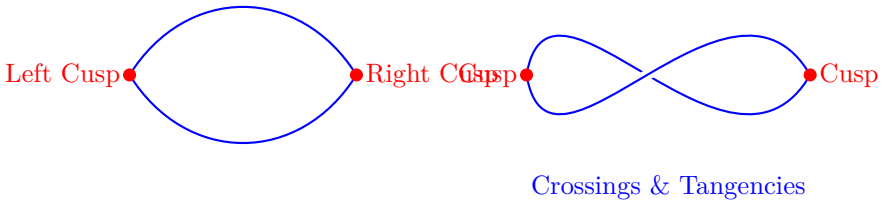

Figure 10: Legendrian front projections in contact topology. The tangencies in the contact plane dictate the appearance of semi-cubical cusps in the front projection. Algebraic links arise as boundaries of complex curves and possess canonical contact and Legendrian structures.

A second combinatorial invariant extracted from a front is the **ruling polynomial** . A graded normal ruling pairs the strands of the front so that cusps are matched and only specified crossings are allowed to switch. The resulting generating function

$$R_\Lambda(z) = \sum_{\mathcal{R}} z^{j(\mathcal{R})}$$

counts graded normal rulings with their standard switch grading. For a one-component front one may take $j(\mathcal{R}) = s(\mathcal{R}) - c(\Lambda) + 1$, where $s(\mathcal{R})$ is the number of switches and $c(\Lambda)$ is the number of right cusps. Although its definition is purely diagrammatic, it is a genuine Legendrian isotopy invariant. Rutherford showed that it recovers the extremal coefficient of the Kauffman polynomial, while Ng–Sabloff and Henry–Rutherford related rulings to augmentations of the Chekanov–Eliashberg algebra over finite and local coefficient rings [Rut06; NS06; HR15].

Example 5.2 (Worked Example: The Cusp Trefoil)**.** *Consider the standard maximal Thurston–Bennequin Legendrian representative of the right-handed trefoil, which is the algebraic knot associated with the cusp $y^2 = x^3$. Its front has three crossings and two right cusps. There is exactly one 2-graded normal ruling: one crossing is used as a switch, while the other two are resolved without switching. Hence*

$$j(\mathcal{R}) = 1 - 2 + 1 = 0, \qquad R_\Lambda(z) = 1.$$

This tiny calculation is already meaningful. It says that the simplest nontrivial algebraic knot carries a nonzero ruling invariant, so its contact geometry is visible at the level of front combinatorics before one invokes augmentation varieties, sheaf moduli, or HOMFLY homology.

For plane curve singularities this matters because algebraic links sit in the same knot-theoretic package as Hilbert schemes and HOMFLY-type invariants. In the sheaf-theoretic model of Shende–Treumann–Zaslow, a positive braid front determines a moduli space of constructible sheaves whose point counts recover the lowest a-degree part of the HOMFLY polynomial [STZ17]. On the algebro-geometric side, refined Hilbert schemes of the singularity recover the HOMFLY polynomial and HOMFLY homology of the link [OS12; ORS18]. Ruling polynomials should therefore be viewed as a Legendrian shadow of the richer enumerative geometry attached to the same plane curve germ.

The contact-geometric perspective on isolated singularities reveals that algebraic links are prime and non-split, serving as a fruitful bridge between complex algebraic geometry and low-dimensional symplectic/contact topology.

5.7 Numerical Invariants of Plane Curves: The δ-invariant

For plane curve singularities, finding the number of vanishing cycles (the Milnor number μ) connects directly to another deeply classical algebraic invariant: the **delta invariant** δ.

Let $(X, 0)$ be a plane curve singularity cut out by $f(x, y) = 0$. In general, $(X, 0)$ may be composed of several irreducible analytic components (branches), corresponding to the irreducible factors of f in the local ring $\mathcal{O}_{\mathbb{C}^2,0}$. Let r be the number of such branches. Topologically, this r precisely equals the number of connected components of the link K.

The invariant δ intuitively measures *howmanysimplenodesareconcentratedattheorigin*. If we resolve the singularity (via a normalization map $\pi : \tilde{X} \to X$), the delta invariant is defined as:

$$\delta = \dim_{\mathbb{C}}(\pi_* \mathcal{O}_{\tilde{X}} / \mathcal{O}_X).$$

Milnor proved a beautifully simple, unifying formula relating the topological Milnor number μ (the number of holes/vanishing cycles in the fiber) to the algebraic invariants δ and r:

Theorem 5.7 (Milnor's Mu-Delta Formula)**.** *For any reduced plane curve singularity with r branches, the Milnor number μ and the delta invariant δ satisfy:*

$$\mu = 2\delta - r + 1.$$

This shows that the δ-invariant completely determines μ. Furthermore, because μ bounds the number of spheres in the fiber, the genus g of the Milnor fiber (which is a Seifert surface for the link K) can be computed directly as:

$$2g = \mu + r - 1 = 2\delta.$$

Thus δ exactly mirrors the genus of the local smoothings of X.

5.8 Exercises

Exercise 5.1. *Compute the Milnor number $\mu = \dim_{\mathbb{C}} \mathbb{C}\{x, y\}/(\partial f/\partial x, \partial f/\partial y)$ for the A_k singularity $f(x, y) = x^{k+1} + y^2$. Verify that the genus formula gives $g = k/2$. Conclude that A_{2n} singularities yield knots while A_{2n-1} singularities yield links with multiple components.*

Exercise 5.2. *Show that the Milnor number of $f(x, y) = x^3 + y^4$ is $\mu = 6$. Using the formula $\mu = 2\delta - r + 1$ and observing that f is irreducible in $\mathbb{C}\{x, y\}$, prove that its δ-invariant is exactly 3.*

Exercise 5.3. *Let $f(x, y, z) = x^2 + y^2 + z^2$. Describe the geometric structure of the Milnor fiber for this isolated surface singularity. Show that the link mapping involves $S^1 \times S^1$.*

6 Homotopy Type of the Milnor Fiber and the Milnor Number

Before investigating the monodromy of the Milnor fibration and the splitting of singularities into Morse critical points (Morsification), we must establish the fundamental topological structure of the Milnor fiber itself. We will see that its topological structure is astonishingly simple: it has the homotopy type of a bouquet of spheres. The number of these spheres is precisely the **Milnor number** μ, which turns out to be an easily computable algebraic invariant, effectively translating the abstract topology into concrete polynomial arithmetic.

6.1 The Homotopy Type Theorem

Let $f : (\mathbb{C}^{n+1}, 0) \to (\mathbb{C}, 0)$ be a holomorphic function with an isolated singularity at the origin. Recall the Milnor fiber $F_t = f^{-1}(t) \cap B_\epsilon$ for a sufficiently small non-zero t. Because F_t is a complex n-dimensional manifold with boundary, its real dimension is $2n$. However, its homotopy type is equivalent to a space of only half that dimension.

Looijenga's treatment of this theorem in [Loo84, Ch. 5, §A–B] makes a point that is worth isolating: the bouquet theorem is not proved by studying one Milnor fiber in isolation, but by comparing *two* nearby fibrations that differ by one equation. This comparison is what he calls *relative monodromy*. It is the inductive bridge from complete intersections of codimension $k-1$ to those of codimension k.

Proposition 6.1 (Basic Construction of Relative Monodromy)**.** *Let*

$$\mathbf{f} = (f_1, \dots, f_k) : (X, x) \to (\mathbb{C}^k, 0)$$

define an isolated complete intersection singularity, and suppose that

$$\mathbf{f}' = (f_1, \dots, f_{k-1}) : (X, x) \to (\mathbb{C}^{k-1}, 0)$$

also defines an isolated singularity. Then one can choose good proper representatives

$$f : \overline{X} \to S' \times \Delta, \qquad f' : \overline{X}' \to S'$$

with $\overline{X} \subset \overline{X}'$ and a homeomorphism

$$H : \overline{X} \xrightarrow{\sim} \overline{X}'$$

such that $f' \circ H = \pi \circ f$, where $\pi : S' \times \Delta \to S'$ is the projection. After shrinking the vertical disc, H can moreover be chosen to be the identity over a smaller neighborhood containing the discriminant of f.

Proof sketch. This is the basic construction in [Loo84, Ch. 5, §A]. One starts with Milnor tubes cut out simultaneously by

$$|z - x| \le \epsilon, \qquad |f'| < \eta', \qquad |f_k| \le \eta.$$

The key geometric claim is that after shrinking these constants, the differentials of $|z-x|^2$ and $|f_k|^2$ never point in opposite directions on the collar region between $\overline{X}$ and $\overline{X}'$. Looijenga proves this by a curve-selection argument: if they did, an analytic arc would force $|f_k|$ to be nondecreasing while remaining inside the central slice where f_k should stay zero, which is impossible.

Once this opposition is ruled out, one constructs a smooth vector field v on the collar that annihilates $df_1, \dots, df_{k-1}$ and makes both $|z-x|$ and $|f_k|$ strictly increase along its integral curves. Integrating v sweeps the boundary piece $\{|f_k| = \eta\}$ out to the outer boundary of $\overline{X}'$, producing a collar decomposition and hence the required homeomorphism H. In effect, forgetting the last coordinate changes the topology only by a controlled boundary cylinder. □

Theorem 6.1 (Relative Cell-Attachment Picture)**.** *In the situation of Proposition 6.1, fix $t \in S'$ outside the discriminant of f' and choose a generic vertical line $\{t\} \times \Delta$ meeting the discriminant of f in finitely many points $s_1, \dots, s_m$. Then:*

1. *the pair $(\overline{X}'_t, \overline{X}_s)$ is relatively homotopy equivalent to a finite relative CW complex of dimension at most $n+1$;*

2. *if all singular points over the s_μ are quadratic, then up to relative homotopy $\overline{X}'_t$ is obtained from $\overline{X}_s$ by attaching one $(n+1)$-cell for each quadratic point.*

Idea of proof. This is the heart of [Loo84, Ch. 5, §B]. Around each discriminant point s_μ one chooses a small disc Δ_μ supporting a local Milnor fibration, and then connects these discs to a regular value $s \in \{t\} \times \Delta$ by a tree Γ in the base. Over the complement of the Δ_μ, Ehresmann triviality retracts the total space to the single regular fiber $\overline{X}_s$. Each local piece over Δ_μ is, by the conical structure of good and excellent representatives, a cone on its boundary intersection $F_{\mu,\alpha}$.

Therefore $\overline{X}'_t$ is obtained from $\overline{X}_s$ by gluing cones on the small Milnor fibers $F_{\mu,\alpha}$. Inductively these small fibers have the homotopy type of finite n-complexes, giving the relative CW-dimension bound. When the singularities are quadratic, each $F_{\mu,\alpha}$ deformation retracts to S^n, so gluing a cone on it is exactly the attachment of one $(n+1)$-cell. This is the precise mechanism behind the bouquet theorem: global topology is assembled from local vanishing spheres one slice at a time. □

For hypersurfaces, the lower-codimension slice f' is a submersion, so the long exact sequence of the pair $(\overline{X}'_t, \overline{X}_s)$ shows that the resulting vanishing cycles form a basis of $\widetilde{H}_n(\overline{X}_s)$. For higher-codimension ICIS they still generate, but need not be a basis. This is exactly where hypersurfaces start to behave more rigidly than general complete intersections.

Theorem 6.2 (Milnor's Bouquet Theorem)**.** *Let $f : (\mathbb{C}^{n+1}, 0) \to (\mathbb{C}, 0)$ be a holomorphic germ with isolated critical point at the origin, and let F_t be its Milnor fiber. Then F_t has the homotopy type of a finite CW-complex of real dimension n. Specifically, it is homotopy equivalent to a wedge sum (bouquet) of n-dimensional spheres:*

$$F_t \simeq \underbrace{S^n \vee S^n \vee \cdots \vee S^n}_{\mu \text{ times}}.$$

The proof proceeds in several steps: first we show the CW-dimension bound using Morse theory, then we establish high connectivity, and finally we apply the Hurewicz and Whitehead theorems.

Lemma 6.1 (Fiber is $(n-1)$-connected)**.** *For an isolated hypersurface singularity $f : (\mathbb{C}^{n+1}, 0) \to (\mathbb{C}, 0)$, the Milnor fiber F_θ is $(n-1)$-connected, i.e., $\pi_i(F_\theta) = 0$ for $i \leq n-1$.*

Proof. By Alexander duality applied to the compact manifold-with-boundary $\overline{F}_\theta \subset S^{2n+1}_\epsilon$, the reduced homology $\tilde{H}_i(\overline{F}_\theta) \cong \tilde{H}^{2n-i}(S_\epsilon \setminus \overline{F}_\theta)$. But $S_\epsilon \setminus \overline{F}_\theta$ deformation retracts onto any other fiber $F_{\theta'}$ (since the base $S^1 \setminus \{e^{i\theta}\}$ is contractible). By Theorem 5.1 (from the Morse index $\geq n$ argument), $F_{\theta'}$ has the homotopy type of a CW-complex of dimension n, so $H^j(F_{\theta'}) = 0$ for $j > n$, hence $\tilde{H}_i(F_\theta) = 0$ for $i < n$.

For simple connectivity when $n \geq 2$: using the Morse function $-s_\theta$ (the negative of the smoothed $|f|$), the closed fiber $\overline{F}_\theta$ can be built from a $2n$-disk D^{2n} by attaching handles of index $\leq n$. These handles are attached inside the ambient sphere S^{2n+1}_ϵ. The complement $S_\epsilon \setminus D^{2n}$ is simply connected, and attaching handles of index $\leq 2n-2$ to $\overline{F}_\theta$ does not change π_1 of the complement (provided $n \leq 2n-2$, i.e., $n \geq 2$). Hence $\pi_1(S_\epsilon \setminus \overline{F}_\theta) = 0$. Together with the deformation retraction, $\pi_1(F_\theta) = 0$ for $n \geq 2$.

Since F_θ is simply connected (for $n \geq 2$) with $\tilde{H}_i(F_\theta) = 0$ for $i < n$, the Hurewicz theorem gives $\pi_i(F_\theta) = 0$ for all $i \leq n-1$. □

Proof of the Bouquet Theorem. **Step 1: CW-dimension bound.** The smooth function $a_\theta(\mathbf{z}) = \log|f(\mathbf{z})|$ on F_θ has all critical points with Morse index $\geq n$ (see the proof of Theorem 5.2 in

§3). After a generic perturbation to a Morse function s_θ that agrees with $|f|$ near the boundary, standard Morse theory shows that F_θ has the homotopy type of a CW-complex with cells only in dimensions $\geq n$. Since F_θ has real dimension $2n$, the complex has dimension at most n (higher cells can be collapsed).

Step 2: High connectivity. By Lemma 6.1, F_θ is $(n-1)$-connected.

Step 3: Bouquet structure via Hurewicz–Whitehead. Since F_θ is $(n-1)$-connected, the homology group $H_n(F_\theta)$ must be free abelian (any torsion would produce nontrivial cohomology in dimension $n+1$, contradicting the CW-dimension bound). By the Hurewicz theorem, $\pi_n(F_\theta) \cong H_n(F_\theta) \cong \mathbb{Z}^\mu$. Choose maps $\alpha_1, \ldots, \alpha_\mu : (S^n, *) \to (F_\theta, *)$ representing a basis for π_n. These combine to give a map

$$\alpha : S^n \vee \cdots \vee S^n \to F_\theta$$

inducing an isomorphism on all homology groups. Since both spaces are simply connected CW-complexes (for $n \geq 2$), Whitehead's theorem implies α is a homotopy equivalence. □

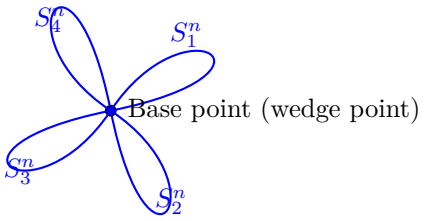

Figure 11: The Milnor fiber retracts onto a bouquet of n-spheres. The reduced homology is completely concentrated in degree n.

Consequently, the reduced homology groups of the Milnor fiber $\tilde{H}_k(F_t; \mathbb{Z})$ are trivial except in the middle dimension:

$$H_n(F_t; \mathbb{Z}) \cong \mathbb{Z}^\mu.$$

The Euler characteristic of the Milnor fiber readily follows:

$$\chi(F_t) = 1 + (-1)^n \mu.$$

We now prove the crucial identity $\mu = \operatorname{rank} H_n(F)$, showing that the topologically defined mapping degree equals the middle Betti number.

Theorem 6.3 (Milnor)**.** *For an isolated hypersurface singularity $f : (\mathbb{C}^{n+1}, 0) \to (\mathbb{C}, 0)$, the middle Betti number of the Milnor fiber F_θ equals the multiplicity μ (the mapping degree of the normalized gradient). Hence $H_n(F_\theta)$ is free abelian of rank μ.*

Proof. Consider the region $M = \{\mathbf{z} \in S_\epsilon \mid \operatorname{Re} f(\mathbf{z}) \geq 0\}$. This is the union of fibers F_θ for $\theta \in [-\pi/2, \pi/2]$ together with the link K, and it has the homotopy type of a single fiber F_θ (since the interior fibers over a contractible arc).

Define the smooth map $\mathbf{v} : S_\epsilon \to S_\epsilon$ by $\mathbf{v}(\mathbf{z}) = \epsilon \cdot \operatorname{grad} f(\mathbf{z}) / \| \operatorname{grad} f(\mathbf{z}) \|$. One verifies three properties:

1. *Fixed points lie in the interior of M*: $\mathbf{v}(\mathbf{z}) = \mathbf{z}$ means $\operatorname{grad} f(\mathbf{z}) = c\mathbf{z}$ with $c > 0$. This forces $\operatorname{Re} f(\mathbf{z}) > 0$, so $\mathbf{z} \in \operatorname{int}(M)$.

2. *No point of M is mapped to its antipode*: by a similar analysis using $\operatorname{grad} \log f$.

3. *The inward normal condition*: for $\mathbf{z} \in \partial M$, the inner product $\langle \mathbf{v}(\mathbf{z}), \mathbf{n}(\mathbf{z}) \rangle > 0$, since the inward normal points in the direction of increasing $\operatorname{Re} f$.

By the Lefschetz fixed point theorem, the sum of fixed point indices of $\mathbf{v}$ on S_ϵ equals $1 + (-1)^{2n+1} d = 1 - d$ where $d = \deg(\mathbf{v})$. A deformation argument (interpolating between $\mathbf{v}$ and the identity via $(1-t)\mathbf{z} + t\mathbf{v}(\mathbf{z})$, which is well-defined on M by property (2)) shows that this Lefschetz number equals $\chi(M) = \chi(F_\theta)$. Hence:

$$\chi(F_\theta) = 1 - \deg(\mathbf{v}).$$

Now, $\deg(\mathbf{v}) = (-1)^{n+1}\mu$, because μ is defined as the degree of $\mathbf{z} \mapsto \overline{\operatorname{grad} f(\mathbf{z})}/\|\operatorname{grad} f(\mathbf{z})\|$, and complex conjugation in $\mathbb{C}^{n+1}$ has degree $(-1)^{n+1}$. Substituting:

$$\chi(F_\theta) = 1 + (-1)^n \mu.$$

Since $\chi(F_\theta) = 1 + (-1)^n \operatorname{rank} H_n(F_\theta)$ (all other homology vanishes except $H_0 \cong \mathbb{Z}$), we conclude $\mu = \operatorname{rank} H_n(F_\theta)$. □

For the differential topology of the fiber, we have the following sharpened result:

Theorem 6.4 (Handlebody Structure)**.** *For an isolated hypersurface singularity and $n \neq 2$, the closed Milnor fiber $\overline{F}_\theta$ is diffeomorphic to a **handlebody**: it is obtained from the disk D^{2n} by simultaneously attaching μ handles of index exactly n.*

This follows from Smale's handle trading results (using the high connectivity of the fiber from Lemma 6.1 and the $(n-2)$-connectivity of K). The case $n = 2$ remains conjectural.

6.2 The Topological and Algebraic Milnor Number

The number μ is an invariant of the singularity. Topologically, it is defined as the local mapping degree of the normalized gradient vector field of f on a small sphere bounding the singularity:

$$\mu = \deg\left(\frac{\operatorname{grad} f}{\|\operatorname{grad} f\|} : S_\epsilon^{2n+1} \to S^{2n+1}\right).$$

Remarkably, this topological number μ can be computed entirely algebraically without any integrations, path lifts, or deformation splitting.

Definition 6.1 (Algebraic Milnor Number)**.** *The **Milnor number** $\mu(f)$ of the isolated singularity $f = 0$ at the origin is defined as the dimension of the local algebra (called the **Milnor algebra** or Jacobi algebra):*

$$\mu(f) = \dim_{\mathbb{C}}\left(\frac{\mathcal{O}_{\mathbb{C}^{n+1},0}}{J_f}\right) = \dim_{\mathbb{C}}\left(\frac{\mathbb{C}\{z_0, \ldots, z_n\}}{(\frac{\partial f}{\partial z_0}, \ldots, \frac{\partial f}{\partial z_n})}\right),$$

*where $J_f = (\frac{\partial f}{\partial z_0}, \ldots, \frac{\partial f}{\partial z_n})$ is the **Jacobian ideal** of f. If f is polynomial, proposition 1.2 shows that the same number is obtained by replacing $\mathbb{C}\{z\}$ with the localized polynomial ring $\mathbb{C}[z]_{(z)}$ or with the formal power series ring $\mathbb{C}[[z]]$.*

Why is this dimension finite? The singularity is isolated at the origin if and only if 0 is the *only* common zero of the partial derivatives near the origin. By Hilbert's Nullstellensatz (adapted to the local analytic setting), this means the radical of the Jacobian ideal $\sqrt{J_f}$ is the maximal ideal $\mathfrak{m} = (z_0, \ldots, z_n)$. Therefore, J_f must contain some power of the maximal ideal, $\mathfrak{m}^k \subset J_f$. Thus, the quotient is isomorphic to a quotient of a finite-dimensional $\mathbb{C}$-vector space (since polynomials up to degree k form a finite basis). Hence, $\mu(f) < \infty$ intrinsically captures the *isolatedness* of the singularity!

6.3 Basic Computation and Subadditivity

The computation of the Milnor number effectively depends on the interplay between the generators of the Jacobian ideal and the maximal ideal of $\mathcal{O}_{\mathbb{C}^{n+1},0}$.

Proposition 6.2 (Properties of the Milnor Number)**.** *For a holomorphic germ f, the algebraic Milnor number*

$$\mu(f) := \dim_{\mathbb{C}}(\mathbb{C}\{z_1, \ldots, z_n\}/J_f)$$

(possibly infinite) satisfies the following foundational characteristics:

1. ***Finite Multiplicity:*** *The parameter $\mu(f)$ is finite if and only if f defines an isolated hypersurface singularity at the origin.*
2. ***Thom-Sebastiani Rule / Multiplicativity:*** *If $f(x)$ and $g(y)$ are holomorphic germs in disjoint sets of variables, and both have isolated critical point at the origin, then*

$$\mu(f \oplus g) = \mu(f(x) + g(y)) = \mu(f) \cdot \mu(g).$$

3. ***Invariance under Right Equivalence:*** *If two singularity germs f and g are right-equivalent, meaning there is a biholomorphic map $\phi : (\mathbb{C}^{n+1}, 0) \to (\mathbb{C}^{n+1}, 0)$ with $\phi(0) = 0$ such that $f \circ \phi = g$, then $\mu(f) = \mu(g)$.*

Proof. Let us sketch the proof for the Thom-Sebastiani Rule, which demonstrates the elegant symmetry of Jacobian quotients. Consider $h(x, y) = f(x) + g(y)$ acting on the product space $\mathbb{C}^n \times \mathbb{C}^m$. The set of variables is completely decoupled between $\{x_1, \ldots, x_n\}$ and $\{y_1, \ldots, y_m\}$. The Jacobian ideal J_h is generated by the partial derivatives $\frac{\partial h}{\partial x_i} = \frac{\partial f}{\partial x_i}$ and $\frac{\partial h}{\partial y_j} = \frac{\partial g}{\partial y_j}$. Therefore, J_h naturally splits into a disjoint union of ideals generated by x-derivatives and y-derivatives. This algebraic separation means the local algebra of h is exactly the tensor product of the constituent local algebras over $\mathbb{C}$:

$$\frac{\mathcal{O}_{\mathbb{C}^{n+m},0}}{J_h} \cong \frac{\mathcal{O}_{\mathbb{C}^n,0}}{J_f} \otimes_{\mathbb{C}} \frac{\mathcal{O}_{\mathbb{C}^m,0}}{J_g}.$$

Therefore, passing to complex vector space dimensions over $\mathbb{C}$, we conclude that $\dim_{\mathbb{C}}(A \otimes_{\mathbb{C}} B) = \dim_{\mathbb{C}}(A) \dim_{\mathbb{C}}(B)$, or formally $\mu(h) = \mu(f) \cdot \mu(g)$. □

Let us precisely compute the Milnor number for our favorite examples.

Example 6.1 (Morse Singularity)**.** *If $f(z) = z_0^2 + z_1^2 + \cdots + z_n^2$, then $\dfrac{\partial f}{\partial z_i} = 2z_i$. The Jacobian ideal is $J_f = (z_0, \ldots, z_n)$. The quotient algebra is $\mathbb{C}\{z_0, \ldots, z_n\}/(z_0, \ldots, z_n) \cong \mathbb{C}$. Thus, $\mu = \dim_{\mathbb{C}}(\mathbb{C}) = 1$. The Milnor fiber is a single S^n.*

Example 6.2 (Brieskorn-Pham Singularities)**.** *Consider a diagonal polynomial* $f(z) = z_0^{a_0} + z_1^{a_1} + \cdots + z_n^{a_n}$*. The partial derivatives are* $a_i z_i^{a_i - 1}$*. The Jacobian ideal is generated by these monomials. The quotient algebra has a basis consisting of monomials* $z_0^{k_0} \cdots z_n^{k_n}$ *where* $0 \leq k_i < a_i - 1$*. The number of such basis elements is exactly:*

$$\mu = (a_0 - 1)(a_1 - 1) \cdots (a_n - 1).$$

Example 6.3 (ADE Singularities)**.** *Let us calculate* μ *for the* D_k *singularity* $f(x, y, z) = x^2 + y^2 z + z^{k-1}$*.*

$$\begin{aligned} \frac{\partial f}{\partial x} &= 2x \\ \frac{\partial f}{\partial y} &= 2yz \\ \frac{\partial f}{\partial z} &= y^2 + (k-1)z^{k-2} \end{aligned}$$

In the quotient ring, $x = 0$*, and* $yz = 0$*. From* $yz = 0$*, we have either* $y = 0$ *or* $z = 0$*. If* $y = 0$*, the third equation gives* $z^{k-2} = 0$*, resulting in a basis* $1, z, z^2, \ldots, z^{k-3}$*. If* $z = 0$*, the third equation gives* $y^2 = 0$*, supplying one extra basis element* y*. Combining them, an explicit* $\mathbb{C}$*-basis for the quotient is* $\{1, z, z^2, \ldots, z^{k-3}, y, z(y \equiv 0)\}$*, although more directly, resolving the module yields* $k - 2$ *basis modes driven by* z*, plus 2 related to* y*, giving exactly* $\mu = k$*. This beautiful alignment where the algebraic Milnor number perfectly coincides with the index ranking of the ADE Lie Algebra notation is not a coincidence!*

By understanding this deep geometric interpretation, we also obtain intuition for the **Thom-Sebastiani Theorem**. If $f(x)$ and $g(y)$ are functions of independent sets of variables, the Milnor number of $f + g$ obeys a crisp multiplicative property:

$$\mu(f(x) + g(y)) = \mu(f) \cdot \mu(g).$$

Topologically, this corresponds precisely to the operation where the Milnor fiber of $f + g$ is the topological join of the Milnor fiber of f and g, preserving the wedge product dimensions perfectly.

6.4 Exercises

Exercise 6.1. *Compute the local Milnor number for the* E_8 *singularity* $f(x, y, z) = x^2 + y^3 + z^5 = 0$*. Provide an explicit basis of monomials for the quotient algebra* $\mathcal{O}_{\mathbb{C}^3,0}/J_f$*. Show that the Milnor fiber is homotopy equivalent to eight* 2*-spheres.*

Exercise 6.2. *Consider the* μ*-constant deformation:* $f_t(x, y) = x^3 + txy^3 + y^4$*. Compute* $\mu(f_0)$ *and* $\mu(f_t)$ *for small* $t \neq 0$*. Demonstrate that the number of connected spheres remains the same, implying isolated singularities typically deform within families of constant Milnor number without changing topological type.*

Exercise 6.3 (Homological Mapping Degree)**.** *Assume that a real analytic map* $F : \mathbb{R}^m \to \mathbb{R}^k$ *admits an isolated* 0 *at the origin. Recall the mapping degree definition for* μ*. Apply this topological definition directly using Brouwer degree (instead of polynomials) to compute the index of the critical point for* $f(x_1, \ldots, x_n) = \sum x_i^2$*.*

7 Geometric Monodromy of the Milnor Fiber

The Milnor fibration gives us a family of smooth manifolds parameterized by a punctured disk. As we traverse a loop around the singularity in the base space, the fiber undergoes a smooth topological twisting and eventually returns to itself. This self-diffeomorphism, and its action on topological invariants, is called the **monodromy**. In this chapter, we introduce both the geometric manifestation of this transformation and its algebraic shadow in the homology of the fiber.

7.1 The Geometric Monodromy and the Mapping Class Group

Let $f : (\mathbb{C}^{n+1}, 0) \to (\mathbb{C}, 0)$ be an isolated hypersurface singularity. Recall the relative Milnor fibration over the punctured disk $D_\delta^* = D_\delta \setminus \{0\}$:

$$f : E^* \to D_\delta^*, \quad \text{where } E^* = B_\epsilon \cap f^{-1}(D_\delta^*)$$

The base space D_δ^* is homotopy equivalent to the circle S^1. Let $\gamma(t) = \delta e^{2\pi i t}$ for $t \in [0, 1]$ be the standard generator of $\pi_1(D_\delta^*, \delta)$.

To construct monodromy carefully, it is better to work in the language of good proper representatives as in Looijenga [Loo84, Ch. 2, §C]. By Theorem 4.1, the boundary map

$$f|_{\partial \overline{X}} : \partial \overline{X} \to S$$

is a globally trivial smooth bundle because S is contractible. Fix such a trivialization once and for all.

Proposition 7.1 (Relative C^∞-Monodromy Representation)**.** *Let $f : \overline{X} \to S$ be a good proper representative of an isolated singularity, and let $s_0 \in S \setminus D_f$. Then every loop $\gamma : [0, 1] \to S \setminus D_f$ based at s_0 determines a diffeomorphism of pairs*

$$h_\gamma : (\overline{X}_{s_0}, \partial \overline{X}_{s_0}) \to (\overline{X}_{s_0}, \partial \overline{X}_{s_0})$$

which restricts to the identity on the boundary. Its relative isotopy class depends only on the homotopy class $[\gamma]$. Hence there is a well-defined homomorphism

$$\rho_{\text{diff}} : \pi_1(S \setminus D_f, s_0) \to \pi_0\big(\text{Diff}^\infty(\overline{X}_{s_0}, \partial \overline{X}_{s_0})\big).$$

Composing with the action on relative homology gives the geometric monodromy representation

$$\rho_{\text{geom}} : \pi_1(S \setminus D_f, s_0) \to \text{Aut}\big(H_*(\overline{X}_{s_0}, \partial \overline{X}_{s_0}; \mathbb{Z})\big).$$

Proof idea. Cover the image of γ by open sets $V_i \subset S \setminus D_f$ over which the fibration is smoothly trivial, and choose the trivializations so that they are compatible with the fixed global trivialization of the boundary bundle. After subdividing $[0, 1]$ so that each subinterval maps into some V_i, one transports the fiber successively along the subdivision and obtains a continuous family of diffeomorphisms

$$h_t : (\overline{X}_{s_0}, \partial \overline{X}_{s_0}) \to (\overline{X}_{\gamma(t)}, \partial \overline{X}_{\gamma(t)}), \qquad h_0 = \text{id}.$$

Because all local trivializations agree with the chosen boundary trivialization, the endpoint h_1 fixes $\partial \overline{X}_{s_0}$ pointwise.

To prove homotopy invariance, one repeats the same construction for a homotopy rectangle $r : [0, 1]^2 \to S \setminus D_f$ between two loops. Subdividing the square into small rectangles contained in trivializing neighborhoods and patching the local identifications inductively yields a two-parameter family $h_{t,t'}$. The upper and lower edges then give the two return maps, and the second parameter supplies the required relative isotopy. Concatenation of loops corresponds to composition of return maps, so ρ_{diff} is a group homomorphism. □

Definition 7.1 (Geometric Monodromy)**.** *When $k = 1$ and $\gamma(t) = \delta e^{2\pi i t}$ is the positive generator of $\pi_1(D^*_\delta, \delta)$, the relative isotopy class of h_γ is called the* ***geometric monodromy*** *of the singularity. If $F = \overline{X}_\delta$ denotes the compact Milnor fiber, this defines an element of the relative mapping class group*

$$\mathrm{Mod}(F, \partial F) = \pi_0(\mathrm{Diff}^+(F, \partial F)).$$

Remark 7.1. *The fact that monodromy acts trivially on the boundary is not a formal consequence of the phase map $f/|f|$ alone. What makes the boundary fixed is the global trivialization of $f|_{\partial \overline{X}}$ coming from the theory of good representatives. This distinction becomes important for ICIS and for families, where the boundary must be controlled independently of any particular phase description.*

The study of plane curve singularities ($n = 1$) can thus be viewed completely through the lens of mapping class groups of punctured surfaces, but now in a way that is compatible with the invariant construction of the Milnor fibration.

7.2 The Algebraic Monodromy

While the geometric monodromy captures the full topological twisting of the fiber, it is often too complex to compute directly. Instead, we study its induced action on the homology groups of F.

Definition 7.2 (Algebraic Monodromy)**.** *The induced automorphism on the integral homology of the Milnor fiber:*

$$h_* : H_k(F; \mathbb{Z}) \to H_k(F; \mathbb{Z})$$

is called the ***algebraic monodromy*** *operator.*

We will prove in later chapters that the Milnor fiber F of an isolated hypersurface singularity in $\mathbb{C}^{n+1}$ has the homotopy type of a bouquet (wedge sum) of n-spheres. Consequently, the only non-trivial reduced homology group is $H_k(F; \mathbb{Z}) = 0$ for $0 < k < n$, and:

$$H_n(F; \mathbb{Z}) \cong \mathbb{Z}^\mu$$

where μ is the Milnor number.

The algebraic monodromy is thus almost entirely captured by the single automorphism:

$$T = h_* : H_n(F; \mathbb{Z}) \to H_n(F; \mathbb{Z}).$$

By choosing a homology basis, T can be represented by a $\mu \times \mu$ integer matrix. Because h is a diffeomorphism, T is invertible over $\mathbb{Z}$, so $\det(T) = \pm 1$. The eigenvalues of T, its characteristic polynomial $\Delta(t) = \det(tI - T)$, and its minimal polynomial are fundamental invariants of the singularity. Specifically, a profound theorem states that the roots of $\Delta(t)$ are always roots of unity (Monodromy Theorem, see §14).

7.3 The Alexander Polynomial and the Monodromy

One of the most profound connections between the purely topological theory of knots and the analytic theory of singularities occurs in dimension $n = 1$, for plane curve singularities. For a plane curve singularity $f(x, y) = 0$, the boundary of the Milnor fiber ∂F is precisely the link K, which is an algebraic knot or link in S^3.

In classic knot theory, a fundamental invariant is the **Alexander polynomial** $\Delta_K(t)$, which can be computed from the fundamental group of the knot complement $\pi_1(S^3 \setminus K)$ using the Fox free calculus, or from the infinite cyclic cover of the knot complement.

On the other hand, from the perspective of singularity theory, we have the **characteristic polynomial** of the algebraic monodromy $h_* : H_1(F;\mathbb{Z}) \to H_1(F;\mathbb{Z})$:

$$P(t) = \det(tI - h_*).$$

Theorem 7.1 (Milnor's Theorem)**.** *Let K be the link of an isolated plane curve singularity. If K is a knot (which occurs if and only if $f(x,y)$ has a single analytically irreducible branch), then the characteristic polynomial of the Milnor monodromy is exactly the Alexander polynomial of the knot:*

$$\det(tI - h_*) = \Delta_K(t).$$

If K is a link with $r > 1$ components (branches), the relationship becomes:

$$\det(tI - h_*) = (t-1)\Delta_K(t, t, \ldots, t)$$

where Δ_K is the multi-variable Alexander polynomial evaluated along the diagonal.

This theorem provides a phenomenal bridge between the geometric deformations inside $\mathbb{C}^2$ and the isotopic invariants of S^3. The roots of the Alexander polynomial (the eigenvalues of the monodromy) are heavily restricted; a theorem of Monodromy states that the eigenvalues must be roots of unity. However, the Alexander polynomial of an algebraic knot contains even more structure:

1. It is monic and reciprocal, $\Delta_K(t^{-1}) = t^{-2g}\Delta_K(t)$.
2. For an analytically irreducible plane curve singularity, the Alexander polynomial completely determines the topological type of the singularity.

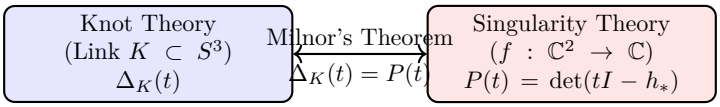

Figure 12: The correspondence between knot invariants and the Milnor monodromy. The algebraic roots constraint forces strong conditions on which knots can appear as links of isolated singularities.

7.4 Monodromy of Homogeneous Polynomials and A_n Singularities

For weighted homogeneous polynomials with isolated critical point at the origin, there is an explicit way to visualize and compute the geometric monodromy without having to solve ODEs for lifted vector fields.

Proposition 7.2 (Homogeneous Singularities)**.** *Suppose $f(z_0, \ldots, z_n)$ is homogeneous of degree d and has an isolated critical point at the origin. Then the geometric monodromy $h : F \to F$ is isotopic to the explicit scaling map:*

$$h(z_0, \ldots, z_n) = e^{2\pi i/d}(z_0, \ldots, z_n).$$

Let us compute the algebraic monodromy for the A_1 singularity $f(x,y) = x^2 + y^2$. This is a homogeneous polynomial of degree 2. The Milnor fiber $F = \{x^2 + y^2 = 1\}$ (taking $\delta = 1$ for simplicity) contracts to the real circle $x^2 + y^2 = 1, x, y \in \mathbb{R}$. The homology $H_1(F;\mathbb{Z}) \cong \mathbb{Z}$ is generated by the cycle

$$\alpha = \{(\cos\theta, \sin\theta) \mid \theta \in [0, 2\pi]\}.$$

The geometric monodromy is $h(x,y) = e^{\pi i}(x,y) = (-x,-y)$, which strictly acts as the antipodal map. The induced action on $H_1(F;\mathbb{Z})$ preserves the manifold but reverses its orientation, meaning it sends the fundamental cycle α to $-\alpha$. Thus, the algebraic monodromy map T is the 1×1 matrix (-1). The characteristic polynomial is exactly $\Delta(t) = t + 1$.

A remarkable property of Brieskorn-Pham curves $f(x,y) = x^a + y^b$ is that their characteristic polynomial can be read off entirely from their exponents. Milnor and Orlik proved that:

$$\Delta(t) = \frac{(t^{ab}-1)(t-1)}{(t^a-1)(t^b-1)}$$

For a general A_n singularity $f(x,y) = x^{n+1} + y^2$ (setting $a = n+1, b = 2$), substituting into the formula gives:

$$\Delta_{A_n}(t) = \frac{(t^{2n+2}-1)(t-1)}{(t^{n+1}-1)(t^2-1)} = \frac{t^{n+1}+1}{t+1}.$$

Notice the roots of this polynomial are precisely the $(2n+2)$-th primitive roots of unity except those that are already roots of $t^{n+1}-1$ or t^2-1. All eigenvalues are roots of unity!

7.5 Exercises

Exercise 7.1. *Consider an annulus $A = S^1 \times [0,1]$. A **Dehn twist** is a diffeomorphism $D : A \to A$ given by $D(\theta, s) = (\theta + 2\pi s, s)$. Show that D is the identity on ∂A. (In §7, we will see the A_1 geometric monodromy is precisely isotopic to a Dehn twist around the core circle of the annulus).*

Exercise 7.2. *Use the Milnor-Orlik formula to compute the characteristic polynomial $\Delta(t)$ for the A_2 cusp singularity $f(x,y) = x^3 + y^2$. Verify that the algebraic monodromy eigenvalues are exactly $e^{i\pi/3}$ and $e^{i5\pi/3}$. What is the trace of the 2×2 monodromy matrix?*

Exercise 7.3. *Suppose T is an algebraic monodromy matrix of size $\mu \times \mu$. Show that the trace of T is exactly the value $\chi(F) - \chi(F^h)$, where χ denotes the Euler characteristic, and F^h is the set of fixed points of the geometric monodromy h. (Hint: Use the Lefschetz Fixed Point Theorem). For the A_1 singularity monodromy $h(x,y) = (-x,-y)$ on $x^2 + y^2 = 1$, calculate the fixed points and verify this formula matches your earlier trace computation.*

8 Picard-Lefschetz Theory: The Local Case

The local monodromy around a critical value is governed by the topology of the singular fiber. In the simplest and most generic case of a non-degenerate critical point (a Morse singularity), the geometry can be described completely explicitly. This is the content of the local Picard-Lefschetz theory, which intrinsically relates the monodromy to a distinguished homology class called the **vanishing cycle** and to an operation generalizing Dehn twists.

8.1 Morse Singularities and the Vanishing Cycle

By the holomorphic Morse Lemma, any non-degenerate isolated critical point of a holomorphic function $f : (\mathbb{C}^{n+1}, 0) \to (\mathbb{C}, 0)$ can be written in suitable local coordinates as a pure quadratic form:

$$f(z_0, \dots, z_n) = z_0^2 + z_1^2 + \cdots + z_n^2.$$

This is the standard A_1 singularity. The Milnor fiber $F_t = f^{-1}(t) \cap B_\epsilon$ for a small real $t > 0$ is given by the equation $\sum z_k^2 = t$. Let us write $z_k = x_k + iy_k$. If we restrict our attention

to the real subspace $\mathbb{R}^{n+1} \subset \mathbb{C}^{n+1}$ (i.e., setting $y_k = 0$), the fiber $F_t \cap \mathbb{R}^{n+1}$ is exactly a real n-dimensional sphere of radius $\sqrt{t}$:

$$S_t^n = \left\{(x_0, \ldots, x_n) \in \mathbb{R}^{n+1} \mid x_0^2 + \cdots + x_n^2 = t\right\}.$$

As $t \to 0$, t acts as a parameter for a family of spheres that shrink continuously and eventually collapse to a single point (the origin) precisely at the critical value $t = 0$.

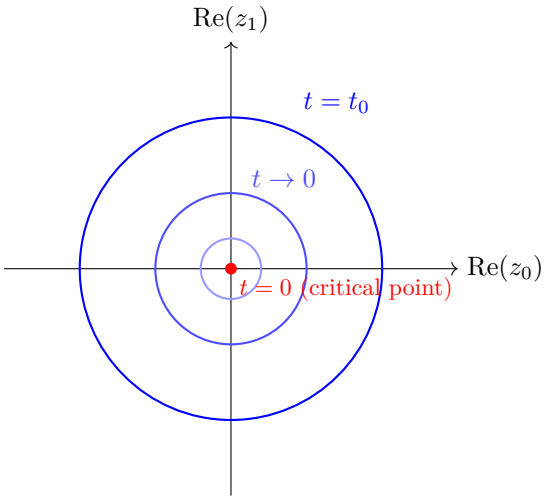

Figure 13: The real locus of the Milnor fiber $x^2 + y^2 = t$ shrinks to the singular point as $t \to 0$, giving rise to the vanishing cycle.

For this reason, the homology class $\delta \in H_n(F_t; \mathbb{Z})$ represented by this n-sphere S_t^n is called the **vanishing cycle**. Because the Milnor fiber $\sum z_k^2 = t$ deformation retracts to its real points, S_t^n is actually the fundamental generator of $H_n(F_t; \mathbb{Z}) \cong \mathbb{Z}$. (Note the Milnor number $\mu = 1$).

8.2 The Lefschetz Thimble (Vanishing Chain)

To understand the algebraic mechanism of the vanishing cycle, we geometricize the vanishing process into an $(n+1)$-dimensional chain spanning the family of fibers. Let $\gamma : [0, 1] \to \mathbb{C}$ be a straight line path in the base space from the critical value 0 to the regular value t. For each $s \in (0, 1]$, the real sphere $S_{\gamma(s)}^n$ lies inside the fiber $F_{\gamma(s)}$.

Definition 8.1 (Lefschetz Thimble)**.** *The union of all these spheres along the path γ, together with the critical point at the origin, forms an $(n+1)$-dimensional topological disk (or cone) Δ in the total space, which is called the* ***Lefschetz thimble****:*

$$\Delta = \bigcup_{s \in (0,1]} S_{\gamma(s)}^n \cup \{0\}.$$

Notice that Δ is an $(n+1)$-chain whose boundary lies entirely inside the regular fiber F_t, and this boundary is precisely the vanishing cycle:

$$\partial \Delta = \delta \subset F_t.$$

The existence of the thimble demonstrates a crucial fact: the vanishing cycle δ is homologous to zero in the total space of the fibration, but is a non-trivial homology class within the fiber F_t itself.

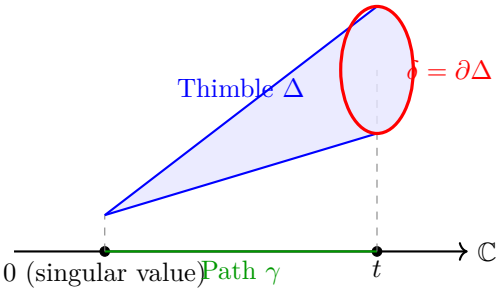

Figure 14: The Lefschetz thimble is an $(n+1)$-dimensional disk sweeping over a path to the critical value. Its boundary is the vanishing cycle $\delta \subset F_t$.

8.3 The Picard-Lefschetz Formula

What happens to the topology of F_t when the base point t travels around a simple closed loop enclosing the critical value 0, for example $\gamma(\theta) = te^{i\theta}$ $(\theta \in [0, 2\pi])$?

To understand the induced monodromy $h_* : H_n(F_t; \mathbb{Z}) \to H_n(F_t; \mathbb{Z})$, we need the intersection form on $H_n(F_t; \mathbb{Z})$. The intersection form $\langle \cdot, \cdot \rangle$ is symmetric if n is even, and skew-symmetric if n is odd. The self-intersection number of the n-dimensional vanishing cycle inside the $2n$-dimensional real manifold F_t evaluates to:

$$\langle \delta, \delta \rangle = \begin{cases} 0 & n \text{ is odd}, \\ (-1)^{n/2} 2 & n \text{ is even}. \end{cases}$$

Looijenga's treatment of the quadratic singularity makes the local computation especially transparent [Loo84, Ch. 3, §A].

Proposition 8.1 (Quadratic Local Model and the Variation Map)**.** *For the Morse singularity*

$$q(z_0, \ldots, z_n) = z_0^2 + \cdots + z_n^2,$$

the compact Milnor fiber is diffeomorphic to the unit disk bundle E of the tangent bundle of S^n. Under this identification, one can choose a geometric monodromy which is the identity on ∂E, and its variation homomorphism

$$\mathrm{var}_*(h) : H_n(E, \partial E) \to H_n(E)$$

satisfies

$$\mathrm{var}_*(h)(c) = -(-1)^{\frac{n(n-1)}{2}} \langle c, \delta \rangle \, \delta, \qquad c \in H_n(E, \partial E),$$

where now $\langle -, - \rangle$ denotes the Lefschetz duality pairing between relative and absolute homology.

Proof idea. The first step is geometric. Write $z = x + iy$ with $x, y \in \mathbb{R}^{n+1}$. For fixed $t > 0$, the equations

$$|x|^2 - |y|^2 = t, \qquad (x, y) = 0$$

identify the Milnor fiber with the disk bundle of TS^n: the real part gives the point of S^n, while the imaginary part gives a tangent vector. A naive monodromy would be scalar multiplication

by -1, but this does not fix the boundary. Looijenga corrects it by inserting a radial twist in the disk-bundle direction, so that the resulting return map is still monodromy but now becomes the identity on ∂E.

The second step is homological. The zero section $S^n \subset E$ represents the vanishing cycle δ, while a single fiber disk $D^n \subset E$ gives a generator of $H_n(E, \partial E)$. One computes $\mathrm{var}_*(h)$ on $[D^n, \partial D^n]$ by projecting to the zero section. This reduces the problem to a map $D^n/\partial D^n \to S^n$ whose degree is $(-1)^{n+1}$. Lefschetz duality then converts this degree computation into the stated formula for $\mathrm{var}_*(h)$. Finally, combining $\mathrm{var}_*(h)$ with the natural map $H_n(E) \to H_n(E, \partial E)$ recovers the usual Picard–Lefschetz formula on absolute homology. □

By explicitly tracking the rotation of the real and imaginary parts of the spheres along the loop $\gamma(\theta)$, one derives the cornerstone of monodromy theory:

Theorem 8.1 (Local Picard-Lefschetz Formula)**.** *The algebraic monodromy $h_* : H_n(F_t; \mathbb{Z}) \to H_n(F_t; \mathbb{Z})$ induced by a simple counterclockwise loop around the critical value associated to δ acts on any homology class $\alpha \in H_n(F_t; \mathbb{Z})$ by the formula:*

$$h_*(\alpha) = \alpha + (-1)^{\frac{n(n+1)}{2}} \langle \alpha, \delta \rangle \delta.$$

This formula immediately shows that the monodromy operates fundamentally as a $reflection$ or a *transvection* centered at the vanishing cycle. If an n-cycle α does not intersect the vanishing cycle δ (i.e., $\langle \alpha, \delta \rangle = 0$), it is invariant under the monodromy. The shift only occurs proportionally to how many times α geometrically crosses δ.

8.4 Generalized Dehn Twists and Geometry

In the geometric picture, the monodromy diffeomorphism $h : F_t \to F_t$ acts as the identity outside a small tubular neighborhood of the vanishing cycle $\delta \cong S^n$.

Let us examine the plane curve case (isolated A_1 curve singularity, $n = 1$). The Milnor fiber F_t is a cylinder (an annulus), and the vanishing cycle δ is its core circle (the equator). The Picard-Lefschetz formula gives:

$$h_*(\alpha) = \alpha - \langle \alpha, \delta \rangle \delta.$$

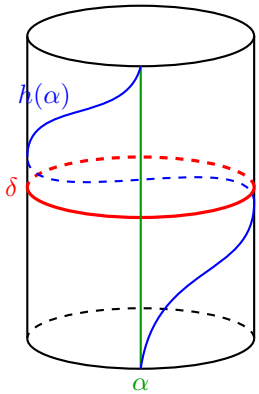

Figure 15: For $n = 1$, the mapping class of the monodromy is a Dehn twist around the core vanishing cycle δ. The blue curve $h(\alpha)$ wraps around the cylinder's circumference exactly once before rejoining the vertical path.

This algebraic operation where a curve is broken at the intersection and a copy of the intersected circle δ is patched into it corresponds precisely to a **Dehn twist**. This brings a beautiful geometric intuition: the local monodromy of any simple non-degenerate singularity is geometrically realized by cutting the manifold along S^n, twisting it by the generalized antipodal map of the normal bundle, and gluing it back together.

For higher n, S^n cannot be *twisted* in the same 1-dimensional sense, but the formula defines exactly what is called a **Generalized Dehn Twist** in higher-dimensional symplectic geometry, which stands at the foundation of modern homological mirror symmetry and Fukaya categories.

8.5 Exercises

Exercise 8.1. *Compute the Picard-Lefschetz monodromy action for the A_1 singularity in dimension $n = 2$ (a surface singularity). Verify using the formula that $h_*(\delta) = -\delta$. Contrast this with the $n = 1$ case where $h_*(\delta) = \delta$, and geometrically explain this difference based on the order of the fundamental group being abelian.*

Exercise 8.2. *Draw an explicit topological picture of a higher-dimensional Lefschetz thimble Δ corresponding to $x^2 + y^2 + z^2 = t$. What is the geometric dimension and topological nature of this thimble? Show that it is an embedded 3-disk $D^3 \subset \mathbb{C}^3$.*

Exercise 8.3. *Suppose an intersection matrix of $H_1(F)$ for some plane curve singularity is given by $\begin{pmatrix} 0 & 1 \\ -1 & 0 \end{pmatrix}$ associated to vanishing cycles δ_1, δ_2. Compute the corresponding Picard-Lefschetz matrices T_1 and T_2 operating on H_1, and calculate the total monodromy matrix of a loop enclosing both assuming they undergo non-degenerate degenerations in sequence.*

9 Introduction to Deformation Theory

In the first half of this course (§§1–8), we extensively mapped out the topography of individual singular points and their algebraic topological invariants [Mil68]. We dissected the geometry via Milnor fibrations, broke apart structures with Brieskorn's Morsifications (§8) and mapped the overarching rigid constraints of holonomy, monodromy, and Hodge structures using differential complexes like the Brieskorn Lattice and Gauss-Manin Connections (§§7, 14). From those intricate local features, a broader global perspective inherently began to emerge—small deformations encode the essence of singularity topologies.

We now pivot officially to the second major theme of modern singularity theory: **Deformation Theory**. Instead of examining a single isolated singularity embedded at the origin point and finding mathematical invariants to describe it statically, we analyze the entire neighborhood—studying practically how that singularity changes, *resolves* or transforms parametrically when we gently perturb its defining equations across a continuous phase space. What is the fundamental parameter space regulating all these topological splittings?

9.1 The Concept of a Deformation and Flatness

Informally, a deformation of a singularity X_0 is a family of spaces X_s parameterized by a base space S, such that the central fiber X_0 (at $s = 0$) is precisely our original singularity. To make this precise, we need the concept of a flat morphism, which ensures that the fibers do not *jump* in size or dimension abruptly.

Definition 9.1 (Deformation of a Germ)**.** *Let $(X_0, 0) \subset (\mathbb{C}^n, 0)$ be the germ of a complex analytic space. A **deformation** of $(X_0, 0)$ over a complex analytic germ (S, s_0) (the base space) consists of:*

1. *A germ of a complex analytic space $(\mathcal{X}, x_0)$ (the total space).*
2. *A flat holomorphic map germ $\pi : (\mathcal{X}, x_0) \to (S, s_0)$.*
3. *An isomorphism of analytic germs $i : (X_0, 0) \xrightarrow{\sim} \pi^{-1}(s_0)$.*

*Two deformations up to isomorphism form an equivalence class, leading to the study of the **Deformation Functor** Def_{X_0}, which maps any base germ (S, s_0) to the set of isomorphism classes of deformations of X_0 over S.*

Definition 9.2 (Flatness in Analytic Geometry)**.** *A map $\pi : (\mathcal{X}, x_0) \to (S, s_0)$ is **flat** at $x_0 \in \mathcal{X}$ if the local ring $\mathcal{O}_{\mathcal{X},x_0}$ is a flat module over the local ring $\mathcal{O}_{S,s_0}$ via the induced pullback homomorphism $\pi^* : \mathcal{O}_{S,s_0} \to \mathcal{O}_{\mathcal{X},x_0}$.*

Geometrically, flatness ensures that the fibers $X_s = \pi^{-1}(s)$ *varycontinuously*. For example, it prevents isolated points from disappearing or entire new connected components of different dimensions from appearing out of nowhere when $s \neq s_0$. For a hypersurface singularity defined by a single equation $f(z) = 0$ in $\mathbb{C}^n$, any deformation defined by a single equation $F(z, s) = 0$ over $S = \mathbb{C}^k$ (where $F(z, 0) = f(z)$) is automatically flat, provided f is not a zero divisor (which is trivial for a non-zero holomorphic function).

For complete intersections, verifying flatness is also straightforward thanks to a fundamental criterion (Looijenga Prop 6.9-6.10): If X_0 is an ICIS of dimension $n - k$ defined by a regular sequence $f_1, \ldots, f_k \in \mathcal{O}_{\mathbb{C}^n,0}$, then any deformation over a smooth base S defined by a mapping $F = (F_1, \ldots, F_k) : (\mathbb{C}^n \times S, 0) \to (\mathbb{C}^k, 0)$ with $F(z, 0) = f(z)$ is automatically flat precisely because $F_1, \ldots, F_k$ remains a regular sequence in the local ring $\mathcal{O}_{\mathbb{C}^n \times S,0}$.

9.2 Induced Deformations and Versality

A core theme in deformation theory is understanding when one deformation can be *pulledback* or induced from another, more general deformation.

Definition 9.3 (Induced Deformation)**.** *Suppose we have a deformation $\mathcal{X} \to S$ of X_0 and a holomorphic germ map $\psi : (S', s_0') \to (S, s_0)$. We can form the fiber product $\mathcal{X}' = \mathcal{X} \times_S S'$, which gives a new deformation $\pi' : \mathcal{X}' \to S'$ of X_0. We say this new deformation is **induced** by ψ, and we write $\mathcal{X}' \cong \psi^*\mathcal{X}$.*

A natural question arises: Is there a *master* deformation from which all other small deformations can be derived? This leads to the concept of a **semi-universal** or **miniversal** deformation (often just called a versal deformation in singularity theory when dealing with unfoldings).

Definition 9.4 (Versal Deformation and Miniversality)**.** *A deformation $\mathcal{X} \to S$ of $(X_0, 0)$ is called **versal** if for any other deformation $\mathcal{X}' \to S'$ of X_0, there exists a smooth analytic map germ $\psi : (S', s_0') \to (S, s_0)$ such that $\mathcal{X}' \cong \psi^*\mathcal{X}$. In other words, every deformation is induced from the versal one. If, in addition, the dimension of the base space S is minimal among all versal deformations, the deformation is called **miniversal** (or semi-universal). The map ψ for a miniversal deformation is not necessarily unique, but its first-order derivative (the differential) $d\psi : T_{S',s_0'} \to T_{S,s_0}$ is uniquely determined.*

In the specific case of functions, an **unfolding** of a function germ $f : (\mathbb{C}^n, 0) \to (\mathbb{C}, 0)$ is a parametrized family $F : (\mathbb{C}^n \times S, 0) \to (\mathbb{C}, 0)$ where $F(z, 0) = f(z)$. We consider two unfoldings $G(z, r)$ and $F(z, s)$ equivalent if one can be induced from the other by coordinate changes.

Definition 9.5 (Versal Unfolding)**.** *An unfolding $F(z, s) = f(z) + \sum_{i=1}^{k} s_i g_i(z)$ is called **versal** if any other unfolding $G(z, r)$ of f can be induced from F by a change of coordinates in the source and the base. That is, there exist smooth map germs $\phi(z, r)$ (with $\phi(z, 0) = z$) and $\psi(r)$ (with $\psi(0) = 0$) such that*

$$G(z, r) = F(\phi(z, r), \psi(r)).$$

9.3 The Tjurina Algebra and Tjurina Number τ

To construct a miniversal deformation algebraically, we look at the tangent space of the deformation functor. For an isolated hypersurface singularity defined by $f = 0$, infinitesimal deformations correspond to perturbations $f + \epsilon g$. Two deformations are trivially isomorphic if they correspond to an analytic change of coordinates on $\mathbb{C}^n$. Such a change naturally induces a vector field $v = \sum \xi_i \dfrac{\partial}{\partial z_i}$. Applying this vector field to f yields $\sum \xi_i \dfrac{\partial f}{\partial z_i}$, producing the Jacobian ideal.

Therefore, the non-trivial first-order deformations modulo trivial biholomorphisms correspond precisely to the quotient by the Jacobian ideal. But when evaluating functions modulo $f = 0$, we must also quotient by (f). This algebraic ring characterizes the full structure of the moduli space direction space and is known as the Tjurina Algebra.

Definition 9.6 (Tjurina Algebra and Tjurina Number τ)**.** *The **Tjurina algebra** of the isolated hypersurface singularity $f = 0$ is defined as the localization ring:*

$$T_f = \frac{\mathcal{O}_{\mathbb{C}^n,0}}{\left(f, \dfrac{\partial f}{\partial z_1}, \ldots, \dfrac{\partial f}{\partial z_n}\right)}.$$

*Its finite complex dimension is called the **Tjurina number** τ:*

$$\tau(f) = \dim_{\mathbb{C}} T_f.$$

For a non-isolated hypersurface germ this quotient need not be finite-dimensional, so the isolated-singularity hypothesis is essential here. For polynomial f, the same dimension is obtained in $\mathbb{C}[z]_{(z)}$ and in $\mathbb{C}[[z]]$ by the same finite-jet argument of proposition 1.2.

Notice the subtle difference between the Milnor number $\mu(f)$ and the Tjurina number $\tau(f)$. The Milnor algebra is the quotient by the Jacobian ideal $J_f = (\dfrac{\partial f}{\partial z_i})$, whereas the Tjurina algebra also modes out by f itself. Therefore, there is a natural surjection from the Milnor algebra to the Tjurina algebra, implying:

$$\tau(f) \leq \mu(f).$$

Saito's Theorem beautifully identifies when equality holds: $\tau(f) = \mu(f)$ if and only if f is quasi-homogeneous (up to a biholomorphic change of coordinates). For instance, for the ADE singularities, both μ and τ coincide perfectly.

9.4 Constructing the Miniversal Deformation

If $g_1, \dots, g_\tau$ project to a $\mathbb{C}$-basis of the Tjurina algebra T_f, then Mather's fundamental theorem on universal unfoldings asserts that the family

$$F(z, s_1, \dots, s_\tau) = f(z) + s_1 g_1(z) + \cdots + s_\tau g_\tau(z)$$

forms a miniversal deformation of $f = 0$.

Example 9.1 (The Fold and The Cusp)**.** *Let $f(x) = x^3$. The derivatives are $3x^2$. The Tjurina algebra is $\mathbb{C}\{x\}/(x^3, x^2) = \mathbb{C}\{x\}/(x^2)$, which has basis $\{1, x\}$, so $\tau = 2$. The miniversal deformation is $F(x, a, b) = x^3 + ax + b$. This is exactly the Whitney Cusp catastrophe we encountered in topological stratifications!*

Let us visualize the parameter space (base space S) for the versal deformation of the A_3 singularity, $f(x) = x^4$. Here $\tau = 3$, and $F(x, a, b, c) = x^4 + ax^2 + bx + c$. The discriminant locus where the fibers become singular forms the famous Swallowtail Catastrophe surface.

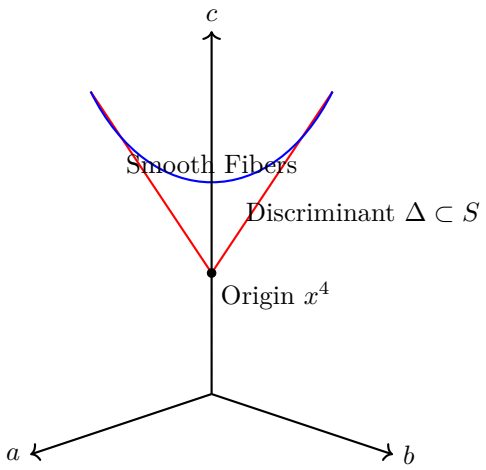

Figure 16: A stylized conceptual diagram of the Swallowtail discriminant surface in the parameter space $S = \mathbb{C}^3$ of the versal deformation of A_3 (x^4). Points on the surface Δ correspond to parameter values where the deformed polynomial possesses degenerate critical points.

The complement of the discriminant $S \setminus \Delta$ is precisely the space where the deformed fibers are smooth. It is the fundamental group of this complement, $\pi_1(S \setminus \Delta)$, that algebraically organizes the monodromy representations we studied earlier. This group is isomorphic to the Braid group for A_k singularities!

9.5 Exercises

Exercise 9.1. *Compute the Milnor number μ and the Tjurina number τ for the singularity $f(x, y) = x^5 + xy^3$. Is f quasi-homogeneous?*

Exercise 9.2. *Using the basis of the Tjurina algebra for the D_4 singularity $f(x, y) = x^2y - y^3$, construct its miniversal deformation. Identify the dimension of the base space S.*

10 Deformation Theory and the Kodaira-Spencer Map

In the previous chapter, we introduced the concept of a parametrized deformation of a singularity and the notion of a versal deformation—a *universaltemplate* from which all other small deformations uniquely branch. However, how can we mathematically guarantee that a specific polynomial family we construct actually *is* versal? To answer this, we must translate the geometric idea of $allpossibledeformationdirections$ into a linear algebraic calculus. This bridges local analytic geometry with homological algebra, giving rise to Kodaira-Spencer theory and the formalism of first-order deformations.

10.1 First-Order Deformations and the Dual Numbers

In differential geometry, the tangent space at a point on a manifold consists of vectors that represent $first-order$ directions of curves passing through that point. A tangent vector $v \in T_pM$ provides a linear derivation: an operation that computes directional derivatives. In algebraic geometry and singularity theory, we emulate this by using schemes over the dual numbers.

Definition 10.1 (The Dual Numbers)**.** *The ring of dual numbers over $\mathbb{C}$ is defined as $D = \mathbb{C}[\epsilon]/(\epsilon^2)$. This is a commutative ring with a single nonzero nilpotent element ϵ strictly satisfying $\epsilon^2 = 0$.*

Geometrically, $\mathrm{Spec}(D)$ represents an $infinitesimalthickpoint$. It contains exactly one topological point (defined by $\epsilon = 0$), but its structure sheaf carries an infinitesimal tangent vector (represented by ϵ). In general, the Zariski tangent space T_pX of any algebraic variety X at a point p is precisely the set of $\mathbb{C}$-algebra homomorphisms $\mathcal{O}_{X,p} \to D$, or equivalently, the set of $\mathbb{C}$-morphisms $\mathrm{Spec}(D) \to X$ mapping the central point to p. This beautiful correspondence indicates that testing over the dual numbers D is analytically identical to computing tangent derivatives.

Definition 10.2 (First-Order Infinitesimal Deformation)**.** *A **first-order deformation** of a singularity $(X_0, 0)$ is a deformation over the base space $S = \mathrm{Spec}(D)$. Algebraically, it corresponds to an analytic space $\mathcal{X}$ that is flat over the ring D such that the restriction to $\epsilon = 0$ (the central fiber) perfectly recovers $X_0 \cong \mathcal{X} \otimes_D \mathbb{C}$.*

For a hypersurface germ $X_0 = \{f(z_1, \dots, z_n) = 0\}$, a first-order deformation corresponds to a perturbed equation:

$$f(z) + \epsilon g(z) = 0$$

Two such deformations defined by g_1 and g_2 are considered isomorphic (over D) if there exists an infinitesimal coordinate change $z_i \mapsto z_i + \epsilon\xi_i(z)$ that transforms one into the other modulo ϵ^2.

Let's compute the effect of such an infinitesimal coordinate change using the Taylor expansion:

$$f(z + \epsilon\xi) + \epsilon g_1(z + \epsilon\xi) \equiv f(z) + \epsilon \sum_{i=1}^{n} \frac{\partial f}{\partial z_i}\xi_i + \epsilon g_1(z) \pmod{\epsilon^2}.$$

Setting this equal to $f(z) + \epsilon g_2(z)$, we see that $g_2(z) - g_1(z) = \sum_{i=1}^{n} \frac{\partial f}{\partial z_i}\xi_i$. In other words, the classes of isomorphic first-order deformations are exactly the elements of the quotient ring:

$$\frac{\mathcal{O}_{\mathbb{C}^n,0}}{(f, \frac{\partial f}{\partial z_1}, \dots, \frac{\partial f}{\partial z_n})}$$

But this is precisely the Tjurina algebra T_f we introduced in §9!

Theorem 10.1 (Tangent Space of the Deformation Functor)**.** *The set of isomorphism classes of first-order deformations of a germ X_0 forms a $\mathbb{C}$-vector space, conventionally denoted as $T^1_{X_0}$. This space is finite-dimensional in the isolated-singularity setting. For a hypersurface germ $f = 0$, we have $T^1_{X_0} \cong T_f$; in particular, if f defines an isolated hypersurface singularity, then*

$$\dim_{\mathbb{C}} T^1_{X_0} = \dim_{\mathbb{C}} T_f = \tau(f).$$

More broadly, for any analytic space germ $(X_0, 0)$, homological algebra provides an elegant and universal interpretation of $T^1_{X_0}$. Specifically, if we consider the module of absolute K$ahler differentials $\Omega^1_{X_0}$, the first-order deformations are classified by the first extension group:

$$T^1_{X_0,0} \cong \mathrm{Ext}^1_{\mathcal{O}_{X_0,0}} \left(\Omega^1_{X_0,0}, \mathcal{O}_{X_0,0}\right).$$

In the particular case of an isolated complete intersection singularity (ICIS) $X_0 \subset \mathbb{C}^n$ defined by an ideal $I = (f_1, \ldots, f_k)$, one can compute this Ext^1 explicitly using the conormal exact sequence:

$$I/I^2 \xrightarrow{d} \Omega^1_{\mathbb{C}^n,0} \otimes \mathcal{O}_{X_0,0} \to \Omega^1_{X_0} \to 0.$$

Dualizing with $\mathrm{Hom}_{\mathcal{O}_{X_0,0}}(\cdot, \mathcal{O}_{X_0,0})$, the cokernel of the dual map precisely captures the deformation direction space $T^1_{X_0,0}$. This yields a concrete presentation: it is the normal module $(I/I^2)^\vee \cong \mathcal{O}^k_{X_0,0}$ modulo the image of ambient tangent vector fields $\theta_{\mathbb{C}^n,0}$ under the Jacobian matrix. Algebraically, $T^1_{X_0,0} = \mathrm{coker}\left(\partial f : \theta_{\mathbb{C}^n,0} \to \mathcal{O}^k_{X_0,0}\right)$. The Tjurina number is perfectly generalized as $\tau(X_0, 0) = \dim_{\mathbb{C}} T^1_{X_0,0}$.

10.2 The Kodaira-Spencer Map

Now, consider a general deformation $\mathcal{X} \to S$ of X_0 over an arbitrary smooth multi-dimensional base S. Pick a point $0 \in S$ corresponding to the central fiber X_0. Every tangent vector $v \in T_{S,0}$ specifies an $infinitesimal curve$ in S passing through 0. By restricting the family $\mathcal{X}$ to this infinitesimal curve, we naturally induce a first-order deformation of X_0. This induced deformation corresponds to a unique element in $T^1_{X_0}$.

Definition 10.3 (Kodaira-Spencer Map)**.** *Let $F : \mathcal{X} \to S$ be a deformation of X_0 over a smooth base S. The* ***Kodaira-Spencer map*** *evaluated at the central fiber is the natural $\mathbb{C}$-linear transformation:*

$$\rho : T_{S,0} \to T^1_{X_0}$$

which maps each tangent vector $v \in T_{S,0}$ to the isomorphism class of the first-order deformation induced by deriving the family F along v.

For a hypersurface family given by $F(z, s) = 0$ with $F(z, 0) = f(z)$, a tangent vector $v = \sum v_j \frac{\partial}{\partial s_j}$ in $T_{S,0}$ maps via the Kodaira-Spencer map to the class:

$$\rho(v) = \left[\sum_j v_j \frac{\partial F}{\partial s_j}(z, 0)\right] \in T_f.$$

For a general ICIS family $\mathcal{X} \to S$, one can work natively with relative differentials to trace $T_{S,0} \to \mathrm{Ext}^1(\Omega^1_{X_0}, \mathcal{O}_{X_0})$.

Proposition 10.1 (Relative Differentials and the Space T^1)**.** *Let $f : (X, x) \to (S, 0)$ be a deformation of an n-dimensional ICIS over a smooth base. Then on the central fiber $X_0 = f^{-1}(0)$ there is an exact sequence*

$$0 \to \mathcal{O}_{X_0,x} \otimes_{\mathbb{C}} T_0(S)^* \to \Omega_{X,x} \otimes_{\mathcal{O}_{X,x}} \mathcal{O}_{X_0,x} \to \Omega_{X_0,x} \to 0.$$

Consequently,

$$T^1_{X_0,x} \cong \mathrm{Ext}^1_{\mathcal{O}_{X_0,x}}(\Omega_{X_0,x}, \mathcal{O}_{X_0,x}),$$

and for an ICIS this group is computed by the cokernel of the Jacobian map from ambient vector fields to the normal module.

Proof sketch. This is the formulation emphasized by Looijenga in [Loo84, Ch. 6, §A–B]. The main point is the injectivity of the left-hand map. On the dense open set where f is a submersion, the sequence is just the standard exact sequence for relative differentials, so injectivity is obvious there. Because the singularity is isolated and the modules involved are coherent, this injectivity extends across the origin. Dualizing the sequence converts the left map into the Jacobian map

$$\partial f : \theta_{X,x} \to \theta(f)_x,$$

whose cokernel is exactly the module denoted $T_{f,x}$ by Looijenga. Reducing modulo the maximal ideal of the base identifies the resulting cokernel with $T^1_{X_0,x}$. This is the intrinsic explanation for why the Tjurina space is an Ext-group rather than merely a quotient written in coordinates. □

A foundational property of the Kodaira-Spencer map is compatibility with base change (Looijenga Prop 6.2): if we pullback $\mathcal{X}/S$ via a morphism $\psi : (S', s'_0) \to (S, s_0)$ to form the new family $\mathcal{X}'$, the Kodaira-Spencer map ρ' for $\mathcal{X}'$ simply factorizes through the differential $d\psi_{s'_0}$ as:

$$\rho' = \rho \circ d\psi_{s'_0}.$$

This property bridges deformation families smoothly and sets the stage for Looijenga Prop 6.3, a fundamental result connecting infinitesimal surjective conditions to local family equivalence:

Proposition 10.2 (Surjective Kodaira-Spencer ensures trivial base extensions)**.** *Let $F : \mathcal{X} \to S$ be a deformation of an isolated singularity X_0 over S. Suppose $\psi : S \to M$ is a smooth map (a submersion) with fiber $S_0 = \psi^{-1}(\psi(s_0))$, and the restriction of the Kodaira-Spencer map $\rho|_{T_{S_0}} : T_{S_0} \to T^1_{X_0}$ remains surjective. Then $\mathcal{X}$ is locally isomorphic to the pullback $\psi^*\mathcal{X}_M$ for some family $\mathcal{X}_M \to M$.*

Idea of 4-step proof. The proof utilizes deep differential topology through integration of liftable vector fields. One first proves that the relative Kodaira-Spencer map injects into the coherent sheaf theoretic structure, leveraging local flatness criteria. A critical observation from commutative algebra is that the restriction surjectivity geometrically forces the relative tangent bundle $T_{\mathcal{X}/M}$ to uniformly lift the kernel vector fields from the base. Finally, these vector fields are analytically integrated into local biholomorphisms, yielding a coordinate exchange over S that fully decomposes the family. □

10.3 Schlessinger's Versality Criterion and the Deformation Functor

In formal deformation theory, rather than dealing directly with convergent analytic germs, one formally considers infinitesimal extensions over the algebraic category $\mathbf{Art}_{\mathbb{C}}$ of local Artinian $\mathbb{C}$-algebras with residue field $\mathbb{C}$.

An object $A \in \mathbf{Art}_{\mathbb{C}}$ is a finite-dimensional local $\mathbb{C}$-algebra with a unique maximal ideal $\mathfrak{m}_A$ such that $\mathfrak{m}_A^k = 0$ for some integer $k \geq 1$. By setting $\mathfrak{m}_A^k = 0$, we forcibly ignore all polynomials of degree k and higher. Analytically, a point equipped with this ring is perceived as carrying higher-order infinitesimal vectors ($jets$) up to degree $k-1$.

The base spaces $S = \mathrm{Spec}(A)$ for $A \in \mathbf{Art}_{\mathbb{C}}$ are all topologically single-point spaces. However, their nilpotent ideals provide a hierarchy of richer tangency structures. For example:

- $A = \mathbb{C}$: Zero-order tangency, testing just a point natively.
- $A = \mathbb{C}[\epsilon]/(\epsilon^2)$: First-order tangency (the dual numbers), measuring tangent spaces.
- $A = \mathbb{C}[x, y]/(x^2, xy, y^2)$: Testing a multi-dimensional tangent plane.
- $A = \mathbb{C}[\delta]/(\delta^3)$: Second-order tangency, checking for an acceleration vector (or curvature).

A formal infinitesimal deformation of X_0 over an Artinian ring A is defined algebraically as a flat scheme $\mathcal{X}_A \to \mathrm{Spec}(A)$ such that its special fiber over $\mathbb{C} \cong A/\mathfrak{m}_A$ is canonically isomorphic to X_0.

We define the formal deformation functor $\mathrm{Def}_{X_0} : \mathbf{Art}_{\mathbb{C}} \to \mathbf{Sets}$ by mapping each local Artinian ring A to the set of isomorphism classes of deformations of X_0 over $\mathrm{Spec}(A)$. We naturally identify $T^1_{X_0} = \mathrm{Def}_{X_0}(\mathbb{C}[\epsilon]/(\epsilon^2))$. In algebraic geometry, evaluating a functor on the dual numbers to retrieve a vector space is effectively what it mathematically means to compute the $TangentSpace$ to a Functor.

According to Michael Schlessinger's fundamental criteria (1968), any functor F on small extensions of Artinian $\mathbb{C}$-algebras admitting a finite-dimensional T^1 tangent space and satisfying specific exactness gluing conditions (fiber products via pullbacks) admits a formal miniversal deformation (a $pro - representablehull$). Thus, we formally rebuild parameters dimension-by-dimension, matching Taylor coefficients modulo progressively higher maximal powers $\mathfrak{m}^k$.

For complex analytic germs, Grauert (1972) and later Kas proved that for isolated hypersurface singularities, this formal miniversal deformation actually converges algebraically, securing the existence of the smooth miniversal space over $S = \mathbb{C}^\tau$.

The Kodaira-Spencer map is the ultimate litmus test for versality, lifting the infinitesimal calculus into smooth geometric maps. Intuitively, if the map ρ is surjective at the origin, the parameter space S provides $enoughindependenttangentdirections$ to trigger every possible infinitesimal perturbation of the singularity.

Theorem 10.2 (Versality Criterion (Schlessinger/Grauert))**.** *A deformation $\pi : \mathcal{X} \to (S, s_0)$ of an isolated singularity X_0 over a smooth analytic base S is versal if and only if the Kodaira-Spencer map:*

$$\rho : T_{S,s_0} \to T^1_{X_0}$$

*is surjective. Furthermore, the deformation is **miniversal** (semi-universal) if and only if ρ is an exact isomorphism of $\mathbb{C}$-vector spaces.*

Idea of proof in Looijenga's analytic setting. The easy direction is base change: if every deformation is induced from $\mathcal{X} \to S$, then every first-order deformation is induced as well, so ρ must be surjective. The converse is where Looijenga's analytic argument becomes useful [Loo84, Ch. 6, §B–C]. One first enlarges any given deformation by adjoining parameters representing a basis of the cokernel of the reduced Kodaira-Spencer map; this produces a deformation whose reduced Kodaira-Spencer map is an isomorphism.

The real work is the comparison theorem between two deformations with surjective Kodaira-Spencer maps. Looijenga interpolates between two defining maps f^0 and f^1 by the family

$f^u = (1-u)f^0 + uf^1$ and shows that the values of u for which surjectivity fails form only a finite set. Over the open complement one upgrades the infinitesimal surjectivity statement to actual liftable vector fields v on the source and w on the base satisfying $df(v) = w \circ F$. A Malgrange-preparation argument is the key algebraic input here: it turns the vanishing of the cokernel into solvability of the lifting equation. Integrating v and w then gives local biholomorphisms intertwining the two families. This proves versality. If the reduced Kodaira-Spencer map is an isomorphism, then the derivative of any inducing map is forced to be unique, which is exactly miniversality. □

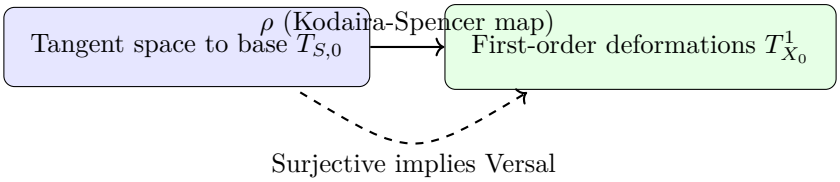

Figure 17: The Kodaira-Spencer Theory directly translates the infinitesimal geometry of base manifolds onto the algebraic obstructions of space embeddings.

Proof Sketch. The *onlyif* part is straight-forward: if a deformation is versal, any first-order deformation over D can be pulled back from S via some map $\mathrm{Spec}(D) \to S$. This tangent direction perfectly hits the targeted first-order class, confirming ρ is surjective.

The *if* direction heavily relies on the formal power series matching and geometric convergence constraints. Given a surjective ρ, one recursively builds a formal mapping $\hat{S}' \to \hat{S}$ lifting any other formal deformation step-by-step using Taylor series matching. The major analytic difficulty lies in proving that this formal mapping actually converges to define a genuine holomorphic map. This deep fact depends on coherence theorems and Artin's Approximation Theorem, ultimately establishing that an infinitesimally comprehensive family (the whole tangent spectrum) rigorously contains all local geometric information of the completely unfolded parameters. □

10.4 Miniversal Construction and Cohen-Macaulay Property

As in (Looijenga 6.7), we can generalize Mather's construction for hypersurfaces to an arbitrary ICIS locally given by $f_1 = \cdots = f_k = 0$. By taking classes $g_1, \ldots, g_\tau \in \mathcal{O}^k_{\mathbb{C}^n,0}$ whose images form a $\mathbb{C}$-basis for $T^1_{X_0} = \mathrm{coker}(\partial f : \theta_{\mathbb{C}^n,0} \to \mathcal{O}^k_{X_0,0})$, we construct a natural deformation space over $S = \mathbb{C}^\tau$ by explicitly perturbing the equations:

$$F_i(z, s_1, \ldots, s_\tau) = f_i(z) + \sum_{j=1}^{\tau} s_j (g_j)_i(z) \quad (1 \le i \le k).$$

Let $\mathcal{X}$ be the zero locus of these F_i in $\mathbb{C}^n \times S$. Because the perturbation is added directly to a regular sequence, $F_1, \ldots, F_k$ remains a regular sequence at the origin. The mapping $\pi : \mathcal{X} \to S$ defined by projection is naturally flat, and the Kodaira-Spencer map evaluates precisely to the linearly independent classes g_j. Therefore, $\mathcal{X}$ forms a miniversal deformation of the ICIS X_0.

A spectacular algebraic realization is the Cohen-Macaulay nature of the Tjurina ideal structure within the total versal family (Looijenga Prop 6.12).

Proposition 10.3 (Cohen-Macaulay Property of Miniversal Deformations)**.** *If $\pi : \mathcal{X} \to S$ is a miniversal deformation of an ICIS X_0 of dimension $n-k$, then the relative deformation module*

$\mathcal{T}_\pi$ *extending the Tjurina structure along the family is a flat Cohen-Macaulay* $\mathcal{O}_S$*-module of relative dimension zero (it is finite over* S*), perfectly bridging local duality theorems and deeper invariants globally across singular strata.*

Proof. This elegantly stems from the exact sequence defined by relative dualizing sheaves and the fundamental theorem that a module finite over a regular local ring S (since S is smooth, $\dim S = \tau$) whose depth equals the dimension of S is necessarily Cohen-Macaulay. It is a critical component ensuring flat base changes cleanly commute with homological data when evaluating Tjurina numbers of nearby fibers along varying perturbations. □

10.5 The Period Mapping and $\tau \leq \mu$

While the Kodaira-Spencer map elegantly aligns tangent spaces with first-order algebraic deformations, it relies on formal module theory. A profoundly analytic method to study the versal deformation space S involves Hodge theory and the integration of holomorphic forms. Consider a miniversal deformation $\pi : \mathcal{X} \to S$ of an isolated hypersurface singularity f. For any $s \in S$ near the origin not lying on the discriminant Δ, the fiber $X_s = \pi^{-1}(s)$ is a smooth Milnor fiber.

By picking a non-vanishing relative differential form $\omega = \frac{dz_1 \wedge \cdots \wedge dz_n}{dF}$ on X_s, we can define the **Period Mapping**. For each homology cycle $\gamma_i \in H_{n-1}(X_s; \mathbb{Z})$, we integrate:

$$\mathcal{P}(s) = \left(\int_{\gamma_1} \omega, \ldots, \int_{\gamma_\mu} \omega \right) \in \mathbb{C}^\mu.$$

This defines a multiple-valued holomorphic map from the discriminant complement $S \setminus \Delta$ into the complex vector space $H^{n-1}(X_s; \mathbb{C}) \cong \mathbb{C}^\mu$. By projecting into projective space (or Grassmannians), one models exactly how the Hodge filtration continuously transforms as we vary the parameters s.

A fundamental theorem in deformation theory tightly links this topological integration map back to the algebraic invariants. Brieskorn and Greuel proved that the derivative of the period mapping (essentially the Gauss-Manin connection evaluated on the Kodaira-Spencer tangent vectors) is an **immersion** near the origin. Since S is τ-dimensional, and the target $H^{n-1}(X_s; \mathbb{C})$ is μ-dimensional, the injectivity of the period map's differential analytically forces the dimensions to satisfy:

$$\tau \leq \mu$$

This analytically rigorously proves the inequality we algebraically observed earlier! The Tjurina number is bounded by the Milnor number because the parameter space of the miniversal deformation embeds locally inside the space of cohomological periods.

10.6 Discriminant-Preserving Derivations and Saito's $\tau = \mu$ Criterion

The boundary of the smooth phase space is determined by the discriminant hypersurface $\Delta \subset S$. Geometrically, determining which vector fields on S are tangent to Δ (i.e., discriminant-preserving derivations $\theta_{S,0}\langle\Delta\rangle$) characterizes the local topology of the singularities.

Let $v \in \theta_{S,0}$ be a holomorphic vector field on the base space. We say v is tangent to the discriminant if $v(h) \in (h)$ where $h = 0$ is the local reduced defining equation for Δ.

Saito profoundly demonstrated that $\tau = \mu$ holds if and only if the singularity is quasi-homogeneous. The most elegant proof connects these derivations. For an isolated complete intersection singularity (ICIS), the Tjurina number and Milnor number align perfectly when there exists a well-defined global $\mathbb{C}^*$-action. In the quasi-homogeneous scenario, the Euler vector

field precisely lifts to the parameter space S, presenting as a weighted scaling structure on the versal deformation $F(z, s)$.

Through Greuel's formulation, this scaling allows the local Gauss-Manin connection to construct a non-degenerate perfect pairing on the Brieskorn lattice, matching the algebraic and topological ranks perfectly.

10.7 Optional: Severi Strata for Plane Curve Singularities

The discriminant of a miniversal deformation of a plane curve singularity carries a much finer structure than the simple dichotomy "smooth fiber versus singular fiber". Let $\pi : \mathcal{C} \to S$ be a miniversal deformation of a reduced plane curve singularity $(C_0, 0) \subset (\mathbb{C}^2, 0)$, let $\Delta \subset S$ be its discriminant, and write $\delta = \delta(C_0, 0)$. Inside Δ one can stratify parameter values by how much of the original delta-invariant survives in the singularities of the nearby fiber.

Definition 10.4 (Severi Strata / Equigeneric Strata)**.** *For $1 \leq k \leq \delta$, define the k-th closed Severi stratum by*

$$D(k) = \left\{ s \in \Delta : \sum_{p \in \mathrm{Sing}(C_s)} \delta(C_s, p) \geq k \right\}.$$

Equivalently, the locally closed pieces $D(k) \setminus D(k+1)$ consist of those fibers whose singular points have total delta-invariant exactly k. The smallest stratum $D(\delta)$ is the ***δ-constant stratum****; it parametrizes deformations for which the full delta of the original singularity survives in the nearby fiber. In the literature these loci are also called the* ***equigeneric strata*** *of the versal deformation [GLS07; Wal04; CMS16].*

Example 10.1 (Node, Cusp, and Tacnode)**.** *Three basic examples already show the range of behaviors.*

1. *For the node $xy = 0$, one has $\delta = 1$ and the miniversal deformation is $xy - s = 0$. The discriminant is just $s = 0$, so there is only one Severi stratum.*
2. *For the cusp $y^2 = x^3$, one again has $\delta = 1$. In the miniversal family $y^2 = x^3 + ax + b$, the discriminant $4a^3 + 27b^2 = 0$ is generically nodal, while the origin is the cusp itself. Thus equigenericity does* not *imply equisingularity.*
3. *For the tacnode $y^2 = x^4$, one has $\delta = 2$. In a miniversal deformation, a generic point of Δ corresponds to a single node (total delta 1), while the smaller locus $D(2)$ is the equigeneric stratum where the total delta remains 2; generically it corresponds to a splitting into two nodes. This is the first genuinely nested Severi picture.*

For the tacnode one can choose a very concrete two-parameter slice of the miniversal base by writing

$$C_{u,v} : y^2 = x^4 - 2ux^2 + v.$$

This is not the most generic slice, but it is the most transparent one for calculations. A point (x, y) is singular on $C_{u,v}$ precisely when

$$y = 0, \qquad 4x(x^2 - u) = 0, \qquad x^4 - 2ux^2 + v = 0.$$

Hence either $x = 0$ and $v = 0$, or $x^2 = u$ and $v = u^2$. Therefore the discriminant in this slice is the union

$$\Pi \cap \Delta = \{v = 0\} \cup \{v = u^2\}.$$

These two branches have different equigeneric meanings.

- On the line $v = 0$ with $u \neq 0$, the fiber has one node at $(0, 0)$, since the quadratic part is $y^2 - 2ux^2$.
- On the parabola $v = u^2$ with $u \neq 0$, the fiber has two nodes at $(\pm\sqrt{u}, 0)$, so the total delta remains 2.
- At $(u, v) = (0, 0)$ the two loci meet tangentially, and the fiber is the original tacnode.

Thus in this explicit slice one sees

$$D(1) \cap \Pi = \{v = 0\} \cup \{v = u^2\}, \qquad D(2) \cap \Pi = \{v = u^2\}.$$

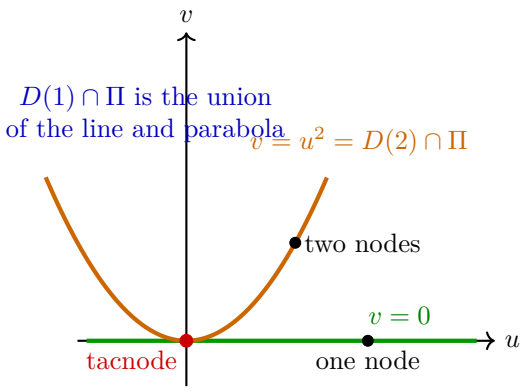

Figure 18: An explicit two-parameter slice of the tacnode versal deformation. The full discriminant $D(1) \cap \Pi$ is the union of the line $v = 0$ and the parabola $v = u^2$, while the smaller equigeneric stratum $D(2) \cap \Pi$ is exactly the parabola. Generic points on the two components correspond to one node and two nodes, respectively.

Example 10.2 (Nodalizing the Tacnode Along Explicit Arcs)**.** *The slice $C_{u,v} : y^2 = x^4 - 2ux^2 + v$ makes the nodalization process completely explicit.*

If we move along the arc

$$\gamma_1(t) = (t, 0),$$

then

$$C_{\gamma_1(t)} : y^2 = x^4 - 2tx^2 = x^2(x^2 - 2t).$$

For $t \neq 0$, the only singular point near the origin is $(0, 0)$, and its quadratic part is $y^2 - 2tx^2$, so it is an ordinary node. This is a path inside $D(1)$ but not inside $D(2)$.

If instead we move along the equigeneric arc

$$\gamma_2(t) = (t^2, t^4),$$

then

$$C_{\gamma_2(t)} : y^2 = x^4 - 2t^2x^2 + t^4 = (x^2 - t^2)^2.$$

For $t \neq 0$, the singular points are exactly $(x, y) = (\pm t, 0)$. At either point, writing $x = \pm t + \xi$ gives

$$y^2 - 4t^2\xi^2 + \textit{higher order terms} = 0,$$

so both singularities are ordinary nodes. Thus the tacnode has split into two nodes, which is the expected δ-nodal deformation along the smaller Severi stratum $D(2)$.

Finally, perturbing transversely off the parabola, for instance to $(u, v) = (t^2, t^4+\varepsilon)$ *with* $\varepsilon \neq 0$*, smooths both nodes simultaneously. In this way the picture*

$$\textit{tacnode} \longrightarrow \textit{two nodes} \longrightarrow \textit{smooth fiber}$$

is visible directly in the parameter plane.

Example 10.3 (Full Discriminant Elimination for the Cusp)**.** *The cusp family already gives a complete elimination computation with almost no machinery. Consider*

$$F(x, y; a, b) = y^2 - x^3 - ax - b.$$

The fiber $F_{a,b} = 0$ *is singular exactly when*

$$F = 0, \qquad \frac{\partial F}{\partial y} = 2y = 0, \qquad \frac{\partial F}{\partial x} = -3x^2 - a = 0.$$

Thus $y = 0$*,* $a = -3x^2$*, and then*

$$b = -x^3 - ax = -x^3 + 3x^3 = 2x^3.$$

Eliminating x *gives the familiar cusp discriminant equation*

$$4a^3 + 27b^2 = 4(-3x^2)^3 + 27(2x^3)^2 = -108x^6 + 108x^6 = 0.$$

Conversely, every point on the discriminant is obtained from the parametrization

$$a = -3t^2, \qquad b = 2t^3.$$

For $t \neq 0$*, the singularity is a node, while at* $t = 0$ *one recovers the cusp itself. So the discriminant is already singular, even though its generic point corresponds to the simplest possible singular fiber.*

Remark 10.1 (Basic Properties)**.** *Three structural facts are worth remembering.*

1. *The generic point of the* δ*-constant stratum corresponds to a* δ*-nodal deformation, so the codimension of the equigeneric locus is exactly* δ*.*
2. *The Severi strata are usually singular even though the miniversal base* S *is smooth. For irreducible plane curve singularities, the* δ*-constant stratum is Lagrangian with respect to the symplectic form obtained from the intersection pairing via the period mapping, and the higher Severi strata are coisotropic [CMS16].*
3. *In many simple and ADE examples these strata are Cohen–Macaulay, which explains why equigeneric deformation theory is more rigid than the full discriminant might suggest.*

Remark 10.2 (Why the δ-Constant Stratum is Lagrangian)**.** *For a plane curve singularity, the Milnor fiber is a surface, so* $H_1(F; \mathbb{C})$ *carries a genuine symplectic intersection form. Away from the discriminant, the period mapping transports this symplectic geometry to the versal base. Now a generic point of the* δ*-constant stratum can be reached by deforming the original singularity into* δ *ordinary nodes. Each node contributes a vanishing cycle, and these vanishing cycles can be chosen pairwise disjoint; hence they span a maximal isotropic subspace of* $H_1(F; \mathbb{C})$*. Tangent directions along the* δ*-constant stratum are precisely those directions for which this maximal isotropic collection continues to collapse simultaneously. This is the geometric reason the* δ*-constant stratum is Lagrangian. If one only asks that fewer cycles remain singular, the isotropic condition is no longer maximal, and one naturally gets the coisotropic behavior of the larger Severi strata.*

Definition 10.5 (Hilbert Scheme of Points on a Singular Curve)**.** *For a plane curve germ* $(C, 0)$*, the punctual Hilbert scheme* $\mathrm{Hilb}^n(C, 0)$ *parametrizes length-*n *subschemes supported at the singular point. More globally, if* C *is a locally planar curve, then* $C^{[n]}$ *denotes the Hilbert scheme of all length-*n *zero-dimensional subschemes on* C*.*

These Hilbert schemes measure how ideals thicken the singular point. For locally planar curves they have pure dimension n and behave far better than one would expect for an arbitrary singular curve. Shende's theorem packages the Euler characteristics of all Hilbert schemes into a single BPS-type expansion. If C is an integral locally planar curve of arithmetic genus g, then there are integers $n_h(C)$ such that

$$\sum_{m\geq 0} q^m \chi(C^{[m]}) = \sum_{h=0}^{g} n_h(C)\, q^{g-h}(1-q)^{2h-2},$$

and these coefficients $n_h(C)$ are exactly the multiplicities of the Severi strata of geometric genus h at the central point of the versal deformation [She12]. In the particularly important case where a rational curve has a single plane singularity of delta-invariant δ, we have $g = \delta$, so the same formula reads

$$\sum_{m\geq 0} q^m \chi(C^{[m]}) = \sum_{h=0}^{\delta} n_h(C)\, q^{\delta-h}(1-q)^{2h-2}.$$

Thus the Hilbert-scheme Euler characteristics do not just correlate with Severi strata; they literally determine their multiplicities.

There is a deeper geometric reason this formula is so effective. The compactified Jacobian $\overline{J}(C)$ of a locally planar integral curve packages rank-one torsion-free sheaves on C, and its topology is remarkably rigid [Pio06]. Migliorini and Shende proved a support theorem saying that, in a family with smooth relative Hilbert schemes, no unexpected perverse summands appear in positive codimension; equivalently, the perverse filtration on $H^*(\overline{J}(C))$ controls the cohomology of *all* Hilbert schemes $C^{[m]}$ at once [MS13]. In the singularity setting, this means the compactified Jacobian sits between Severi geometry and knot theory:

- Severi strata measure how singularities persist in the versal base;
- Hilbert schemes measure the zero-dimensional geometry of the singular fiber;
- the compactified Jacobian and its perverse filtration organize these Hilbert schemes into a single package.

When the curve has a single plane singularity, Oblomkov–Shende related generating series of Euler characteristics of refined punctual Hilbert schemes to the HOMFLY polynomial of the link, and Oblomkov–Rasmussen–Shende lifted this relationship to HOMFLY homology [OS12; ORS18]. In this way:

- Severi strata record how much of the original δ survives under deformation;
- Hilbert schemes record how length-n subschemes pile up at the singular point;
- knot polynomials record the topology of the boundary link of the same germ.

They are different shadows of one and the same local plane curve singularity.

10.8 Deeper Obstruction Theory: $T^2_{X_0}$

What happens beyond first-order deformations? If $T^1_{X_0}$ classifies the tangent space, there are natural higher cohomology groups $T^i_{X_0}$ defined via the cotangent complex (or Schlessinger's module $\mathrm{Ex}_{\mathbb{C}}(R, R)$).

Specifically, $T^2_{X_0}$ precisely houses the **obstructions** to lifting deformations. If one begins with a first-order deformation over $\mathbb{C}[\epsilon]/(\epsilon^2)$, it may not be possible to find a second-order polynomial matching the flatness criteria over $\mathbb{C}[\epsilon]/(\epsilon^3)$. The failure to lift creates a uniquely defined cocycle class perfectly living inside $T^2_{X_0}$.

If $T^2_{X_0} = 0$, the singularity is said to be **unobstructed**. Every infinitesimal deformation extends formally to a full, smooth analytic family.

For instance:

- **Isolated Hypersurface Singularities:** Always unobstructed, $T^2_{X_0} = 0$. Small perturbations $f + sg$ are inherently flat without matching conditions.
- **Isolated Complete Intersections (ICIS):** Always unobstructed, $T^2_{X_0} = 0$. (Pioneering result by Kas and Schlessinger).
- **Non-complete Intersections:** A generic space curve singularity (e.g., the cone over a rational normal curve of high degree) is often heavily obstructed, featuring a massive $T^2_{X_0}$ space. Their versal deformation base spaces S are famously no longer smooth $\mathbb{C}^\tau$, but comprise intersecting singular components of varying dimensions!

10.9 Exercises

Exercise 10.1. *Consider the singularity $f(x, y) = x^4 + y^4$, representing an isolated singularity of Milnor number $\mu = 9$. Suppose we propose a family parameterised by $S = \mathbb{C}^2$: $F(x, y, s_1, s_2) = x^4+y^4+s_1x^2y^2+s_2xy$. Compute the explicit Tjurina algebra basis for f. Use the Kodaira-Spencer map to evaluate the span of $\rho(\frac{\partial}{\partial s_1})$ and $\rho(\frac{\partial}{\partial s_2})$. Conclude whether this 2-parameter deformation is versal.*

Exercise 10.2. *Let $T^1_{X_0}$ designate the set of first-order deformations. There exists a higher cohomology group $T^2_{X_0}$ reflecting obstructions to extending a given first-order deformation over D to a second-order deformation over $\mathbb{C}[\epsilon]/(\epsilon^3)$. For complete intersection hypersurface singularities, it is known that $T^2_{X_0} = 0$. Explain intuitively why this implies any generic polynomial generator $g(z)$ yields an unobstructed valid direction for a full analytic deformation $f(z) + sg(z)$.*

11 Fitting Ideals and Critical Spaces

When investigating singularities of functions $f : (\mathbb{C}^n, 0) \to (\mathbb{C}, 0)$, the critical points simply occur where the partial derivatives vanish. However, for a generic holomorphic mapping between varieties $F : X \to Y$, understanding the singularities goes beyond merely checking when the rank of the Jacobian matrix drops. To do this robustly, particularly to track the scheme structure and multiplicities of the critical locus, we use the algebraic concept of a **Fitting ideal**. It allows us to inherently capture the singular locus independent of the particular coordinates chosen.

11.1 Fitting Ideals of Modules

Let R be a commutative ring (typically the local coordinate ring $\mathcal{O}_{X,x}$ of a variety), and let M be a finitely generated R-module.

Any finitely generated R-module M admits a free presentation:

$$R^p \xrightarrow{\phi} R^q \to M \to 0,$$

where the map ϕ is represented by a $q \times p$ matrix A with entries in R. The shape of this matrix encodes all the relations amongst a set of q generators of M.

Definition 11.1 (Fitting Ideals)**.** *For every integer $k \geq 0$, the k-th **Fitting ideal** of M, denoted $Fitt_k(M)$, is defined as the ideal in R generated by all $(q-k) \times (q-k)$ minors (determinants of submatrices) of A. If $q - k \leq 0$, we define $Fitt_k(M) = R$. If $q - k > \min(p, q)$, we define $Fitt_k(M) = 0$.*

A remarkable consequence of basic linear algebra is that the ideal $\mathrm{Fitt}_k(M)$ does not depend on the choice of presentation. It is an intrinsic invariant of the module M. They form an ascending chain:

$$0 \subset \mathrm{Fitt}_0(M) \subset \mathrm{Fitt}_1(M) \subset \cdots \subset \mathrm{Fitt}_q(M) = R.$$

Proposition 11.1. *The 0-th Fitting ideal $Fitt_0(M)$ is contained in the annihilator ideal $\mathrm{Ann}_R(M)$. Furthermore, they define the same reduced space (their radicals are equal): $\sqrt{Fitt_0(M)} = \sqrt{\mathrm{Ann}_R(M)}$. Thus, the support of M, $Supp(M) = \mathrm{Spec}\,(R/\,\mathrm{Ann}_R(M))$, is exactly defined by $V(Fitt_0(M))$.*

In analytic geometry, the k-th Fitting ideal is naturally associated to the locus where M requires at least $k+1$ generators.

Proposition 11.2 (Base Change for Fitting Ideals)**.** *Let $\varphi : R \to S$ be a homomorphism of commutative rings and let M be a finitely generated R-module. Then for every $k \geq 0$,*

$$Fitt_k(S \otimes_R M) = Fitt_k(M) \cdot S.$$

Equivalently, on analytic spaces the Fitting ideal sheaf of a coherent module pulls back under arbitrary base change.

Proof idea. Take a finite presentation $R^p \xrightarrow{A} R^q \to M \to 0$. After tensoring with S one gets the presentation $S^p \xrightarrow{\varphi(A)} S^q \to S \otimes_R M \to 0$. The relevant minors of $\varphi(A)$ are simply the images under φ of the corresponding minors of A. Since Fitting ideals are presentation-independent, the formula follows. This is the commutative-algebra input behind Looijenga's repeated observation that critical and discriminant spaces commute with base change [Loo84, Ch. 4, §D–E]. □

11.2 The Module of Relative Differentials

To define singularities of morphisms, we need a module that captures $first derivatives$. This is exactly the sheaf of relative Kähler differentials $\Omega^1_{X/Y}$.

Let $\varphi : X \to Y$ be a morphism of varieties (or analytic spaces) corresponding algebraically to a ring homomorphism $\varphi^{\#} : A \to B$.

Definition 11.2 (Relative Differentials)**.** *The module of relative differentials $\Omega^1_{B/A}$ is generated over B by symbols db for all $b \in B$, subject to the relations:*

1. $d(b_1 + b_2) = db_1 + db_2$ *(additivity)*
2. $d(b_1 b_2) = b_1 db_2 + b_2 db_1$ *(Leibniz rule)*

3. $d(a) = 0$ *for any* $a \in \varphi^{\#}(A)$ *(functions from the base are constant relative to* A*)*

If $Y = \mathbb{C}$, then $\Omega^1_{X/\mathbb{C}}$ is just the absolute cotangent sheaf Ω^1_X. If $B = \mathbb{C}[x_1, \ldots, x_n]/(f_1, \ldots, f_m)$, we have an explicit presentation:

$$B^m \xrightarrow{J} B^n \to \Omega^1_{B/\mathbb{C}} \to 0$$

where J is exactly the Jacobian matrix $\mathrm{Jac}(f) = (\partial f_i/\partial x_j)$.

11.3 The Critical Space

Now suppose $F : X \to Y$ is a morphism between non-singular spaces of dimensions n and p, respectively. The relative differential $\Omega^1_{X/Y}$ captures the behavior of the derivative of F. The map F is a submersion (smooth) precisely when its differential dF is surjective. Algebraically, this occurs exactly where $\Omega^1_{X/Y}$ is locally free of rank $n - p$.

Definition 11.3 (Critical Locus and Critical Space)**.** *The* ***critical locus*** *of the morphism* $F : X \to Y$ *is defined as the support of the singular behavior, i.e., where* $\Omega^1_{X/Y}$ *is not a free module of rank* $n - p$*.*

Using Fitting ideals, we define the ***critical space*** *scheme-theoretically. The critical ideal* I_C *is defined as the* $(n - p)$*-th Fitting ideal:*

$$I_C = Fitt_{n-p}(\Omega^1_{X/Y}).$$

The scheme $C = \mathrm{Spec}(\mathcal{O}_X/I_C)$ *is called the critical space.*

Proposition 11.3 (Critical Space Commutes with Base Change)**.** *Consider a cartesian diagram of analytic germs*

$$\begin{array}{ccc} (X', x') & \xrightarrow{\tilde{g}} & (X, x) \\ {\scriptstyle F'}\downarrow & & \downarrow{\scriptstyle F} \\ (Y', y') & \xrightarrow{g} & (Y, y) \end{array}$$

and assume the fibers of F *have pure dimension* n*. Then the critical ideal of* F' *is generated by the pullback of the critical ideal of* F*; equivalently, the critical space of* F' *is the scheme-theoretic pullback of the critical space of* F*.*

Proof idea. This is one of the main structural points of [Loo84, Ch. 4, §A]. Locally embed X in a smooth ambient space by equations $\phi_1, \ldots, \phi_r$ and extend F to a map in ambient coordinates. The critical ideal is generated by the maximal minors of the Jacobian matrix of $(\phi_1, \ldots, \phi_r, F_1, \ldots, F_p)$. After base change, the new ambient presentation is obtained by adjoining equations for the base, so the enlarged Jacobian matrix differs from the old one only by obvious identity blocks in the base directions. Its maximal minors therefore generate exactly the pullback of the old critical ideal. In the language of relative differentials, this is the same statement as saying that the defining Fitting ideal of $\Omega^1_{X/Y}$ is compatible with base change via Proposition 11.2. □

For $F : \mathbb{C}^n \to \mathbb{C}^p$, this implies I_C is generated by all maximal $p \times p$ minors of the Jacobian matrix of F. Notice that by viewing it as a Fitting ideal, the scheme structure (the multiplicity of the critical point) is coordinate-free.

Example 11.1 (Map to $\mathbb{C}$)**.** *Let $f : \mathbb{C}^2 \to \mathbb{C}$ be given by $f(x, y) = x^2 y$. The relative dimension is $n - p = 2 - 1 = 1$. The Jacobian matrix is $(2xy, x^2)$. The module $\Omega^1_{\mathbb{C}^2/\mathbb{C}}$ has presentation:*

$$\mathcal{O}^1_{\mathbb{C}^2} \xrightarrow{\begin{pmatrix} 2xy & x^2 \end{pmatrix}} \mathcal{O}^2_{\mathbb{C}^2} \to \Omega^1_{\mathbb{C}^2/\mathbb{C}} \to 0$$

Here $q = 2$, $p = 1$. We are interested in $Fitt_1(\Omega^1_{\mathbb{C}^2/\mathbb{C}})$, which is $(2-1) \times (2-1) = 1 \times 1$ minors. The ideal generated by 1×1 minors is exactly $I_C = (2xy, x^2)$. The critical space is $C = V(x^2, 2xy)$, which restricts exactly to the y-axis (where $x = 0$), but importantly, the structure as a non-reduced scheme gives it multiplicity 2 at the origin.

11.4 Exercises

Exercise 11.1. *Compute the critical space structure for the map $F : \mathbb{C}^2 \to \mathbb{C}^2$ given by $F(x, y) = (x^2, y^2)$. Write down the presentation matrix and explicitly calculate $Fitt_0(\Omega^1_{\mathbb{C}^2/\mathbb{C}^2})$. Show that the critical space is supported on the union of the axes $\{x = 0\} \cup \{y = 0\}$.*

Exercise 11.2. *Let A be a ring and $M = A \oplus (A/I)$. Find a presentation matrix for M and calculate its Fitting ideals $Fitt_0(M)$ and $Fitt_1(M)$.*

Exercise 11.3. *Show that if X is defined by a single irreducible polynomial $f(x, y, z) = 0$ in $\mathbb{C}^3$, then the singular locus $\mathrm{Sing}(X)$ defined as the vanishing of the Jacobian criteria exactly coincides with the support of $V(Fitt_2(\Omega^1_{X/\mathbb{C}}))$.*

12 Thom Singularity Spaces and Discriminants

In the previous chapter, we identified the critical space C of a mapping $F : X \to Y$ using the Fitting ideals of the relative differential sheaf $\Omega^1_{X/Y}$. But not all critical points are born equal—some are *moresingular* than others. To organically stratify the singular behavior, we introduce the Thom-Boardman singularity classes. Moreover, mapping the critical space into the target space Y produces the **discriminant**, a highly intrinsic object that parameterizes the singular fibers of a family of varieties.

12.1 Thom-Boardman Singularity Strata

Let $F : M \to N$ be a smooth mapping between manifolds of dimension n and p. At any point $x \in M$, the differential $dF_x : T_xM \to T_{F(x)}N$ has a certain rank. The critical points are exactly those where the rank is strictly less than $\min(n, p)$.

Rene Thom and J.M. Boardman introduced a way to systematically classify the degeneracy of dF_x.

Definition 12.1 (First Order Boardman Symbol)**.** *For each integer $i \geq \max(0, n-p)$, we define the set:*

$$\Sigma^i(F) = \{x \in M \mid \dim \ker(dF_x) = i\} = \{x \in M \mid \mathrm{rank}(dF_x) = n - i\}.$$

If F is reasonably generic (a condition formalized by Thom's *Transversality Theorem*), $\Sigma^i(F)$ is a smooth submanifold of M. Since $\Sigma^i(F)$ is a manifold, we can restrict F to this stratum $F|_{\Sigma^i(F)} : \Sigma^i(F) \to N$. We can then ask for the critical points of *this* restricted map!

Definition 12.2 (Higher Order Boardman Symbols)**.** *By iterating this process, taking the kernel dimension j of the differential of the restriction of F on Σ^i, we obtain the second-order singularity strata $\Sigma^{i,j}(F)$. Continuing this indefinitely yields an infinite sequence of non-increasing integers $I = (i_1, i_2, i_3, \dots)$ representing the **Thom-Boardman symbol** $\Sigma^I(F)$.*

For example, a Morse singularity (a generic fold) corresponds to $\Sigma^{1,0}$. A single coordinate differentiation brings the rank down by 1 (the Σ^1 condition), but the second derivative (Hessian) is non-degenerate, so restricting to the critical manifold drops no further rank (the 0 condition). A cusp corresponds to $\Sigma^{1,1,0}$.

12.2 The Discriminant Space

Looking at the base space Y offers a different but ultimately more parameter-geometric perspective.

Definition 12.3 (Discriminant Space)**.** *Let $F : X \to Y$ be a finite proper morphism. Let $C \subset X$ be its critical space (defined by the scheme structure $Fitt_{n-p}(\Omega^1_{X/Y})$ discussed in §11). The **discriminant space** $D \subset Y$ is defined as the scheme-theoretic image of the critical space. Algebraically, since F is finite, the pushforward $F_*\mathcal{O}_C$ is a finitely generated $\mathcal{O}_Y$-module. The discriminant ideal is defined as:*

$$I_D = Fitt_0(F_*\mathcal{O}_C).$$

Theorem 12.1 (Base Change and Purity of the Discriminant)**.** *Let $f : (\mathbb{C}^{n+k}, 0) \to (\mathbb{C}^k, 0)$ define an ICIS, and let C_f be its critical space. Then:*

1. *the discriminant space defined by $I_{D_f} = Fitt_0(f_*\mathcal{O}_{C_f})$ commutes with base change;*
2. *the ideal $I_{D_f} \subset \mathcal{O}_{\mathbb{C}^k,0}$ is principal.*

In particular, the discriminant of an ICIS is naturally a hypersurface, possibly with non-reduced scheme structure.

Proof idea. The first assertion is the direct analogue of the critical-space base-change property and is exactly why Looijenga defines the discriminant using $\mathrm{Fitt}_0(f_*\mathcal{O}_{C_f})$ rather than by a naive set-theoretic image [Loo84, Ch. 4, §E]. Because $f|_{C_f}$ is finite, the pushforward $f_*\mathcal{O}_{C_f}$ is a coherent $\mathcal{O}_{\mathbb{C}^k,0}$-module, and Proposition 11.2 shows that its 0-th Fitting ideal behaves well under pullback.

For the second assertion, one uses the Cohen–Macaulay property of the critical space. Looijenga proves that $\mathcal{O}_{C_f,0}$ is Cohen–Macaulay of dimension $k-1$. Viewed as a finite module over the regular local ring $R = \mathcal{O}_{\mathbb{C}^k,0}$ of dimension k, it therefore has depth $k-1$. By the Auslander–Buchsbaum formula, its projective dimension over R is 1. Hence it admits a square presentation

$$0 \to R^q \xrightarrow{A} R^q \to f_*\mathcal{O}_{C_f} \to 0.$$

But then $\mathrm{Fitt}_0(f_*\mathcal{O}_{C_f})$ is generated by the determinant of A, so it is principal. This is Looijenga's purity theorem for the discriminant in the ICIS case. □

Geometrically, the support of D is $F(\mathrm{Supp}(C))$. It consists of all points $y \in Y$ such that the fiber $F^{-1}(y)$ is singular (or non-reduced). If X and Y have the same dimension (e.g., F is a finite branched covering), the discriminant D is a principal divisor (a hypersurface) in Y, given locally by a single equation.

Remark 12.1 (Reduced Discriminant and Quadratic Singularities)**.** *Looijenga pushes this one step further: regular points of the discriminant correspond exactly to fibers containing a single quadratic singularity. The proof compares the multiplicity-one condition on the discriminant with the quadratic local normal form for the critical space. So the reducedness of the discriminant is not a cosmetic scheme-theoretic refinement; it is a precise measure of whether the generic singular fiber is Morse in the target direction.*

12.3 Versal Unfoldings and the Cusp Catastrophe

To see this in action, we compute the critical space and the discriminant of the universal deformation (unfolding) of the A_2 singularity.

Let $f(x) = x^3$. We unfold it into a family of functions parameterised by $u \in \mathbb{C}$:

$$F(x, u) = x^3 + ux.$$

We define the geometric mapping space $\Phi : \mathbb{C}^2_{(x,u)} \to \mathbb{C}^2_{(y,u)}$ given by mapping (x, u) to its function value and parameters:

$$\Phi(x, u) = (F(x, u), u) = (x^3 + ux, u).$$

1. The Critical Space C: The topological setting treats mapping $X = \mathbb{C}^2$ to $Y = \mathbb{C}^2$. The differential matrix is:

$$d\Phi = \begin{pmatrix} \frac{\partial y}{\partial x} & \frac{\partial y}{\partial u} \\ \frac{\partial u}{\partial x} & \frac{\partial u}{\partial u} \end{pmatrix} = \begin{pmatrix} 3x^2 + u & x \\ 0 & 1 \end{pmatrix}$$

The rank drops below 2 precisely when the determinant vanishes, i.e., $3x^2 + u = 0$. Thus, the critical space $C \subset \mathbb{C}^2$ is the smooth parabola $u = -3x^2$.

2. The Discriminant Space D: The discriminant is the image of C under Φ. We substitute the critical relation $u = -3x^2$ into the mapping equations $y = x^3 + ux$:

$$y = x^3 + (-3x^2)x = -2x^3.$$

We can eliminate x by squaring y and cubing u:

$$y^2 = (-2x^3)^2 = 4x^6 = 4\left(-\frac{u}{3}\right)^3 = -\frac{4}{27}u^3.$$

Rearranging, we obtain the defining equation of the discriminant space in the base Y:

$$\Delta(u, y) = 4u^3 + 27y^2 = 0.$$

This describes an algebraic cusp curve in the (u, y) plane!

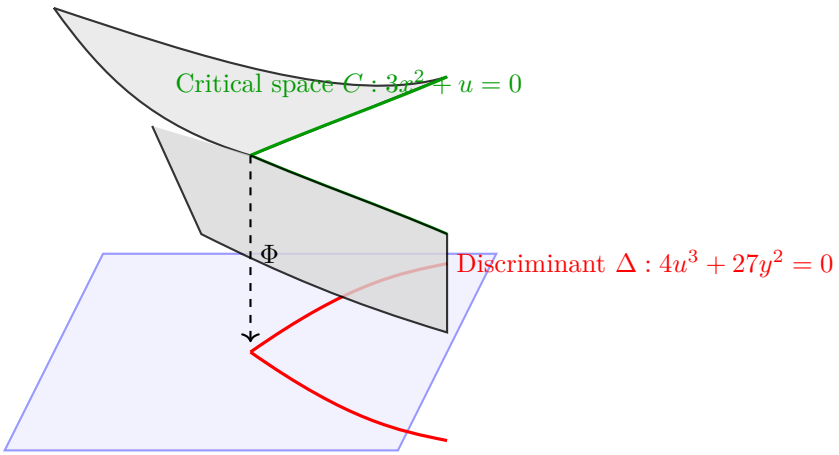

Figure 19: The Cusp Catastrophe: The unfolding space X (the pleated surface) maps via Φ to the parameter space Y. The critical space C (the green fold lines) maps precisely onto the discriminant space Δ (the red cusp), where fibers transition from having 3 real preimages to 1.

This tells us that for polynomials $P(x) = x^3 + ux - y$, the nature of the roots completely changes depending on whether (u, y) lies inside the cusp, outside the cusp, or exactly on the discriminant Δ (where $P(x)$ has multiple roots). For generic unfoldings, the discriminant is precisely this **bifurcation set** where the topology of the underlying space jumps.

12.4 Exercises

Exercise 12.1. *Consider the A_3 singularity (the swallowtail catastrophe). Its universal unfolding is $f(x, u, v) = x^4 + ux^2 + vx$. Let $\Phi : \mathbb{C}^3 \to \mathbb{C}^3$ map $(x, u, v) \mapsto (x^4 + ux^2 + vx, u, v)$. Find the equation defining its critical space C. Then, geometrically or algebraically project it to the base to find the parametric equations of the swallowtail discriminant surface in $\mathbb{C}^3$.*

Exercise 12.2. *Compute the Thom-Boardman symbol for the critical point at the origin of the E_6 singularity defined by $f(x, y) = x^3 + y^4$. Describe how the rank of the Hessian drops.*

Exercise 12.3. *Let A be a finitely generated $\mathbb{C}[u]$-module representing the pushforward $\Phi_*(\mathcal{O}_C)$ of $C : \{3x^2 + u = 0\}$ mapping to the u-line via $u \mapsto u$. What is the rank of this module? Determine its 0-th Fitting ideal and show how it predicts a non-reduced point.*

13 Vanishing Lattices, Monodromy Groups and Adjacency

So far we have mostly discussed absolute monodromy—the monodromy associated to a single, isolated critical point. However, analyzing more complex singularities or global phenomena often requires studying deformations that break a complicated singularity into a collection of simpler, typically non-degenerate, Morse singularities. Tracking these simpler singularities collectively leads to the concepts of **vanishing lattices** and **monodromy groups**, which bridge local singularity theory with the global topology of the parameter spaces.

13.1 Fundamental Group of the Discriminant Complement

Consider a miniversal deformation $F : \mathcal{X} \to S$ of an ICIS X_0 with discriminant locus $D \subset S$. The complement $S \setminus D$ is exactly the locus where the deformed fibers X_s remain smooth. The topology of $S \setminus D$ fundamentally controls how vanishing cycles globally transport when parameters continuously vary.

A deep result (Looijenga Lemma 7.1) shows that if F is a good representative of the miniversal deformation, there is a natural surjection from the fundamental group of the complement to the monodromy group. More precisely, for hypersurface singularities, if we slice S with a generic complex line L intersecting D transversally at μ points, the induced map on fundamental groups $\pi_1(L \setminus (L \cap D)) \to \pi_1(S \setminus D)$ is surjective. This algebraically implies that the global fundamental group is generated by the simple loops around the generic divisor components, tightly linking global parameter topology to Picard-Lefschetz local twists.

Proposition 13.1 (Generic Line Generators for the Local Fundamental Group)**.** *Let $D \subset S = T \times \Delta$ be the discriminant of a good representative of a versal deformation, with T contractible and the last coordinate axis transverse to the tangent cone of D. For generic $t \in T$ and $s = (t, \eta) \in (T \times \partial\Delta) \setminus D$, the inclusion of the slice induces a surjection*

$$\pi_1(S_t \setminus D_t, s) \twoheadrightarrow \pi_1(S \setminus D, s).$$

If D is irreducible, then the standard small loops around the points of D_t form a single conjugacy class in $\pi_1(S \setminus D, s)$.

Proof sketch. This packages the content of [Loo84, Ch. 7, §A]. Over the complement of the discriminant of the projection $D \to T$, the map $S \setminus D \to T$ is a locally trivial fibration with a section $t \mapsto (t, \eta)$. The section splits the homotopy exact sequence, so every loop is represented by a product of a loop in the fibre slice and a loop in the section. Because the bad set in T has real codimension at least 2, any loop can first be homotoped off it. Since the section itself is contractible, only the slice loop contributes to the fundamental group, proving surjectivity.

For the conjugacy statement, one uses irreducibility of D: the smooth locus D_{reg} is connected, so a small loop around one branch point can be slid along an arc in D_{reg} to a loop around any other branch point. In the complement this sliding becomes conjugation. This is exactly why the local Picard-Lefschetz transformations coming from a generic line slice lie in one conjugacy class. □

13.2 Deformations and Non-Degenerate Splitting

Let $f : (\mathbb{C}^{n+1}, 0) \to (\mathbb{C}, 0)$ be an isolated hypersurface singularity germ with Milnor number μ. We can unfold f into a family of functions parameterised by $s \in U \subset \mathbb{C}^k$:

$$F : X \times U \to \mathbb{C} \times U, \quad F(x, s) = (f_s(x), s).$$

A remarkable theorem by Brieskorn (and topologically anticipated by Milnor) guarantees that if we choose a generic small deformation s, the isolated critical point of $f_0 = f$ splits into exactly μ distinct non-degenerate (Morse) critical points $p_1, \ldots, p_\mu$ of the deformed function f_s.

Theorem 13.1 (Brieskorn's Splitting Theorem/Morsification)**.** *Every isolated hypersurface singularity $f : (\mathbb{C}^{n+1}, 0) \to (\mathbb{C}, 0)$ admits a **Morsification**. That is, arbitrarily close to f in the space of holomorphic functions, there exists a function f_s defined on the same domain such that f_s has exactly μ critical points, all of which are real Morse singularities (non-degenerate quadratic singularities with distinct critical values).*

Proof Sketch. Consider the miniversal deformation $F(x, s) = f(x) + \sum_{i=1}^{\tau} s_i g_i(x)$ where $\{g_1, \ldots, g_\tau\}$ projects to a basis of the Tjurina algebra. The discriminantal locus $\Delta \subset S$ consists of parameters s where the perturbed function has degenerate critical points. A dimension-counting argument using the transversality of the jet bundles of F shows that the stratum of functions possessing a degenerate critical point has codimension ≥ 1 in the parameter space S. Moreover, the condition that two critical values coincide (a multi-local discriminant condition) independently has codimension 1. Therefore, the complement $S \setminus \Delta$ is generic and dense. For any parameter point $s \in S \setminus \Delta$, the resulting function f_s has only Morse critical points with distinct critical values. Finally, by the conservation of multiplicity of the critical set mapping (rooted in the continuity of the local topological degree or algebraic dimension of finite morphisms), the total sum of the Milnor numbers at the split critical points must equal the original Milnor number $\mu(f)$. Since each Morse point has a local Milnor number of 1, there must be exactly μ such points! □

Let the critical values of f_s be $c_1, \ldots, c_\mu = f_s(p_1), \ldots, f_s(p_\mu)$. The set $\{c_1, \ldots, c_\mu\} \subset \mathbb{C}$ lies inside a small disk D. The fiber F_t over a regular value $t \in D \setminus \{c_1, \ldots, c_\mu\}$ is diffeomorphic to the original Milnor fiber.

13.3 Distinguished Bases of Vanishing Cycles

For a generic deformation s, we can construct a path system from the regular value t to each of the distinct critical values c_i. By Picard-Lefschetz theory (§8), each path γ_i to c_i uniquely defines a Lefschetz thimble Δ_i and a corresponding vanishing cycle $\delta_i \in H_{n-1}(F_t; \mathbb{Z})$.

Definition 13.1 (Distinguished Basis)**.** *A set of paths $\gamma_1, \dots, \gamma_\mu$ in $D \setminus \{c_i\}$ from t to the critical values $c_1, \dots, c_\mu$ is called a* ***strongly distinguished system of paths*** *if they do not self-intersect or mutually intersect except at the basepoint t, and they are ordered cyclically. The ordered set of vanishing cycles $(\delta_1, \dots, \delta_\mu)$ generated by such a path system forms a* ***distinguished basis*** *of the homology $H_{n-1}(F_t; \mathbb{Z})$.*

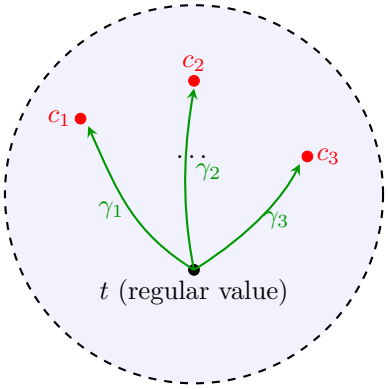

Figure 20: A strongly distinguished system of paths avoiding the critical values in the s-parameter base disk. Each path γ_i dictates a vanishing cycle δ_i.

The profound consequence is that the Milnor number effectively counts the *number of independent splits*, thus $H_{n-1}(F) \cong \mathbb{Z}^\mu$ is freely generated by $\{\delta_1, \dots, \delta_\mu\}$.

13.4 Factorization of the Total Monodromy

Now, consider a large loop Γ enclosing all μ critical values. This loop represents the classical, absolute geometric monodromy of the original un-deformed singularity f. Topologically in the punctured disk, the loop Γ is homotopic to the concatenated product of simple loops σ_i going along γ_i, circling c_i, and returning.

This topological factorization leads directly to the core theorem of relative monodromy.

Theorem 13.2 (Brieskorn, Deligne)**.** *Let $T_1, \dots, T_\mu$ be the local Picard-Lefschetz monodromy operators associated with the critical values $c_1, \dots, c_\mu$ (representing generalized Dehn twists around δ_i). Then the total, absolute algebraic monodromy T of the singularity factorizes as their composed product:*

$$T = T_\mu \circ T_{\mu-1} \circ \cdots \circ T_1.$$

By selecting a distinguished basis, we represent the total monodromy simply as a product of reflections (in the higher-dimensional analogue). Thus, studying the complicated twisting of A_k, D_k, E_k singularities boils down to understanding the intersection graph (Dynkin diagram) of their basic vanishing cycles δ_i.

13.5 The Monodromy Group and the Vanishing Lattice

Definition 13.2 (Vanishing Lattice and Monodromy Group)**.** *Let F_t be a smooth fiber. The* ***monodromy group*** *$\Gamma \subset \mathrm{Aut}(H_n(F_t, \mathbb{Z}))$ is the image of the natural representation $\pi_1(S \setminus D, t) \to \mathrm{Aut}(H_n(F_t, \mathbb{Z}))$. Since Picard-Lefschetz transformations preserve the intersection form, Γ is a*

subgroup of the orthogonal group. The ***vanishing lattice*** *is the $\mathbb{Z}$-submodule $V \subset H_n(F_t, \mathbb{Z})$ spanned by all vanishing cycles.*

A fundamental theorem states that for hypersurface singularities (except for odd-dimensional quadratic singularities), all vanishing cycles form a single, transitive Γ-orbit. Furthermore, Γ is generated by the Picard-Lefschetz reflections associated with the distinguished vanishing cycles. We can decompose the vanishing lattice $V \otimes \mathbb{Q}$ and Γ into unipotent (radical) and semi-simple pieces, denoted Γ_u and Γ_s, dictating the arithmetic structure of the singularity's intersection lattice.

Theorem 13.3 (Structure of the Vanishing Lattice)**.** *Let F_t be a Milnor fiber of a versal deformation of an ICIS and let $\Gamma \subset \mathrm{Aut}(H_n(F_t; \mathbb{Z}))$ be its monodromy group.*

1. *Any distinguished system of vanishing cycles generates $H_n(F_t; \mathbb{Z})$; in the hypersurface case it is a basis.*
2. *The corresponding Picard-Lefschetz transformations generate Γ and belong to a single conjugacy class in Γ.*
3. *Except for odd-dimensional quadratic singularities, all vanishing cycles form a single Γ-orbit.*

Idea of proof. This is the structural content of [Loo84, Ch. 7, §B]. The generation statement comes from relative monodromy: after choosing a generic line in the base, Chapter 5 identifies the Milnor fiber of the original singularity as the result of attaching cells along the vanishing spheres coming from the slice. In the hypersurface case there is no lower-codimension Milnor fiber left over, so these vanishing cycles are already a basis.

The second point combines Proposition 13.1 with the Picard-Lefschetz formula. Surjectivity of the slice fundamental group shows that monodromy is generated by loops around the slice discriminant points, and Picard-Lefschetz identifies each such loop with a pseudo-reflection in its vanishing cycle. Conjugacy of the loops implies conjugacy of the reflections.

For the orbit statement one first uses connectedness of the smooth discriminant to move any vanishing cycle to any other up to sign. If n is even, a Picard-Lefschetz reflection already changes the sign of the vanishing cycle. If n is odd and the singularity is not an ordinary double point, Looijenga uses adjacency to an A_2-singularity to produce another vanishing cycle intersecting the first in ± 1; a short Picard-Lefschetz computation with the two corresponding reflections then changes δ to $-\delta$. The only exception is the odd-dimensional quadratic singularity, where the monodromy is trivial and one is left only with the pair $\pm\delta$. □

13.6 Adjacency and the Splitting Lemma

When we deform a singularity, its topological complexity breaks down. If a singularity X can be deformed into a singularity Y (meaning Y appears as an isolated singularity on some fiber of the miniversal deformation of X), we say X is **adjacent** to Y, denoted $X \to Y$. This adjacency defines a partial ordering on the space of all isolated complete intersection singularities $\mathrm{CIS}(n)$. Moving downward in this poset strictly decreases the Milnor number μ, the Tjurina number τ, the embedding codimension, and the topological modality.

Proposition 13.2 (Adjacency Embeds Vanishing Lattices)**.** *If an n-dimensional ICIS (X_0, x) is adjacent to (Y_0, y), then the vanishing lattice of (Y_0, y) embeds primitively into the vanishing lattice of (X_0, x) in a way compatible with the intersection form. In particular,*

$$\mu(Y_0, y) \leq \mu(X_0, x), \qquad \tau(Y_0, y) \leq \tau(X_0, x),$$

and adjacency can only move toward simpler singularities.

Proof sketch. This is the geometric meaning of Looijenga's specialization exact sequence and adjacency discussion in [Loo84, Ch. 7, §B–C]. Choose a versal deformation of (X_0, x) and a nearby parameter where the fiber has a unique singular point of type (Y_0, y). Comparing a generic nearby smooth fiber with this special fiber gives an exact sequence of middle homology in which the local Milnor lattice of (Y_0, y) injects into the Milnor lattice of (X_0, x).

The map is induced by inclusion of a local Milnor ball, so it preserves the intersection form; primitiveness comes from the fact that the quotient is again the middle homology of a fiber and hence torsion-free. The Milnor number inequality is therefore immediate. The inequality for τ is the deformation-theoretic shadow of the same picture: in a versal family, the dimension of T^1 is upper semicontinuous, so specialization cannot increase the Tjurina number. This is why vanishing lattices serve as an effective absolute measure of complexity. □

A major geometric consequence is the **Splitting Lemma** (Looijenga Lemma 7.16), which states that if a function germ has a degenerate critical point but non-zero Hessian rank r, it is locally right-equivalent to $f(x_1, \dots, x_{n-r}) + Q(x_{n-r+1}, \dots, x_n)$, splitting out the Morse (quadratic) non-degenerate part Q. As a corollary, any isolated hypersurface singularity that is not of type A_1 (Morse) can uniformly deform to A_2 (the split cusp).

13.7 Braid Group Action on Bases

What if we chose a different set of paths? The collection of all possible distinguished bases for a fixed singularity forms an orbit under an action. This action is operated by the **Braid Group** $\mathcal{B}_\mu$. A standard braid generator σ_i swaps the i-th and $(i+1)$-th paths. If the path γ_i completely crosses over γ_{i+1}, the old vanishing cycle δ_{i+1} undergoes the local monodromy T_i of the first cycle!

Hence, a braid generator creates a new basis:

$$(\delta_1, \dots, \delta_i, \delta_{i+1}, \dots) \mapsto (\delta_1, \dots, T_i(\delta_{i+1}), \delta_i, \dots).$$

This technique allows us to transform one geometric presentation of a singularity's Milnor fiber into another. This *Hurwitzmove* algebra heavily connects singularity theory to algebraic knot theory and representation theory.

13.8 Exercises

Exercise 13.1. *The Morse critical points of a generic polynomial typically lie at distinct heights (critical values). Assume $n = 2$ (curves), and we have a basis of two vanishing cycles δ_1, δ_2 with intersection number $\langle \delta_1, \delta_2 \rangle = 1$. By Picard-Lefschetz, write down matrices for T_1 and T_2. Then compute $T = T_2 T_1$, find its characteristic polynomial, and deduce which ADE singularity this corresponds to.*

Exercise 13.2. *Apply the Hurwitz move (braid group operation) σ_1 on a distinguished basis (δ_1, δ_2) to obtain a new basis $(\delta_1', \delta_2') = (\delta_1 - \langle \delta_2, \delta_1 \rangle \delta_1, \delta_1)$. Verify that the intersection matrix of the new basis is isomorphic to the old one. This proves that the Dynkin diagram relies only on the orbit, not the specific path choice.*

14 The Monodromy Theorem and the Gauss-Manin Connection

In §8, we broke a singularity apart using Morsifications (Brieskorn's theorem), and in §6 we saw how this splitting topologically builds the Milnor fiber as a finite bouquet of μ spheres. This gave us a deep understanding of the middle homology $H_n(F_t;\mathbb{Z}) \cong \mathbb{Z}^\mu$ as a free abelian group generated by non-degenerate vanishing cycles. Simultaneously in §7, we observed that the induced monodromy action (Picard-Lefschetz matrices) circling critical paths governed the topological linking of these cycles mathematically.

Now, a central algebraic question naturally arises for these geometric systems: what are the concrete, universal linear algebraic properties of these global monodromy transformations? Which kinds of eigenvalues can the monodromy operator h_* possess? Is there a way to extract these topological twists purely from calculus and differential equations? The answers lie deep at the intersection of algebraic geometry and topology, culminating in the foundational Monodromy Theorem, which we will rigorously investigate by lifting the topological problems to analytic differential equations via the Gauss-Manin Connection.

14.1 The Monodromy Theorem

Let $h_* : H_n(F_t;\mathbb{Z}) \to H_n(F_t;\mathbb{Z})$ denote the algebraic monodromy operator acting on the middle homology of the Milnor fiber. Over $\mathbb{C}$, we can consider the $\mathbb{C}$-linear extension operator acting on $H_n(F_t;\mathbb{C})$.

Theorem 14.1 (The Monodromy Theorem)**.** *Let $f : (\mathbb{C}^{n+1}, 0) \to (\mathbb{C}, 0)$ be the germ of an isolated complete intersection singularity. Then the algebraic monodromy operator h_* satisfies two fundamental rigidity properties:*

1. ***Quasi-Unipotency:*** *All eigenvalues of h_* are roots of unity.*
2. ***Bounded Nilpotency index:*** *The operator has a bounded Jordan block size. Specifically, $(h_*^N - I)^m = 0$ for some integer $N > 0$ and some integer $m \leq n + 1$.*

The first part (eigenvalues being roots of unity) was proved independently by Brieskorn, Grothendieck, and Deligne in various algebraic and analytic contexts. The second part was proven by Landman. This theorem provides a powerful constraint: while local topology can appear incredibly twisted, its linear manifestation via monodromy is exceptionally orderly.

Idea of proof via relative monodromy. Looijenga's proof strategy in [Loo84, Ch. 5, §C], following Lê's carrousel philosophy, again proceeds by slicing. One first enlarges f to a map

$$g : \overline{X} \to \Delta \times \Delta'$$

whose discriminant is a plane curve and whose critical points away from the origin are generically quadratic. Fix $s \in \Delta^*$. The relative cell-attachment picture from Theorem 6.1 implies that the pair

$$(f^{-1}(s), g^{-1}(s,t))$$

has relative cohomology concentrated in degree n: each quadratic point contributes one vanishing sphere, and hence one generator in middle degree. Since g is topologically trivial in the t-direction away from the discriminant, the long exact sequence of this pair shows that all interesting monodromy is pushed into that middle relative cohomology group.

The problem is then reduced to a two-dimensional statement about a local system on a bidisk with branch curve $D \subset \Delta \times \Delta'$. Looijenga proves a key proposition saying that if every analytic arc transverse to D sees quasi-unipotent monodromy of index at most $n-1$, then the first relative cohomology sheaf over Δ^* has quasi-unipotent monodromy of index at most n. This closes the induction on the fiber dimension. In Lê's language, the carrousel controls how a loop in the base decomposes into loops around the branches of the discriminant, and the nilpotent index grows by at most one at each slicing step. □

Three Proofs of Quasi-Unipotency

The three independent proofs of quasi-unipotency are landmark achievements, each reflecting a fundamentally different mathematical perspective:

1. **Brieskorn's Analytic Proof** [Bri70]: Brieskorn demonstrated that the Gauss-Manin connection on the relative de Rham cohomology has a *regular singular point* at $t = 0$. By the classical theory of linear ODEs with regular singularities (Fuchs–Levelt theory), the monodromy of such a system is necessarily quasi-unipotent. We will develop this proof in detail in §14.3 below.

2. **Grothendieck's Algebraic Proof**: Grothendieck's approach is purely algebro-geometric, using the theory of étale cohomology and ℓ-adic sheaves. Given a proper morphism $f : X \to S$ with S a curve, Grothendieck showed that the higher direct image sheaves $R^q f_* \mathbb{Q}_\ell$ form a lisse ℓ-adic sheaf on $S \setminus D$ (the complement of the discriminant). The key input is Grothendieck's **local monodromy theorem**: for any lisse ℓ-adic sheaf on a punctured disk, the action of the inertia group (which generates monodromy) is quasi-unipotent. This follows from the fact that the inertia group of a local field has a pro-ℓ part of finite index, combined with a rigidity argument for ℓ-adic representations. The proof reduces the analytic statement about period integrals to a purely algebraic statement about Galois representations.

3. **Clemens–Schmid's Topological–Hodge Theoretic Proof**: A third approach, developed later by Clemens and Schmid, uses Hironaka's resolution of singularities [Kul98]. After resolving the total space so that the singular fiber becomes a normal crossing divisor $D = \bigcup m_i E_i$, one studies the *nearby cycles functor* ψ_f. The monodromy acts on $\psi_f(\mathbb{Q})$, and quasi-unipotency follows from the structure of the weight filtration on the nearby cycles complex, which is controlled by the combinatorics of the normal crossing divisor.

These three perspectives—analytic (Brieskorn), algebraic (ℓ-adic, Grothendieck), and geometric (resolution, Clemens–Schmid)—are unified by the modern theory of $\mathcal{D}$-modules, where the regular singularity of the Gauss-Manin connection, the quasi-unipotency of monodromy, and the existence of the V-filtration are all manifestations of the *regularity* property of holonomic $\mathcal{D}$-modules.

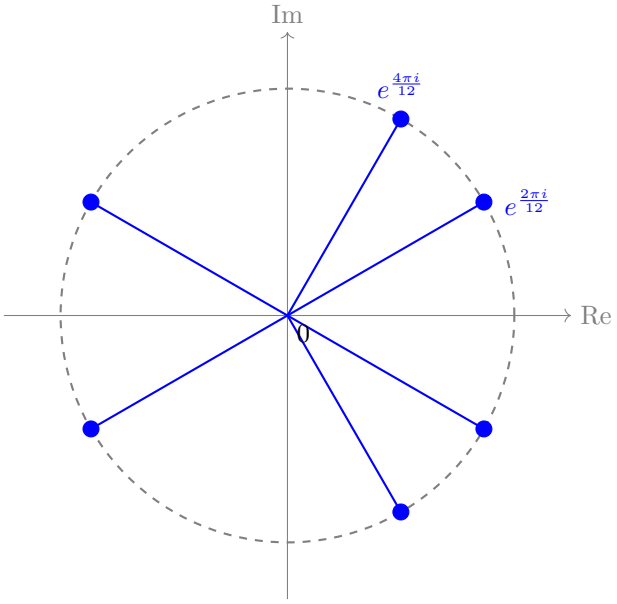

Figure 21: The eigenvalues of the monodromy operator are meticulously constrained to lie exclusively on the unit circle as rationality necessitates them to be roots of unity.

14.2 The Gauss-Manin Connection

To investigate the monodromy analytically, one looks at integration of holomorphic differential forms over the homology cycles of the Milnor fibers. Consider the Milnor fibration $f : X \to S$ where S is a small punctured disk Δ^*. For any absolute cohomology class $[\omega] \in H^n(X)$, we can restrict it to the fibers F_t to get a family of cohomology classes $[\omega_t] \in H^n(F_t; \mathbb{C})$. As t varies, these classes form sections of a vector bundle over Δ^* known as the **cohomology bundle** (or the Milnor bundle).

This bundle comes equipped with a natural flat connection, called the **Gauss-Manin Connection**, denoted by ∇_{GM}. Given a cycle $\gamma(t) \in H_n(F_t; \mathbb{Z})$ varying continuously with t, the integration of a holomorphic n-form ω over $\gamma(t)$, $I(t) = \int_{\gamma(t)} \omega$, satisfies a differential equation governed by this connection.

Definition 14.1 (Gauss-Manin Connection)**.** *The* ***Gauss-Manin connection*** ∇_{GM} *is defined analytically by differentiating the period integrals. Let v be a vector field on the base S. For a section ω of the relative De Rham cohomology bundle $H^n(X/S)$,*

$$\nabla_v[\omega] = [\mathcal{L}_{\tilde{v}}\omega]$$

where $\tilde{v}$ is any smooth vector field on X lifting v, and $\mathcal{L}$ is the Lie derivative.

The monodromy h_* acting on the homology is exactly the analytic continuation of these period integrals along the generator of $\pi_1(\Delta^*)$. In linear algebraic terms, h_* is the **holonomy** of the flat Gauss-Manin connection.

The De Rham Realization

The Gauss-Manin connection has an algebraic incarnation via the relative de Rham complex. Consider the map $f : X \to S$ with $X \subset \mathbb{C}^{n+1}$. The **relative de Rham complex** is:

$$\Omega^\bullet_{X/S} : \quad \mathcal{O}_X \xrightarrow{d_{X/S}} \Omega^1_{X/S} \xrightarrow{d_{X/S}} \Omega^2_{X/S} \xrightarrow{d_{X/S}} \cdots$$

where $\Omega^p_{X/S} = \Omega^p_X/(df \wedge \Omega^{p-1}_X)$ is the sheaf of relative p-forms. The cohomology sheaves $\mathcal{H}^q = R^q f_* \Omega^\bullet_{X/S}$ over S recover the cohomology of the fibers: for $s \in S$ smooth, the stalk $\mathcal{H}^q_s \cong H^q(F_s; \mathbb{C})$.

The Gauss-Manin connection $\nabla : \mathcal{H}^q \to \mathcal{H}^q \otimes \Omega^1_S$ is then defined algebraically by the connecting homomorphism in the long exact sequence associated to the short exact sequence of complexes:

$$0 \to f^*\Omega^1_S \otimes \Omega^{\bullet-1}_{X/S} \to \Omega^\bullet_X / f^*\Omega^{\geq 2}_S \to \Omega^\bullet_{X/S} \to 0.$$

This algebraic description makes the flatness of ∇ (i.e., $\nabla^2 = 0$) manifest, since it arises from a purely algebraic short exact sequence.

Proposition 14.1 (Relative de Rham Comparison for Good Representatives)**.** *Let $f : X \to S$ be a good Stein representative of a deformation of an isolated singularity, and write*

$$\mathcal{H}^p_f := H^p(f_* \Omega^\bullet_f).$$

Then there is a natural exact sequence of $\mathcal{O}_S$-modules

$$0 \to R^p f_* H^0(\Omega^\bullet_f) \to \mathcal{H}^p_f \to f_* H^p(\Omega^\bullet_f) \to 0.$$

Over $S \setminus D_f$, the natural map identifies $\mathcal{H}^p_f$ with

$$(R^p f_* \mathbb{C}_X) \otimes_{\mathbb{C}} \mathcal{O}_{S \setminus D_f},$$

while at the special point one recovers the local relative de Rham cohomology:

$$(\mathcal{H}^p_f)_0 \cong H^p(\Omega^\bullet_{f,x}) \qquad (p > 0).$$

Idea of proof. This is the structural content of Looijenga's Chapter 8A. For a Stein representative the spectral sequence with $E_1^{ab} = R^b f_* \Omega^a_f$ degenerates immediately, so $\mathcal{H}^p_f$ is computed by global sections of the relative de Rham complex. The second spectral sequence, starting from $R^a f_* H^b(\Omega^\bullet_f)$, has only the $b = 0$ row and the finite critical-locus contribution $a = 0$ in higher rows, because the higher cohomology sheaves are supported on the finite critical space. Comparing the two spectral sequences yields the exact sequence above.

Away from the discriminant, f is a smooth locally trivial fibration, so the relative Poincaré lemma identifies $\Omega^\bullet_f$ with $f^{-1}\mathcal{O}_S$ and hence identifies $\mathcal{H}^p_f$ with the local system $R^p f_* \mathbb{C}_X$ tensored by $\mathcal{O}_S$. At the origin, shrinking the Stein representative and passing to the inductive limit kills the higher direct image term, leaving exactly the stalk $H^p(\Omega^\bullet_{f,x})$. This is the precise sense in which the relative de Rham complex packages all nearby Milnor fibers simultaneously. □

Proposition 14.2 (Lie-Derivative Formula for Gauss–Manin)**.** *Assume $f = (f_1, \ldots, f_k) : X \to S \subset \mathbb{C}^k$ is a good Stein representative, let $s \in S$, and let $\eta \in \theta_{S,s}$ be liftable to a vector field ξ on X. If $[\omega] \in H^p(f_* \Omega^\bullet_f)_s$ is represented by a d_f-closed relative form such that*

$$d\omega = \sum_{\kappa=1}^{k} df_\kappa \wedge \omega_\kappa,$$

then the Gauss–Manin covariant derivative is given by

$$\nabla_\eta([\omega]) = [L_\xi \omega],$$

and over $S \setminus D_f$ one has the coordinate formula

$$\nabla([\omega]) = \sum_{\kappa=1}^{k} dt_\kappa \otimes [\omega_\kappa].$$

In particular, the algebraic connection defined from the relative de Rham complex coincides with the topological flat connection coming from parallel transport of cycles.

Idea of proof. This is Looijenga's Chapter 8B construction. If two lifts of η differ by a vertical vector field, Cartan's formula

$$L_\xi = i_\xi d + d i_\xi$$

shows that their difference acts trivially on relative cohomology; hence $[L_\xi \omega]$ depends only on η. For a smooth parameter value choose transported cycles Z_t in the fibers. Stokes' formula applied to the cylinder traced by Z_t gives

$$\frac{d}{dt_\kappa} \int_{Z_t} \omega = \int_{Z_t} \omega_\kappa,$$

so horizontality of period integrals is equivalent to the vanishing of the classes $[\omega_\kappa]$. This identifies the Lie-derivative construction with the usual topological connection on $(R^p f_* \mathbb{C}_X) \otimes \mathcal{O}_{S \setminus D_f}$. □

14.3 The Brieskorn Lattice and Its Hierarchy

Brieskorn's proof of the quasi-unipotency of the monodromy leverages the analytic theory of differential equations, specifically the fact that the Gauss-Manin Connection possesses a **regular singular point** at $t = 0$. To formally state this, we construct a hierarchy of specialized modules of differential forms.

Definition 14.2 (Brieskorn Modules H_0' and H_0'')**.** *Let $f : (\mathbb{C}^{n+1}, 0) \to (\mathbb{C}, 0)$ be an isolated hypersurface singularity. Let Ω^p denote the stalk of holomorphic p-forms at the origin of $\mathbb{C}^{n+1}$. We define two modules:*

$$H_0' = \frac{\Omega^n}{df \wedge \Omega^{n-1}}$$

$$H_0'' = \frac{\Omega^{n+1}}{df \wedge d\Omega^{n-1}}$$

Both are modules over the local ring $\mathbb{C}\{t\}$ (where $t = f$). The map $d : H_0' \to H_0''$ sending $[\omega] \mapsto [d\omega]$ is well-defined and $\mathbb{C}\{t\}$-linear. There is also a multiplication map $df\wedge : H_0' \to H_0''$ sending $[\omega] \mapsto [df \wedge \omega]$.

The relationship between these modules encodes the Gauss-Manin connection:

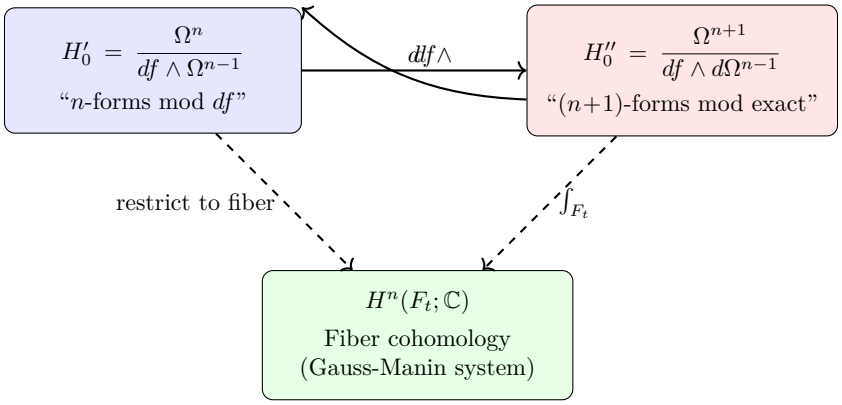

Figure 22: The Brieskorn modules H_0' and H_0'' are algebraic incarnations of the Gauss-Manin system. The exterior derivative d and the wedge product $df\wedge$ connect them, while both relate to the fiber cohomology via restriction and integration.

Remark 14.1. *There is an important notational distinction: the module H_0'' in Brieskorn's original paper uses $\Omega^{n+1}/(df \wedge d\Omega^{n-1})$, while some authors (including Kulikov) define it as $\Omega^{n+1}/(df \wedge \Omega^n)$. These differ by the image of exact forms. The former is the* ***Brieskorn lattice****, while the latter is the* ***saturated Brieskorn module****. Both are free $\mathbb{C}\{t\}$-modules of rank μ, but their ∂_t-module structures differ. Following Kulikov §1.4, we adopt the convention $H_0'' = \Omega^{n+1}/(df \wedge d\Omega^{n-1})$.*

A fundamental algebraic result by Brieskorn identifies the size of this module.

Theorem 14.2 (Brieskorn, 1970)**.** *For an isolated hypersurface singularity, both H_0' and H_0'' are free $\mathbb{C}\{t\}$-modules of rank equal to the Milnor number μ.*

Proof Sketch. The proof relies heavily on the coherence of relative differential forms and the finiteness criteria given by the Preparation Theorem. Consider the sequence of $\mathcal{O}_{\mathbb{C}^{n+1},0}$-modules given by exterior multiplication by df:

$$0 \to \Omega^0 \xrightarrow{df\wedge} \Omega^1 \xrightarrow{df\wedge} \dots \xrightarrow{df\wedge} \Omega^{n+1} \to \frac{\Omega^{n+1}}{df \wedge \Omega^n} \to 0$$

Because f has an isolated singularity, the critical locus is just the origin. Outside the origin, $df \neq 0$, so the sequence of vector bundles is exact. By the De Rham lemma, the cohomology of this sequence is supported only at the origin. Consequently, the quotient H_0'' is coherent. By applying the Weierstrass Preparation Theorem relative to the map f, one shows that the stalk of this coherent sheaf is a freely finitely generated module over the base ring $\mathbb{C}\{t\}$. The rank is determined by evaluating the module at the origin, which reduces precisely to the Milnor algebra $\Omega^{n+1}/(df \wedge \Omega^n + f\Omega^{n+1}) \cong \mathcal{O}_{\mathbb{C}^{n+1},0}/J_f$, yielding rank μ. □

14.4 The Connection Operator and Regular Singularity

With the free module structure established, we can define the covariant derivative associated to the Gauss-Manin connection. The key insight is that differentiation with respect to t (the value of f) translates into an algebraic operation on the Brieskorn lattice.

Definition 14.3 (The Operator ∂_t on H''_0)**.** *For a class $[\omega] \in H''_0$ represented by an $(n+1)$-form ω, we define the action of ∂_t by:*

$$\partial_t[\omega] = [\eta] \quad \text{where} \quad d\eta = \omega \text{ modulo } df \wedge d\Omega^{n-1}.$$

More precisely, since ω is an $(n+1)$-form, there exists a unique n-form η (modulo $df \wedge \Omega^{n-1}$ and $\ker d$) such that $d\eta \equiv \omega \pmod{df \wedge d\Omega^{n-1}}$. This makes H''_0 into a module over the ring $\mathbb{C}\{t\}[\partial_t]$.

The operator ∂_t is meromorphic: while ∂_t does not preserve H''_0 itself, the operator $t\partial_t$ does preserve a slightly enlarged lattice. Concretely:

Proposition 14.3 (Kulikov, Prop. 1.4.2)**.** *The operator $t\partial_t$ maps a localized version of H''_0 (namely $H''_0[t^{-1}]$) into itself. At the fiber level, for a cohomology class $[\omega_t] \in H^n(F_t; \mathbb{C})$ obtained by restricting $[\omega] \in H''_0$, we have*

$$\nabla_{\partial_t}[\omega_t] = \partial_t[\omega_t]$$

i.e., the Gauss-Manin connection is represented by the algebraic ∂_t operator.

Theorem 14.3 (Brieskorn's Regular Singularity Theorem)**.** *The Gauss-Manin connection ∇ has a **regular singular point** at $t = 0$. Specifically, there exists a $\mathbb{C}\{t\}$-lattice $\mathcal{L} \subset H''_0[t^{-1}]$ such that $t\partial_t(\mathcal{L}) \subset \mathcal{L}$. As a consequence, any period integral $I(t) = \int_{\gamma(t)} \omega$ satisfies a linear differential equation (the Picard-Fuchs equation) with a regular singularity at the origin.*

Proof Outline (following Malgrange and Looijenga Chapter 8). Choose a good Stein representative $f : X \to \Delta$ and generators $\omega_1, \ldots, \omega_\mu$ of the relative de Rham cohomology sheaf. By Proposition 14.1, these classes form a basis of the cohomology bundle over Δ^*, and Proposition 14.2 gives the connection matrix on this basis.

The key point is that regularity is proved from period estimates rather than from a direct pole computation. One triangulates $\overline{X}$ and the base disk so that f becomes simplicial and the origin is a subcomplex. On each simplex of the punctured disk, the integrals of the forms ω_j over simplices in the fibers vary continuously and remain bounded. If $c_1(t), \ldots, c_\mu(t)$ is an integral basis of $H_n(F_t; \mathbb{Z})/\text{torsion}$, one forms the squared period determinant

$$d(t) = \det olimits^2\big(\langle c_i(t), [\omega_j(t)]\rangle\big).$$

Boundedness of the simplex integrals implies that $d(t)$ extends holomorphically across $t = 0$ after multiplication by a suitable power of t.

Now choose a basis of horizontal sections $\zeta_1, \ldots, \zeta_\mu$ and write

$$\zeta_i = \sum_j \phi_{ij}(t)[\omega_j].$$

By Cramer's rule, each coefficient $\phi_{ij}(t)$ is a quotient of bounded period determinants by $d(t)$, so some power of t times $\phi_{ij}(t)$ remains bounded near the origin. Thus horizontal sections have tempered growth. Deligne's regularity criterion for integrable meromorphic connections now implies that the Gauss-Manin connection is regular singular. Classical Fuchs theory then yields expansions of the form

$$I(t) = t^\alpha \sum_{k=0}^{m} \frac{(\log t)^k}{k!} \phi_k(t),$$

which forces the semisimple monodromy eigenvalues to be roots of unity and recovers quasi-unipotence. $\square$

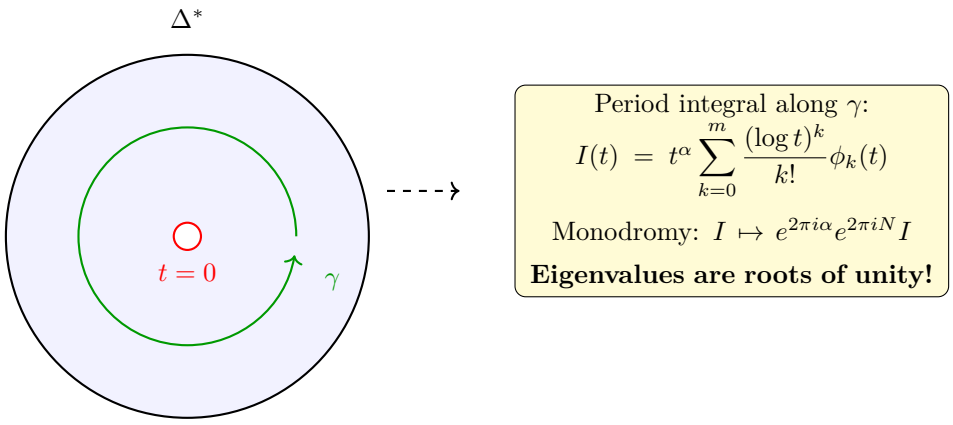

Figure 23: The regular singularity of the Gauss-Manin connection at $t = 0$ forces period integrals to have controlled asymptotic behavior. The monodromy (analytic continuation around the puncture) produces eigenvalues that are roots of unity.

14.5 The Picard-Fuchs Equation: Explicit Computation

For concrete singularities, the Gauss-Manin connection can be rendered as an explicit ordinary differential equation (the **Picard-Fuchs equation**) satisfied by the period integrals. Let us work this out in a fundamental example.

Example 14.1 (Picard-Fuchs for A_2: $f(x, y) = x^3 + y^2$)**.** *The Milnor number is $\mu = 2$. Choose a basis of the Brieskorn module H_0'':*

$$\omega_0 = dx \wedge dy, \quad \omega_1 = x\, dx \wedge dy.$$

These represent classes in $\Omega^2/(df \wedge d\Omega^0)$.

The period integrals are $I_k(t) = \int_{\gamma(t)} \frac{\omega_k}{df}$ where the division by df converts the 2-form into a 1-form on the fiber. Since $df = 3x^2 dx + 2y\, dy$, on the fiber $\{x^3 + y^2 = t\}$ we can express:

$$I_0(t) = \int_{\gamma(t)} \frac{dx}{2y}, \quad I_1(t) = \int_{\gamma(t)} \frac{x\, dx}{2y}.$$

The period integrals can be evaluated by the scaling substitution $x = t^{1/3}u$ ($y = \sqrt{t - tu^3} = t^{1/2}\sqrt{1 - u^3}$), which shows:

$$I_k(t) = t^{(k+1)/3 - 1/2} \cdot C_k, \qquad k = 0, 1,$$

for nonzero constants C_k. In terms of the Gauss–Manin operator $t\partial_t$:

$$t\partial_t I_0 = -\frac{1}{6} I_0,$$
$$t\partial_t I_1 = \frac{1}{6} I_1.$$

These first-order ODEs have a regular singularity at $t = 0$. The solutions are:

$$I_0(t) = c_0 \cdot t^{-1/6}, \quad I_1(t) = c_1 \cdot t^{1/6}.$$

Analytic continuation $t \mapsto e^{2\pi i}t$ sends $I_0 \mapsto e^{-2\pi i/6}\, I_0$ and $I_1 \mapsto e^{2\pi i/6}\, I_1$. The two monodromy eigenvalues are $e^{\pm 2\pi i/6} = e^{\pm i\pi/3}$, which are exactly the roots of $\Delta_{A_2}(t) = t^2 - t + 1 = 0$. ✓

In the language of the spectrum, the spectral numbers are obtained by the shift spectral number = *exponent $+1$, giving $\alpha_1 = 5/6$ and $\alpha_2 = 7/6$.*

Example 14.2 (Picard-Fuchs for A_n: $f(x,y) = x^{n+1} + y^2$)**.** *More generally, for $f = x^{n+1} + y^2$, the Brieskorn module has basis $\omega_k = x^k dx \wedge dy$ for $k = 0, 1, \ldots, n-1$. The same scaling substitution $x = t^{1/(n+1)}u$ gives*

$$I_k(t) = c_k \cdot t^{(k+1)/(n+1) - 1/2}, \quad 0 \le k \le n-1.$$

In terms of the Gauss–Manin operator:

$$t\partial_t I_k = \frac{2(k+1) - (n+1)}{2(n+1)} I_k.$$

The monodromy eigenvalues are $e^{2\pi i(2(k+1)-(n+1))/(2(n+1))}$ for $k = 0, \ldots, n-1$. The spectral numbers (shifting by $+1$) are:

$$s_k = \frac{2(k+1) + (n+1)}{2(n+1)}, \quad k = 0, \ldots, n-1,$$

which range from $\frac{n+3}{2(n+1)}$ (at $k = 0$) to $\frac{3n+1}{2(n+1)}$ (at $k = n-1$), consistently symmetric about $\frac{n+1}{2} \cdot \frac{2}{n+1} = 1$.

14.6 Computation for Diagonal Singularities

For a Brieskorn-Pham polynomial $f(z) = z_0^{a_0} + z_1^{a_1} + \cdots + z_n^{a_n}$, the characteristic polynomial of the monodromy operator was elegantly isolated. By the Thom-Sebastiani structure, the geometric monodromy operator splits into a tensor product of the monodromy operators of the individual variables $z_k^{a_k}$.

For a single variable $f(z) = z^a$, the Milnor fiber is $\{z \in \mathbb{C} \mid z^a = 1\}$, which consists of a points. The degree 0 homology has rank $a - 1$ (reduced). The monodromy merely cycles these a points perfectly. The eigenvalues are $e^{2\pi ik/a}$ for $1 \le k \le a-1$.

For the full diagonal polynomial f, the eigenvalues on the middle homology $H_n(F)$ are exactly all the products:

$$\lambda = \prod_{j=0}^{n} \exp\left(\frac{2\pi i k_j}{a_j}\right), \quad 1 \le k_j \le a_j - 1.$$

Indeed, they are explicitly roots of unity.

14.7 Exercises

Exercise 14.1. *Compute the characteristic polynomial of the monodromy operator h_* for the ordinary cusp singularity $f(x,y) = x^2 + y^3$. List the explicit roots of unity that occur as eigenvalues.*

Exercise 14.2. *The differential equation satisfied by the period integral $I(t) = \int_{\gamma(t)} \frac{dx \wedge dy}{df}$ for $f(x,y) = x^2 + y^3$ is a hypergeometric differential equation. Set up the Gauss-Manin connection operator $t\partial_t$ for this singularity and explicitly show the regular singular point structure.*

15 Mixed Hodge Structures on the Milnor Fiber

To fully comprehend the deep topological invariants of an isolated hypersurface singularity beyond Betti numbers and monodromy, one must invoke Hodge theory. For smooth projective varieties, classical Hodge theory imposes an elegant decomposition on cohomology. Although the Milnor fiber F is an open manifold—and hence lacks a pure Hodge structure—it miraculously admits a canonically defined **Mixed Hodge Structure (MHS)** , a monumental result established independently by Steenbrink and Varchenko. This structure, especially computable in the quasi-homogeneous case, weaves together our knowledge of the Gauss-Manin connection, local algebras, and algebraic periods.

15.1 The Construction of the MHS

Let $f : (\mathbb{C}^{n+1}, 0) \to (\mathbb{C}, 0)$ be the germ of an isolated hypersurface singularity. Deligne developed the idea that the cohomology of any algebraic variety carries a mixed Hodge structure: a combination of an increasing *weight filtration* $W_\bullet$ (measuring how far the space is from being compact and smooth) and a decreasing *Hodge filtration* $F^\bullet$ (reflecting holomorphic differential form types).

For the Milnor fiber F, Steenbrink defined this MHS on the middle cohomology $H^n(F; \mathbb{C})$ by utilizing a resolution of singularities of the central fiber $f^{-1}(0)$. Because the monodromy operator h_* must be considered, the Gauss-Manin connection plays a critical role. Specifically, if we decompose the quasi-unipotent monodromy into its semisimple and nilpotent parts $h_* = h_s h_u$, we can write $h_u = \exp(N)$ where $N = \log h_u$ is a nilpotent operator. This nilpotent operator N acts dynamically to shift the weight filtration $W_\bullet$ of the MHS.

Theorem 15.1 (Steenbrink, Varchenko)**.** *The middle cohomology $H^n(F; \mathbb{Q})$ of the Milnor fiber carries a natural Mixed Hodge Structure $(F^\bullet, W_\bullet)$. The weight filtration is indexed from 0 to $2n$, and the nilpotent operator $N = \log h_u$ acts as a morphism of MHS of type $(-1, -1)$.*

The *Hodge numbers* associated to this structure, $h^{p,q} = \dim_{\mathbb{C}} \mathrm{Gr}_F^p \mathrm{Gr}_{p+q}^W H^n(F; \mathbb{C})$, provide an incredibly fine geometric invariant. Summing these recovers the Milnor number: $\sum_{p,q} h^{p,q} = \mu$.

15.2 The Spectrum of a Singularity

A tremendous simplification occurs if we organize the eigenvalues of the semisimple monodromy h_s along with the Hodge filtration index. This leads to the **Spectrum** $\mathrm{Sp}(f)$ of the singularity, an invariant consisting of μ rational numbers $0 < \alpha_1 \leq \alpha_2 \leq \cdots \leq \alpha_\mu < n + 1$.

For each eigenvector $v \in H^n(F; \mathbb{C})$ with eigenvalue $\lambda = e^{2\pi i \alpha}$ lying in the graded piece Gr_F^p, we record the spectral number $\alpha = p + \nu$, where $\nu \in (0, 1]$ is the fractional part ensuring $e^{2\pi i \nu} = \lambda$.

Proposition 15.1 (Symmetry of the Spectrum)**.** *The spectrum of an isolated hypersurface singularity enjoys central symmetry about $\frac{n+1}{2}$. That is, the multiplicity of the spectral number α is identical to the multiplicity of $n + 1 - \alpha$.*

15.3 Calculations for Quasi-homogeneous Singularities

If f is a *quasi-homogeneous* polynomial, its MHS and spectrum can be computed purely combinatorially from the monomial basis of the Milnor algebra!

Let $f(z_0, \ldots, z_n)$ be quasi-homogeneous with weights $w_0, \ldots, w_n > 0$ such that $f(\lambda^{w_0} z_0, \ldots, \lambda^{w_n} z_n) = \lambda f(z)$. The degree of f is normalized to 1. The Milnor algebra is $M_f = \mathbb{C}[z_0, \ldots, z_n]/(\frac{\partial f}{\partial z_i})$. For

any monomial class $[z^K] = [z_0^{k_0} \cdots z_n^{k_n}] \in M_f$, we can assign an internal degree:

$$\deg(z^K) = \sum_{i=0}^{n} w_i(k_i + 1).$$

(The $+1$ comes formally from considering the differential form $z^K dz_0 \wedge \cdots \wedge dz_n$).

Theorem 15.2 (Steenbrink's Formula)**.** *For a quasi-homogeneous isolated singularity f, the spectral numbers $\{\alpha_1 \ldots, \alpha_\mu\}$ of the Milnor fiber's MHS are exactly the internal degrees* $\deg(z^K)$ *evaluated over a monomial basis of the Milnor algebra M_f.*

Let us exhibit the sheer computational power of this theorem.

Example 15.1 (The A_2 Singularity, $n = 1$)**.** *Consider $f(x, y) = x^2+y^3$. To make f homogeneous of degree 1, we must set weights: $w_x = 1/2$, $w_y = 1/3$. The Milnor algebra is $\mathbb{C}[x, y]/(x, y^2)$, which has a basis composed of* 1 *and* y*. Here $\mu = 2$. Let's compute their degrees:*

$$\deg(1) = w_x(0 + 1) + w_y(0 + 1) = \frac{1}{2} + \frac{1}{3} = \frac{5}{6}.$$
$$\deg(y) = w_x(0 + 1) + w_y(1 + 1) = \frac{1}{2} + \frac{2}{3} = \frac{7}{6}.$$

Hence, the spectrum of A_2 is $(\frac{5}{6}, \frac{7}{6})$. Notice that these perfectly sum to $2 = \frac{1+1+2}{2} = \frac{n+1}{2} \cdot 2$, confirming spectral symmetry ($n = 1$, symmetry center is 1*). The monodromy eigenvalues are $e^{2\pi i(5/6)} = e^{-2\pi i/6}$ and $e^{2\pi i(7/6)} = e^{2\pi i/6}$, which matches the classic roots.*

Example 15.2 (The D_4 Singularity, $n = 2$)**.** *Let $f(x, y, z) = x^2y - y^3 + z^2$ (a slight variant of D_4). Set weights $w_x = 1/2$, $w_y = 1/3$, $w_z = 1/2$ ... wait, for $x^2y - y^3$ to balance, we need $2w_x + w_y = 3w_y = 1 \implies w_y = 1/3$, so $w_x = 1/3$. Let $w_z = 1/2$. The Jacobian ideal is $(\frac{\partial f}{\partial x} = 2xy, \frac{\partial f}{\partial y} = x^2 - 3y^2, \frac{\partial f}{\partial z} = 2z)$. The Milnor algebra has basis: $1, x, y, x^2$ (modding out z and $x^2 - 3y^2$). So $\mu = 4$. Degrees:*

$$\deg(1) = \frac{1}{3} + \frac{1}{3} + \frac{1}{2} = \frac{7}{6}.$$
$$\deg(x) = \frac{2}{3} + \frac{1}{3} + \frac{1}{2} = \frac{9}{6} = \frac{3}{2}.$$
$$\deg(y) = \frac{1}{3} + \frac{2}{3} + \frac{1}{2} = \frac{9}{6} = \frac{3}{2}.$$
$$\deg(x^2) = \frac{3}{3} + \frac{1}{3} + \frac{1}{2} = \frac{11}{6}.$$

The spectrum is $(\frac{7}{6}, \frac{3}{2}, \frac{3}{2}, \frac{11}{6})$. Symmetry center is $(2 + 1)/2 = 1.5$. The elements mirror around 1.5.

15.4 Newton Polygons and Non-Degenerate Singularities

While quasi-homogeneous polynomials form a remarkably computable class, isolating exact weights is not always naturally feasible. A much more expansive and powerful generalized combinatorial tool comes from Newton Polygons (and generally Newton Polyhedra in higher dimensions). This technique bridges the analytic topology with convex geometry.

Definition 15.1 (Newton Polyhedron and Boundary)**.** *Let $f(z) = \sum a_k z^k$ be a Taylor series germ at the origin in $\mathbb{C}^{n+1}$, where $k = (k_0, \ldots, k_n) \in \mathbb{Z}^{n+1}_{\geq 0}$ and $z^k = z_0^{k_0} \cdots z_n^{k_n}$. The **Newton Polyhedron** $\Gamma_+(f)$ is defined dynamically as the convex hull in $\mathbb{R}^{n+1}$ of the union of all quadrants translated by the support of polynomial:*

$$\Gamma_+(f) = \text{Conv}(\{k + \mathbb{R}^{n+1}_{\geq 0} \mid a_k \neq 0\}).$$

*The **Newton Boundary** $\Gamma(f)$ is the union of all the compact faces of $\Gamma_+(f)$.*

The Newton boundary encapsulates the *dominant* lowest degree terms of the polynomial, essentially filtering out the higher-order deformation terms that don't influence local topological properties. For a 2-variable polynomial, it is literally the innermost polygon line formed sequentially by connecting the lowest coordinate degrees.

We say f is **non-degenerate with respect to its Newton boundary** if for every compact face $\Delta \subset \Gamma(f)$, the truncated polynomial $f_\Delta(z) = \sum_{k \in \Delta} a_k z^k$ defines a smooth, non-singular hypersurface inside the complex algebraic torus $(\mathbb{C}^*)^{n+1}$. By Kouchnirenko's theorem, *most* singularities with a given Newton boundary are automatically non-degenerate.

Theorem 15.3 (Kouchnirenko's Formula for the Milnor Number)**.** *If $f(z)$ is isolated and non-degenerate with respect to its Newton boundary, and its Newton polyhedron intersects every coordinate axis, then its Milnor number μ is a topological invariant determined exclusively by the geometric volume of the region beneath the Newton boundary! For $n = 1$ (curves), if the Newton boundary cuts the axes at points $(A, 0)$ and $(0, B)$ and binds an area S_- with the axes, we have:*

$$\mu = 2S_- - A - B + 1.$$

In general dimension $n + 1$, μ equates to $(n + 1)!$ times the Newton volume minus the adjusted lower-coordinate dimensional volumes.

Newton polygons powerfully extend our MHS computations. Just as Steenbrink used the internal degrees $\sum w_i k_i$ for spectra, analogous formulas by Danilov, Kouchnirenko, and Varchenko demonstrate that the Hodge numbers $h^{p,q}$ directly correspond to the number of generic lattice points $\mathbb{Z}^{n+1}$ contained at specifically controlled depth levels inside the Newton geometry.

Example 15.3 (A Non-degenerate Computation)**.** *Let $f(x, y) = x^5 + y^5 + x^2y^2$. It is decisively not quasi-homogeneous because the x^2y^2 term destroys any homogeneous pure scaling. However, plotting its exponents $(5, 0)$, $(0, 5)$ and $(2, 2)$, we see the convex hull naturally forms a Newton boundary composed of two edge segments: one connecting $(5, 0) \to (2, 2)$ and another $(2, 2) \to (0, 5)$. The area S_- bounded between the coordinate axes $x = 0$, $y = 0$ and this multi-segment interior boundary consists of a 2×2 square plus two triangles of base 3 and height 2.*

$$S_- = (2 \times 2) + \frac{1}{2}(3 \times 2) + \frac{1}{2}(3 \times 2) = 4 + 3 + 3 = 10.$$

The intercepts on the axes are obviously $A = 5$ and $B = 5$. Plugging into Kouchnirenko's Area Formula directly outputs:

$$\mu = 2(10) - 5 - 5 + 1 = 20 - 10 + 1 = 11.$$

Indeed, a rigorous computer algebra calculation matching the finite sum of Jacobian moduli for $(x^5 + y^5 + x^2y^2)$ yields precisely 11! Newton Polygons convert an agonizing algebraic ideal reduction into a grade-school polyhedral geometry exercise.

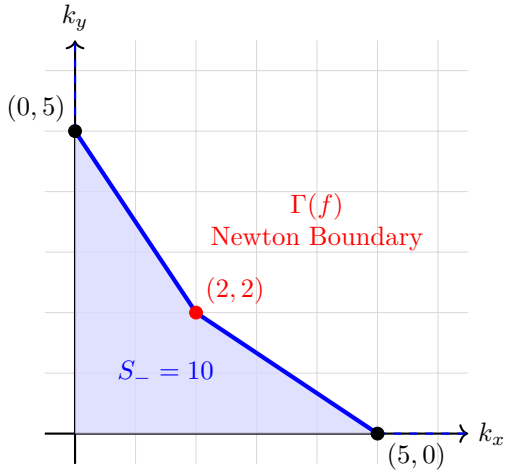

Figure 24: The Newton Polygon for $f(x,y) = x^5 + y^5 + x^2y^2$. The Newton boundary filters the topological complexity, perfectly predicting the Milnor number by calculating the discrete continuous geometric area S_- subtended by the inner faces.

Example 15.4 (Recovering the Brieskorn-Pham / Diagonal Formula)**.** *Consider the classic diagonal Brieskorn-Pham singularity $f(x,y) = x^a + y^b$. The monomials only possess components $(a,0)$ and $(0,b)$. The Newton boundary $\Gamma(f)$ is an incredibly simple straight line segment connecting these two points. The region S_- bounded by the axes and this single boundary segment is a straight right triangle with base a and height b. Its continuous geometric interior area is exactly the classic Euclidean triangle area $S_- = \frac{1}{2}ab$. The intercepts on the coordinate axes are explicitly $A = a$ and $B = b$.*

Using Kouchnirenko's Area Formula computationally yields:

$$\mu = 2\left(\frac{1}{2}ab\right) - a - b + 1 = ab - a - b + 1 = (a-1)(b-1).$$

This spectacularly reproduces the identical algebraic formula we derived in §6 via the purely algebraic dimension count of the Jacobian ideal's basis, demonstrating a profound internal consistency between ideal topology and convex integer geometry!

Example 15.5 (A Genuine Three-Edge Newton Polygon)**.** *Consider*

$$f(x,y) = x^8 + x^5y + x^3y^4 + y^9.$$

Its support points $(8,0)$, $(5,1)$, $(3,4)$, and $(0,9)$ are all vertices of the lower convex hull, so $\Gamma(f)$ has three distinct compact edges. This is the first truly multi-slope situation: different boundary segments record different dominant balances between x and y, and the Newton polygon is no longer reducible to one triangle or one weighted-homogeneous line.

The region S_- is the polygon with vertices $(0,0)$, $(8,0)$, $(5,1)$, $(3,4)$, $(0,9)$. Using the shoelace formula,

$$S_- = \frac{1}{2}\big((8\cdot 1 + 5\cdot 4 + 3\cdot 9) - (1\cdot 3)\big) = \frac{1}{2}(55-3) = 26.$$

Since the axis intercepts are $A = 8$ and $B = 9$, Kouchnirenko's formula gives

$$\mu = 2S_- - A - B + 1 = 2(26) - 8 - 9 + 1 = 36.$$

Non-degeneracy is checked edge-by-edge. For the first edge, $f_{\Delta_1} = x^8 + x^5 y$*, so on* $\{f_{\Delta_1} = 0\} \cap (\mathbb{C}^*)^2$ *we get* $y = -x^3$*, and then*

$$x\partial_x f_{\Delta_1} = 8x^8 + 5x^5 y = 3x^8 \neq 0.$$

For the middle edge, $f_{\Delta_2} = x^5 y + x^3 y^4 = x^3 y(x^2 + y^3)$*, hence* $y^3 = -x^2$ *on the torus zero set, and*

$$x\partial_x f_{\Delta_2} = 5x^5 y + 3x^3 y^4 = 2x^5 y \neq 0.$$

For the last edge, $f_{\Delta_3} = x^3 y^4 + y^9 = y^4(x^3 + y^5)$*, so* $y^5 = -x^3$ *and*

$$x\partial_x f_{\Delta_3} = 3x^3 y^4 \neq 0.$$

Thus every compact face is smooth inside $(\mathbb{C}^*)^2$*, so the polynomial is Newton non-degenerate and its Milnor number is indeed* $\mu = 36$*.*

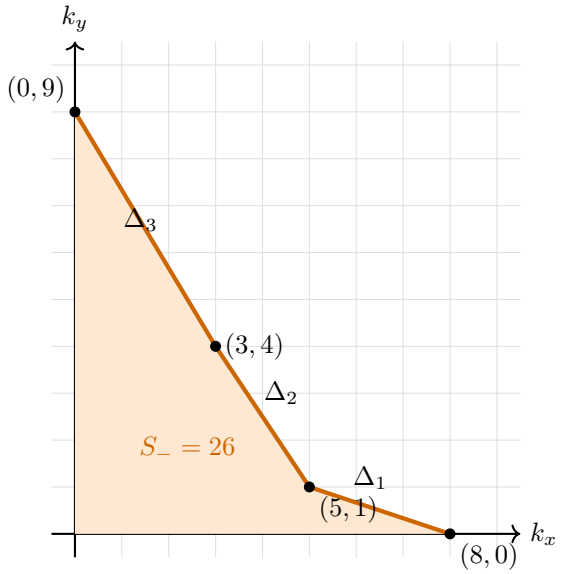

Figure 25: A three-edge Newton polygon for $f(x, y) = x^8 + x^5 y + x^3 y^4 + y^9$. The three compact faces encode three different dominant balances, but the Milnor number is still extracted from the single combinatorial area S_-.

15.5 Algorithmic Computation with Newton Polygons

The practical power of Newton polygons lies in their algorithmic nature. We summarize a step-by-step procedure for computing the Milnor number and verifying non-degeneracy, which can be implemented in computer algebra systems such as `SINGULAR` or `Macaulay2`.

1. **Input:** A polynomial $f(z_0, \ldots, z_n) = \sum a_k z^k$.
2. **Compute the support:** Extract $\operatorname{supp}(f) = \{k \in \mathbb{Z}^{n+1}_{\geq 0} : a_k \neq 0\}$.
3. **Construct $\Gamma_+(f)$:** Compute the convex hull of $\bigcup_{k \in \operatorname{supp}(f)} (k + \mathbb{R}^{n+1}_{\geq 0})$. In practice, this reduces to computing the *lower* convex hull of the support points.

4. **Identify compact faces:** Enumerate all compact faces Δ of $\Gamma_+(f)$ (edges in 2D, faces/edges in 3D).

5. **Non-degeneracy check:** For each compact face Δ, form $f_\Delta = \sum_{k\in\Delta} a_k z^k$. Verify that $\{f_\Delta = 0\} \cap (\mathbb{C}^*)^{n+1}$ is smooth by checking that $\nabla f_\Delta \neq 0$ on this set. In `SINGULAR`, this is done by computing the ideal $(f_\Delta, z_0\partial_{z_0} f_\Delta, \ldots, z_n\partial_{z_n} f_\Delta)$ and verifying it equals (1) in $\mathbb{C}[z_0^{\pm 1}, \ldots, z_n^{\pm 1}]$.

6. **Compute the Milnor number:** Apply Kouchnirenko's volume formula: $\mu = (-1)^{n+1} + (n+1)! \cdot V_0 - n! \sum_i V_i + \cdots$, where V_0 is the volume of the region below $\Gamma(f)$ and V_i are the volumes of the codimension-1 faces projected onto coordinate hyperplanes.

Example 15.6 (Complete Computation: $f(x,y) = x^4 + x^2y^3 + y^6$). ***Step 1–2:*** *Support* $= \{(4,0),(2,3),(0,6)\}$.

Step 3: *The Newton boundary consists of one line segment from* $(4,0)$ *to* $(2,3)$ *and another from* $(2,3)$ *to* $(0,6)$. *The supporting lines are* $3k_x + 2k_y = 12$ *(edge* L_1*) and* $3k_x + 2k_y = 12$ *(same line!). In fact, all three support points are collinear:* $3(4) + 2(0) = 12$, $3(2) + 2(3) = 12$, $3(0) + 2(6) = 12$. *So* $\Gamma(f)$ *is a single edge.*

Step 4: *One compact face* $\Delta = L_1$ *with* $f_\Delta = x^4 + x^2y^3 + y^6 = f$ *itself.*

Step 5 (Non-degeneracy): *Check* $f_\Delta = x^4 + x^2y^3 + y^6$ *on* $(\mathbb{C}^*)^2$. *We compute* $x\partial_x f = 4x^4 + 2x^2y^3$ *and* $y\partial_y f = 3x^2y^3 + 6y^6$. *Setting* $f = x\partial_x f = y\partial_y f = 0$ *on* $(\mathbb{C}^*)^2$*: from* $x\partial_x f = 2x^2(2x^2 + y^3) = 0$ *and* $x \neq 0$, *get* $y^3 = -2x^2$. *Then* $f = x^4 - 2x^4 + 4x^4 = 3x^4 \neq 0$. *So* f *is non-degenerate.*

Step 6 (Milnor number): *The intercepts are* $A = 4$, $B = 6$. *The area below the boundary segment is* $S_- = \frac{1}{2}(4)(6) = 12$. *Thus* $\mu = 2(12) - 4 - 6 + 1 = 15$.

Note that all three support points satisfy $3k_x + 2k_y = 12$. *Equivalently,* f *is weighted homogeneous either with normalized weights* $(w_x, w_y) = (\frac{1}{4}, \frac{1}{6})$ *and weighted degree* 1, *or with integral weights* $(3,2)$ *and weighted degree* 12. *This is exactly why the Newton boundary collapses to a single compact face, and the Milnor algebra computation agrees with Kouchnirenko's formula, again giving* $\mu = 15$.

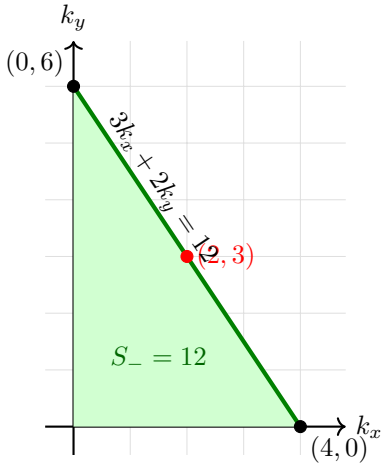

Figure 26: For $f(x,y) = x^4 + x^2y^3 + y^6$, all support points lie on the same supporting line, so the Newton boundary is a single compact face. The middle point $(2,3)$ does not create a new edge; it only enriches the face polynomial.

Example 15.7 (A Degenerate Face Polynomial)**.** *Consider*

$$g(x,y) = x^6 + 2x^3y^3 + y^6 = (x^3+y^3)^2.$$

Its support points are $(6,0)$*,* $(3,3)$*, and* $(0,6)$*, all lying on the single segment* $k_x + k_y = 6$*. Geometrically the Newton polygon looks completely harmless: it is the same triangle one would draw for a perfectly good weighted-homogeneous singularity. The problem is not the polygon itself, but the face polynomial on the compact edge:*

$$g_\Delta = x^6 + 2x^3y^3 + y^6 = (x^3+y^3)^2.$$

On $(\mathbb{C}^*)^2$*, every point with* $x^3+y^3=0$ *satisfies* $g_\Delta = 0$*, and along the same locus we also have*

$$x\partial_x g_\Delta = 6x^3(x^3+y^3) = 0, \qquad y\partial_y g_\Delta = 6y^3(x^3+y^3) = 0.$$

Hence $\{g_\Delta = 0\} \subset (\mathbb{C}^*)^2$ *is singular, so* g *is degenerate with respect to its Newton boundary. In fact the singularity at the origin is not isolated, because both partial derivatives vanish along the curve* $x^3+y^3=0$*.*

This is the basic warning one must keep in mind when using Newton polygons: the convex geometry suggests what might happen, but the non-degeneracy condition is what prevents repeated factors on the faces from destroying the local topology.

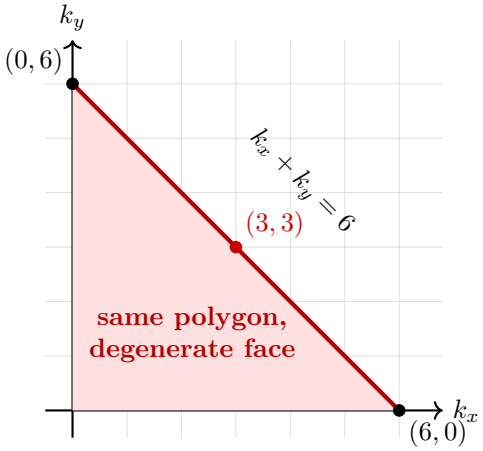

Figure 27: The Newton polygon for $g(x,y) = x^6 + 2x^3y^3 + y^6$ looks innocuous, but the face polynomial is $(x^3+y^3)^2$, so the torus hypersurface on the compact face is singular. This is precisely the kind of situation excluded by Newton non-degeneracy.

Example 15.8 (A Three-Dimensional Newton Polyhedron)**.** *The same combinatorics works in higher dimension, but one must now keep track of volumes and coordinate-plane areas. Consider*

$$f(x,y,z) = x^4 + y^4 + z^4 + xyz.$$

The support points are

$$A = (4,0,0), \qquad B = (0,4,0), \qquad C = (0,0,4), \qquad D = (1,1,1).$$

The inner point D breaks the diagonal simplex into three compact faces $\Delta_{xy} = \triangle ABD$, $\Delta_{xz} = \triangle ACD$, and $\Delta_{yz} = \triangle BCD$. Thus the region under the Newton boundary is the union of three tetrahedra:

$$\mathrm{Vol}(OABD) = \mathrm{Vol}(OACD) = \mathrm{Vol}(OBCD) = \frac{16}{6},$$

so the total Newton volume is

$$V = \frac{16}{6} + \frac{16}{6} + \frac{16}{6} = 8.$$

Each coordinate-plane section is still a triangle of area 8:

$$P_x = \mathrm{Area}(OBC) = 8, \qquad P_y = \mathrm{Area}(OAC) = 8, \qquad P_z = \mathrm{Area}(OAB) = 8,$$

and the axis intercept lengths are $L_x = L_y = L_z = 4$. Therefore the three-variable version of Kouchnirenko's formula gives

$$\mu = 6V - 2(P_x + P_y + P_z) + (L_x + L_y + L_z) - 1 = 6(8) - 2(24) + 12 - 1 = 11.$$

Non-degeneracy is especially transparent here. On the face Δ_{xy} we have $f_{\Delta_{xy}} = x^4 + y^4 + xyz$, and on $(\mathbb{C}^*)^3$ the logarithmic derivative in the z-direction is

$$z\partial_z f_{\Delta_{xy}} = xyz \neq 0.$$

So $f_{\Delta_{xy}} = 0$ cannot have a critical point on the torus. The same argument works for Δ_{xz} and Δ_{yz}, using $y\partial_y$ or $x\partial_x$ respectively. Hence f is Newton non-degenerate, and the combinatorial computation predicts $\mu = 11$.

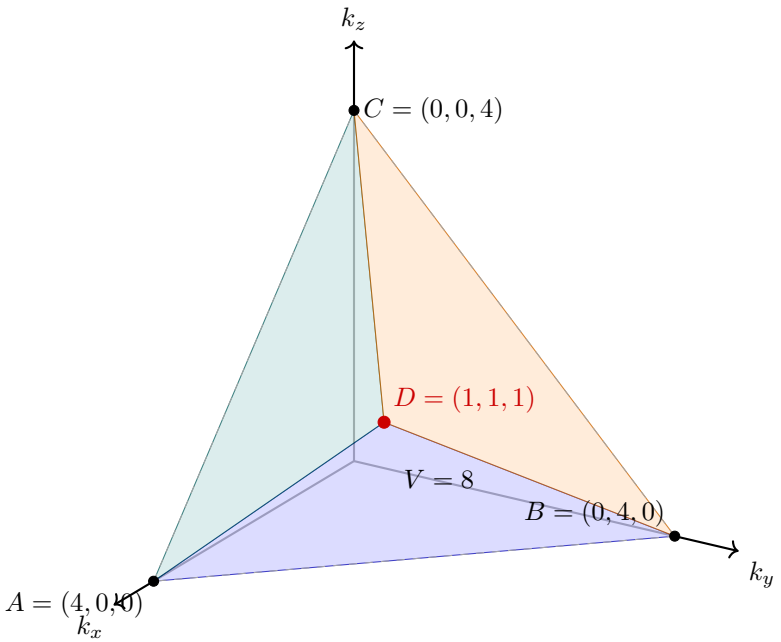

Figure 28: A three-dimensional Newton polyhedron for $f(x, y, z) = x^4 + y^4 + z^4 + xyz$. The interior support point $(1, 1, 1)$ breaks the diagonal simplex into three compact triangular faces, and the Newton volume is computed by summing the three tetrahedra beneath them.

15.6 Exercises

Exercise 15.1. *Compute the spectrum for the E_8 singularity $f(x,y) = x^3 + y^5$ ($n = 1$). Find its $\mu = 8$ spectral numbers and verify that it is symmetric about 1. Use this to show that the monodromy operator has no fixed points on the middle homology (no eigenvalue is exactly 1).*

Exercise 15.2. *Explain why for an isolated hypersurface singularity inside $\mathbb{C}^{n+1}$, if $n > 0$, the lowest spectral number α_1 strictly bounds the canonical threshold, and explicitly argue why $\alpha_1 = \sum w_i > 1$ correlates to the singularity being rational.*

Exercise 15.3. *Let $f(x,y) = x^3 + xy^4$. Draw the Newton polygon, verify non-degeneracy with respect to the Newton boundary, and compute μ using Kouchnirenko's formula. Compare your result with a direct computation via $\dim_{\mathbb{C}} \mathbb{C}\{x,y\}/(\partial_x f, \partial_y f)$.*

15.7 The Limit Mixed Hodge Structure and Filtrations

The deep machinery behind Steenbrink's result is the construction of the **Limit Mixed Hodge Structure**. When we consider the Milnor fibration over the punctured disk S^*, the local system of cohomology $H^n(F_t; \mathbb{C})$ forms a flat vector bundle equipped with the Gauss-Manin connection ∇. However, to capture the geometry of the singular fiber at $t = 0$, we must study the asymptotic behavior of the periods as $t \to 0$.

Schmid's Nilpotent Orbit Theorem governs this degeneration. If we trivially trivialize the bundle by pulling back along the universal cover $\tilde{S}^* \to S^*$, the multi-valued periods become single-valued functions involving $\log(t)$. The monodromy transformation $h_* = h_s e^N$ dictates that the periods have logarithmic singularities.

The **Weight Filtration** $W_\bullet$ on the limiting cohomology H^n_∞ is uniquely determined by the nilpotent operator $N = \log(h_u)$. It is the unique increasing filtration

$$0 \subset W_0 \subset W_1 \subset \cdots \subset W_{2n} = H^n_\infty$$

such that $N(W_k) \subset W_{k-2}$ for all k, and the induced maps on the graded quotients

$$N^k : \mathrm{Gr}^W_{n+k} \xrightarrow{\sim} \mathrm{Gr}^W_{n-k}$$

are isomorphisms for all $k \geq 0$. This mirrors the Hard Lefschetz theorem locally.

The **Hodge Filtration** $F^\bullet$, on the other hand, is defined analytically using the Gauss-Manin connection and the Brieskorn lattice H''_0. By extending the flat bundle to a canonical extension over the origin (Deligne's extension), and pulling back the Hodge bundles of the individual fibers, one defines a limiting Hodge filtration $F^\bullet_{lim}$ on H^n_∞. The celebrated result of Schmid and Steenbrink is that $(W_\bullet, F^\bullet_{lim})$ constitutes a Mixed Hodge Structure on $H^n(F; \mathbb{C})$.

Alternatively, the Hodge filtration can be recovered purely algebraically from the V-filtration of Kashiwara and Malgrange on the Brieskorn module, showing that the mixed Hodge theory is intimately tied to the theory of $\mathcal{D}$-modules and b-functions (Bernstein-Sato polynomials). We develop this algebraic approach in the next subsection.

15.8 The V-Filtration and the Canonical Lattice

The V-filtration, introduced independently by Kashiwara and Malgrange, provides a purely algebraic construction of the limit MHS that bypasses the need for resolutions of singularities. It works directly on the meromorphic Gauss-Manin connection module $\mathcal{M}$ and exploits the root decomposition of the operator $t\partial_t$.

Root Decomposition of the Meromorphic Connection

Recall from the previous section that the Brieskorn module H_0'' is a free $\mathbb{C}\{t\}$-module of rank μ. By inverting t, we obtain the **meromorphic connection module**:

$$\mathcal{M} = H_0''[t^{-1}] = H_0'' \otimes_{\mathbb{C}\{t\}} \mathbb{C}\{t\}[t^{-1}].$$

The operator $t\partial_t$ acts on $\mathcal{M}$, and the regularity theorem guarantees that this action has a well-controlled structure.

Since the monodromy $T = h_*$ is quasi-unipotent, its eigenvalues $\lambda = e^{2\pi i\beta}$ are roots of unity with $\beta \in \mathbb{Q}$. For each such eigenvalue, we choose a determination of the logarithm: $\alpha = -\frac{1}{2\pi i}\log\lambda \in \mathbb{Q}$, normalized so that $-1 < \alpha \leq 0$.

The module $\mathcal{M}$ decomposes into a direct sum of **root subspaces**:

$$\mathcal{M} = \widehat{\bigoplus}_{\alpha\in\mathbb{Q}} C_\alpha,$$

where C_α is the generalized eigenspace on which $(t\partial_t - \alpha)$ is nilpotent. Concretely, $C_\alpha = \{\omega \in \mathcal{M} : (t\partial_t - \alpha\,\mathrm{id})^N\omega = 0 \text{ for } N \gg 0\}$.

The key algebraic properties of this decomposition are:

- **Multiplication by** t: The operator $t : C_\alpha \xrightarrow{\sim} C_{\alpha+1}$ is an isomorphism for all α.
- ∂_t **operator**: The operator $\partial_t : C_\alpha \to C_{\alpha-1}$ is an isomorphism for all $\alpha \neq 0$.
- On C_α, we can write $t\partial_t = \alpha\,\mathrm{id} + N_\alpha$ where N_α is nilpotent.

Definition 15.2 (V-filtration (Kashiwara–Malgrange))**.** *The* V***-filtration*** *on* $\mathcal{M}$ *is the decreasing filtration defined using the order function:*

$$V^\alpha\mathcal{M} = \{\omega \in \mathcal{M} : \alpha(\omega) \geq \alpha\} = \widehat{\bigoplus}_{\beta\geq\alpha} C_\beta,$$
$$V^{>\alpha}\mathcal{M} = \{\omega \in \mathcal{M} : \alpha(\omega) > \alpha\} = \widehat{\bigoplus}_{\beta>\alpha} C_\beta.$$

The associated graded is $\mathrm{Gr}_V^\alpha\mathcal{M} = V^\alpha/V^{>\alpha} \cong C_\alpha$.

Each term $V^\alpha\mathcal{M}$ is a free $\mathbb{C}\{t\}$-module of rank μ, invariant under $t\partial_t$ (i.e., it is a *saturated lattice*). The V-filtration is characterized by two conditions:

1. $t \cdot V^\alpha \subset V^{\alpha+1}$ and $\partial_t \cdot V^\alpha \subset V^{\alpha-1}$;
2. On each graded piece Gr_V^α, the operator $t\partial_t - \alpha$ is nilpotent.

The Canonical Lattice (Deligne Extension)

A crucial application of the V-filtration is the construction of Deligne's **canonical extension**.

Definition 15.3 (Canonical Lattice)**.** *The* ***canonical lattice*** *is defined as:*

$$\mathcal{L} = V^{>-1}\mathcal{M} = \bigoplus_{-1<\alpha\leq 0} \mathcal{O}_S \cdot C_\alpha.$$

It is the unique $\mathbb{C}\{t\}$*-lattice in* $\mathcal{M}$ *satisfying:*

1. *The connection* ∇ *has at most a* logarithmic pole *on* $\mathcal{L}$*:* $\nabla(\mathcal{L}) \subset \mathcal{L} \otimes \Omega^1_S(\log 0)$*, i.e.,* $t\partial_t$ *preserves* $\mathcal{L}$*.*

2. *The eigenvalues of the residue* $\mathrm{Res}_0 \nabla = (t\partial_t)|_{\mathcal{L}/t\mathcal{L}}$ *lie in the half-open interval* $(-1, 0]$*.*

The zero fiber $\mathcal{L}/t\mathcal{L} \cong \bigoplus_{-1<\alpha\leq 0} C_\alpha$ is canonically identified with the space $H = H^n(F_\infty; \mathbb{C})$ of multivalued horizontal sections (the "canonical fiber" of the local system). This identification is the key bridge connecting the algebraic V-filtration to the topological monodromy.

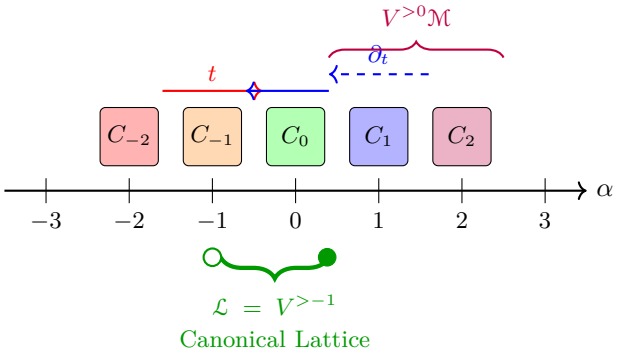

Figure 29: The root decomposition $\mathcal{M} = \widehat{\bigoplus} C_\alpha$ and the V-filtration. The canonical lattice $\mathcal{L} = V^{>-1}\mathcal{M}$ collects the root subspaces with $\alpha \in (-1, 0]$. Multiplication by t shifts the index by $+1$, while ∂_t shifts by -1.

From the Brieskorn Lattice to the Hodge Filtration

The Hodge filtration on $H = \mathcal{L}/t\mathcal{L}$ is now defined purely in terms of the relative position of the Brieskorn lattice $\mathcal{H}^{(0)} = H''_0$ inside the canonical lattice $\mathcal{L}$.

By Malgrange's theorem, $\mathcal{H}^{(0)} \subset V^{>-1}\mathcal{M} = \mathcal{L}$. The Hodge filtration is then defined as (following Scherk–Steenbrink and Varchenko):

$$F^p\mathcal{L} = \partial_t^{n-p}\mathcal{H}^{(0)} \cap \mathcal{L} = \partial_t^{n-p}(V^{>n-p-1}\mathcal{H}^{(0)}).$$

Here ∂_t^{n-p} shifts the V-filtration index by $-(n-p)$, so the intersection with $\mathcal{L}$ ensures we remain in the canonical lattice. On the zero fiber, the induced filtration becomes:

$$F^p(\mathcal{L}/t\mathcal{L}) = \partial_t^{n-p}\left(\frac{V^{>n-p-1}\mathcal{H}^{(0)}}{V^{>n-p}\mathcal{H}^{(0)}}\right).$$

Proposition 15.2 (Spectrum via the V-filtration)**.** *The spectral numbers* $\alpha_1, \ldots, \alpha_\mu$ *of the singularity* f *are determined by the* V*-filtration of the Brieskorn lattice: the spectral number* α *has multiplicity*

$$n_\alpha = \dim_{\mathbb{C}} \mathrm{Gr}_V^\alpha \mathcal{H}^{(0)}/t \cdot \mathrm{Gr}_V^{\alpha+1}\mathcal{H}^{(0)}.$$

Equivalently, a $\mathbb{C}\{t\}$*-basis* $\omega_1, \ldots, \omega_\mu$ *of* $\mathcal{H}^{(0)}$ *ordered by their* V*-filtration orders* $\alpha(\omega_1) \leq \alpha(\omega_2) \leq \cdots \leq \alpha(\omega_\mu)$ *gives the spectral numbers as* $\alpha_i = \alpha(\omega_i)$*.*

This algebraic characterization makes the spectrum computable without any reference to resolutions or period integrals—one only needs to determine the position of the Brieskorn lattice $\mathcal{H}^{(0)}$ relative to the V-filtration on $\mathcal{M}$.

The Bernstein-Sato Polynomial

The V-filtration is intimately connected to the **Bernstein-Sato polynomial** (or b-function) of f. This is the minimal polynomial $b_f(s) \in \mathbb{C}[s]$ satisfying a functional equation:

$$b_f(s) f^s = P(s, z, \partial_z) \cdot f^{s+1}$$

for some differential operator $P \in \mathcal{D}[s]$, where $\mathcal{D} = \mathbb{C}\{z_0, \ldots, z_n\}\langle \partial_{z_0}, \ldots, \partial_{z_n} \rangle$ is the ring of local differential operators.

Theorem 15.4 (Malgrange, Kashiwara)**.** *If $\widetilde{b}_f(s) = b_f(s)/(s+1)$ denotes the reduced Bernstein–Sato polynomial, then its roots are precisely the negatives of the spectral numbers:*

$$\{\text{roots of } \widetilde{b}_f(s)\} = \{-\alpha : \alpha \in \mathrm{Sp}(f)\}.$$

In particular, the roots of $b_f(s)$ are negative rational numbers in the interval $(-n-1, 0)$, and $s = -1$ is always a root.

Example 15.9 (The b-function of A_μ)**.** *For $f(x) = x^{\mu+1}$ (a one-variable singularity with $n = 0$), the spectral numbers are $\alpha_k = \frac{k}{\mu+1}$ for $k = 1, \ldots, \mu$. The Bernstein-Sato polynomial is:*

$$\widetilde{b}_f(s) = \prod_{k=1}^{\mu} \left(s + \frac{k}{\mu+1} \right), \qquad b_f(s) = (s+1)\widetilde{b}_f(s).$$

For A_2: $f = x^3$ gives

$$b_f(s) = (s+1)\left(s + \frac{1}{3}\right)\left(s + \frac{2}{3}\right).$$

Example 15.10 (The b-function of $f(x, y) = x^2 + y^3$ (A_2 in two variables))**.** *Here $n = 1$ and $\mu = 2$. The spectral numbers are $\alpha_1 = 5/6$ and $\alpha_2 = 7/6$. The Bernstein-Sato polynomial is:*

$$b_f(s) = (s+1)\left(s + \frac{5}{6}\right)\left(s + \frac{7}{6}\right).$$

The reduced polynomial is therefore

$$\widetilde{b}_f(s) = \left(s + \frac{5}{6}\right)\left(s + \frac{7}{6}\right),$$

and its roots are exactly the negatives of the spectral numbers.

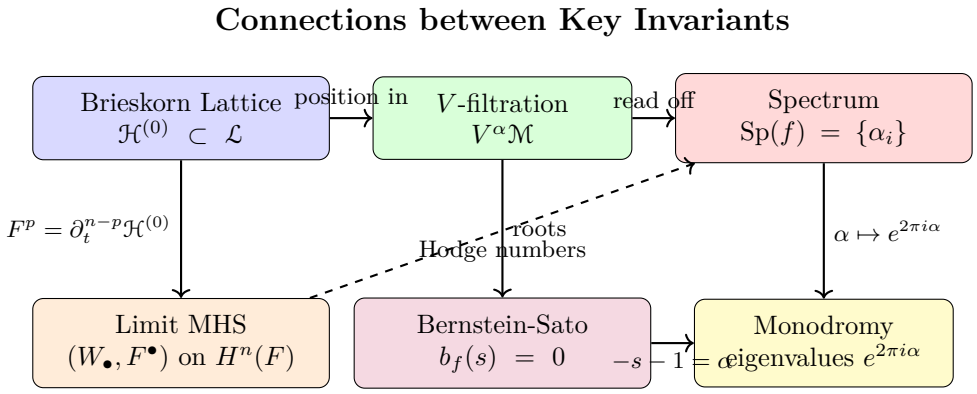

Figure 30: The web of relationships between the Brieskorn lattice, the V-filtration, the spectrum, the limit MHS, the Bernstein-Sato polynomial, and the monodromy eigenvalues. All paths are consistent: the algebraic (V-filtration) and analytic (limit MHS) approaches yield the same invariants.

Exercise 15.4. *Let $f(x,y,z) = x^a + y^b + z^c$ be a Brieskorn-Pham singularity ($n = 2$). Using the spectral formula for quasi-homogeneous singularities with weights $w_x = 1/a$, $w_y = 1/b$, $w_z = 1/c$, compute the spectral numbers and verify that the roots of the Bernstein-Sato polynomial are $\{-(\alpha+1) : \alpha \in \mathrm{Sp}(f)\}$. Do this explicitly for $(a,b,c) = (3,3,3)$.*

Exercise 15.5. *Show that the smallest spectral number $\alpha_{\min}$ of an isolated hypersurface singularity satisfies $\alpha_{\min} > 0$, and equals the **log canonical threshold** $\mathrm{lct}(f)$ of f. Use this to argue that the b-function always has -1 as its largest root.*

15.9 Spectral Pairs and the Steenbrink Spectral Sequence

To compute the Hodge numbers systematically, one constructs the **Steenbrink Spectral Sequence**. By replacing the singular fiber with a divisor with normal crossings $D = \cup D_i$ via a resolution of singularities function $\pi : X \to \mathbb{C}^{n+1}$, one forms a double complex of logarithmic differential forms $\Omega^\bullet_{X/S}(\log D)$.

This complex naturally carries two filtrations: the weight filtration (measuring the number of logarithmic poles along the intersections $D_i \cap D_j$) and the Hodge filtration. The associated spectral sequence

$$E_1^{p,q} \Rightarrow H^{p+q}(F;\mathbb{C})$$

degenerates at the E_2 page (and strictly depends only on E_1), calculating the MHS completely in terms of the combinatorics of the resolution graph and the cohomology of the smooth intersections of the exceptional divisors.

Steenbrink's E_1-Page Computation via Resolution

Let us describe Steenbrink's method more explicitly [Ste77; SS85]. Starting from a resolution $\pi : Y \to \mathbb{C}^{n+1}$ of the map f such that the total transform $(\pi^* f)^{-1}(0) = \sum_i m_i E_i$ is a normal crossing divisor, the E_1-page of the spectral sequence is computed from the cohomology of the strata of the exceptional divisor.

For each non-empty intersection $E_I = \bigcap_{i \in I} E_i$ (where $I \subset \{1, \ldots, r\}$ with $|I| = k+1$), define its "open" part $E_I^\circ = E_I \setminus \bigcup_{j \notin I} E_j$. The E_1-terms are:

$$E_1^{p,q} = \bigoplus_{|I|=q-p+1} H^{2p-q}(E_I^\circ; \mathbb{C})(\alpha_I)$$

where α_I denotes a Tate twist encoding the eigenvalue of the semisimple monodromy on that stratum, determined by the multiplicities m_i.

The differentials $d_1 : E_1^{p,q} \to E_1^{p+1,q}$ are given by Gysin maps (push-forward along codimension-1 inclusions of strata) combined with restriction maps. The E_2-page then gives the Hodge numbers:

$$h^{p,q} = \dim E_2^{p,q} = \dim E_\infty^{p,q}.$$

Example 15.11 (Steenbrink's Method for the A_2 Surface Singularity)**.** *Consider $f(x, y, z) = x^2 + y^2 + z^3$ ($n = 2$, $\mu = 2$). One blow-up at the origin gives a resolution where the exceptional divisor has one component $E_1 \cong \mathbb{P}^2$ with multiplicity $m_1 = 2$ (from the quadratic terms), and the strict transform of $\{f = 0\}$ intersects E_1 in a smooth conic C.*

The relevant strata are:

- $E_1^\circ = \mathbb{P}^2 \setminus C$*: This has* $\chi(E_1^\circ) = \chi(\mathbb{P}^2) - \chi(C) = 3 - 2 = 1$.
- $C^\circ = C$*: a smooth conic, so* $\chi(C) = 2$.

From the multiplicities and the eigenvalue computation, the semisimple monodromy eigenvalue on E_1° is $e^{2\pi i \cdot 1/2} = -1$ (since $m_1 = 2$, the local monodromy of z^2 around 0 gives eigenvalue $e^{\pi i}$). For the strict transform component, the eigenvalue is $e^{2\pi i \cdot 1/3}$.

The E_1-page computation then yields Hodge numbers $h^{1,1} = 1$ and $h^{2,2} = 1$ (with appropriate weight shifts), confirming the spectrum $\mathrm{Sp}(A_2) = (5/6,\, 7/6)$ obtained via the quasi-homogeneous method.

Varchenko's Formula: Spectrum from the Newton Polygon

For *non-degenerate* singularities (in the sense of Kouchnirenko), Varchenko [Var81] gave a purely combinatorial formula for the spectrum in terms of the Newton polyhedron, extending Steenbrink's quasi-homogeneous formula to the vastly larger class of Newton non-degenerate singularities.

Theorem 15.5 (Varchenko's Spectral Formula)**.** *Let $f : (\mathbb{C}^{n+1}, 0) \to (\mathbb{C}, 0)$ be a convenient, Newton non-degenerate isolated singularity with Newton polyhedron $\Gamma_+(f)$. For each integer lattice point $k = (k_0, \ldots, k_n) \in \mathbb{Z}_{>0}^{n+1}$ (i.e., with all coordinates strictly positive), define the* ***Newton distance****:*

$$\nu(k) = \inf\{t > 0 : k/t \in \Gamma_+(f)\}.$$

Then the spectrum of f consists of the values $\nu(k)$ for all $k \in \mathbb{Z}_{>0}^{n+1}$ satisfying $\nu(k) \leq 1$, together with the values $n + 1 - \nu(k)$ for those with $\nu(k) > 1$ (reflected through the symmetry center), counted with appropriate multiplicities determined by the faces of $\Gamma(f)$.

More precisely, the **spectral polynomial** can be expressed as an alternating sum over the faces of the Newton boundary:

$$\mathrm{SP}(f)(t) = \sum_{\Delta \preceq \Gamma(f)} (-1)^{\operatorname{codim} \Delta} \sum_{k \in \mathrm{cone}(\Delta) \cap \mathbb{Z}_{>0}^{n+1}} t^{\nu_\Delta(k)},$$

where $\nu_\Delta(k)$ is the distance function relative to the face Δ.

Example 15.12 (Spectrum via Newton Polygon: $f(x,y) = x^5 + x^2y^2 + y^5$)**.** *Recall from the earlier example that this non-degenerate polynomial has Newton boundary with two edges:* $(5,0) \to (2,2)$ *and* $(2,2) \to (0,5)$*, and* $\mu = 11$*.*

The Newton distance for a lattice point (a,b) *is determined by finding the parameter* t *such that* $(a/t, b/t)$ *lies on the Newton boundary. For the edge* L_1 *from* $(5,0)$ *to* $(2,2)$*, the supporting line is* $2k_x + 3k_y = 10$*, giving* $\nu_{L_1}(a,b) = (2a+3b)/10$*. For the edge* L_2 *from* $(2,2)$ *to* $(0,5)$*, the line is* $3k_x + 2k_y = 10$*, giving* $\nu_{L_2}(a,b) = (3a+2b)/10$*.*

The interior lattice points of $\mathbb{Z}^2_{>0}$ *contributing to the spectrum are those with* $\nu(k) \leq 2$ *(since* $n+1=2$*). Computing* $\nu(k) = \min(\nu_{L_1}(k), \nu_{L_2}(k))$ *for each point and listing the spectral values gives:*

$$\mathrm{Sp}(f) = \left(\frac{1}{2}, \frac{7}{10}, \frac{4}{5}, \frac{9}{10}, 1, 1, 1, \frac{11}{10}, \frac{6}{5}, \frac{13}{10}, \frac{3}{2}\right).$$

Note the symmetry about $\alpha = 1$ *(center for* $n = 1$*) and the appearance of the eigenvalue* 1 *(spectral number* $= 1$*) with multiplicity 3, indicating nontrivial Jordan blocks in the monodromy. This example illustrates how the Newton polygon approach handles non-quasi-homogeneous cases that are inaccessible to the direct weight formula.*

Beyond the spectrum, we can define the **Spectral Pairs**. For each eigenvector of the monodromy, we keep track of both its Hodge level and its weight level. A spectral pair is a tuple $(\alpha, w) \in \mathbb{Q} \times \mathbb{Z}$ where α is a spectral number and w indicates the weight of the corresponding Jordan block of the nilpotent operator N. The multiplicity of a spectral pair $h_{\alpha,w}$ completely captures the MHS.

A remarkable property of the spectrum revolves around the **Thom-Sebastiani Formula** . If we have two isolated singularities $f(x)$ and $g(y)$ in disjoint sets of variables, their sum $f(x)+g(y)$ is also an isolated singularity. What is its spectrum? Scherk and Steenbrink proved that the MHS of the join is the tensor product of the constituent MHSs. At the level of spectra, this means the spectral polynomial $\mathrm{SP}(f) = \sum t^\alpha$ satisfies:

$$\mathrm{SP}(f(x) + g(y)) = \mathrm{SP}(f) \cdot \mathrm{SP}(g)$$

meaning the spectral numbers of $f+g$ are precisely the all-pairs sums $\alpha_i(f) + \alpha_j(g)$.

15.10 Semicontinuity of the Spectrum

Deformation theory tightly constrains how the spectrum can vary. If an isolated singularity f_0 is deformed into a family of isolated singularities $\{f_s\}$ (perhaps splitting into multiple singular points $x_{s,i}$), the total Milnor number is conserved: $\mu_0 = \sum_i \mu_i(f_s)$. Varchenko proved a deep **Semicontinuity Theorem** for the spectrum. If we list the spectra in increasing order, the spectral numbers can only *increase* under deformation. Specifically, for any interval $(-\infty, a]$, the number of spectral numbers in this interval for the deformed singularities cannot exceed the number for the original central singularity:

$$\sum_i |\{\alpha \in \mathrm{Sp}(f_{s,i}) \mid \alpha \leq a\}| \leq |\{\alpha \in \mathrm{Sp}(f_0) \mid \alpha \leq a\}|$$

This implies that lower spectral numbers are more rigid, and provides powerful necessary conditions for adjacency (whether one singularity can deform into another). If $X \to Y$ is a valid deformation, then the spectrum of Y must be bounded below by the spectrum of X.

Exercise 15.6. *Use the Thom-Sebastiani formula to compute the spectrum of the* E_6 *singularity* $f(x,y,z) = x^3 + y^4 + z^2$ *knowing the spectra of* A_2 *and* A_3*. Check that the sum of the spectral numbers conforms to the symmetry centered at* $3/2$*.*

Exercise 15.7. *Verify Varchenko's semicontinuity theorem for the deformation of $D_4 \to A_3+A_1$. (Compare their lowest spectral numbers α_1). Why does a drop in α_1 relate geometrically to a drop in the modality or arnold complexity of the singularity?*

16 Period Mappings and the Torelli Problem

Having constructed the mixed Hodge structure on the Milnor fiber, we now ask: *to what extent does the MHS determine the singularity?* This is the local analogue of the classical Torelli problem for smooth projective varieties. The tool for addressing this is the **period mapping**, which associates to each deformation parameter the MHS of the corresponding Milnor fiber.

16.1 The Period Domain and Period Map

Let $f : (\mathbb{C}^{n+1}, 0) \to (\mathbb{C}, 0)$ be an isolated hypersurface singularity with Milnor number μ, and let $F : (\mathbb{C}^{n+1} \times \mathbb{C}^{\mu}, 0) \to (\mathbb{C}, 0)$ be its miniversal unfolding parametrized by a base S. For each $s \in S$ outside the discriminant D_f, the Milnor fiber F_s has a well-defined MHS on $H^n(F_s; \mathbb{C})$.

Definition 16.1 (Period Domain)**.** *The **period domain** $\mathcal{D}$ is the classifying space for Hodge filtrations $F^\bullet$ on a fixed complex vector space $H \cong \mathbb{C}^\mu$ that are compatible with a given intersection form $\langle \cdot, \cdot \rangle$ and satisfy the Hodge-Riemann bilinear relations. In the context of isolated singularities with n even, the relevant period domain is:*

$$\mathcal{D} = \{F^\bullet \in \mathrm{Flag}(f^0, f^1, \ldots, f^n; H) : \textit{bilinear relations hold}\}$$

where $f^p = \dim F^p H$ are the Hodge numbers. For n odd, one uses the skew-symmetric version.

The **period map** is then defined as follows. Fix a base point $s_0 \in S \setminus D_f$ and a marking (trivialization) of the local system $H^n(F_s; \mathbb{Z})$ over a simply connected open set:

$$\Phi : S \setminus D_f \to \Gamma \backslash \mathcal{D}, \quad s \mapsto [F^\bullet(s)]$$

where $\Gamma \subset \mathrm{GL}(H_\mathbb{Z})$ is the monodromy group acting on the period domain.

Theorem 16.1 (Griffiths Transversality)**.** *The period map satisfies the **infinitesimal period relation**: if v is a tangent vector to S at s, then*

$$\nabla_v F^p \subset F^{p-1}$$

for all p. That is, the Gauss-Manin connection can decrease the Hodge filtration level by at most one step in any direction.

This means Φ is not an arbitrary map into $\mathcal{D}$, but is constrained to be an **integral map** of the contact distribution on $\mathcal{D}$ defined by $F^p \mapsto F^{p-1}$. This restriction is what makes the Torelli problem tractable.

16.2 The Infinitesimal Torelli Theorem

The most powerful result available for singularities is the *infinitesimal* version of Torelli: the injectivity of the differential of the period map.

Theorem 16.2 (Infinitesimal Torelli for Singularities (Hertling)). *Let f be an isolated hypersurface singularity. The differential of the period map*

$$d\Phi_{s_0} : T_{s_0}S \to T_{\Phi(s_0)}(\Gamma\backslash\mathcal{D})$$

can be identified with the multiplication map in the Milnor algebra:

$$T_{s_0}S \cong M_f \xrightarrow{\cdot} \mathrm{Hom}(\mathrm{Gr}_F^p H, \mathrm{Gr}_F^{p-1} H)$$

This is injective for many singularity types, including all simple and unimodal singularities. When it is injective, we say the infinitesimal Torelli theorem holds.

The map $d\Phi$ is closely related to the **Kodaira-Spencer map** studied earlier in the deformation theory chapter. The image of a deformation direction $\delta \in M_f$ under $d\Phi$ essentially records how the periods of holomorphic forms change, which is computed by the cup product with the Kodaira-Spencer class.

16.3 μ-constant Deformations and Period Mapping

A particularly important class of deformations is the **μ-constant stratum** $S_\mu \subset S$: the locus in the base of the miniversal unfolding where the Milnor number remains constant at each singular point. Along S_μ, the topology of the singularity (Milnor fiber, monodromy) does not change, but the complex structure and hence the Hodge filtration can vary.

Theorem 16.3 (Varchenko). *For a μ-constant deformation $\{f_s\}_{s\in S_\mu}$:*

1. *The monodromy group is constant along S_μ.*
2. *The spectrum $\mathrm{Sp}(f_s)$ is constant along S_μ.*
3. *The period map $\Phi|_{S_\mu} : S_\mu \to \Gamma\backslash\mathcal{D}$ is a well-defined holomorphic map.*

The restriction of the period map to the μ-constant stratum carries the essential geometric information: two singularities that are topologically equivalent but analytically distinct are distinguished precisely by their position in the period domain.

Example 16.1 (Period Map for Simple Elliptic Singularities). *The simplest non-trivial example arises for the simple elliptic singularities $\tilde{E}_6$, $\tilde{E}_7$, $\tilde{E}_8$. Consider $\tilde{E}_6 : f = x^3 + y^3 + z^3 + axyz$ with modulus $a \in \mathbb{C}$, $a^3 \neq -27$.*

The Milnor number is $\mu = 8$ for all values of a, so this is a μ-constant family parametrized by a. The period map associates to each a the Hodge structure on $H^2(F_a;\mathbb{C})$. Since the Milnor fiber is homotopy equivalent to a smooth elliptic curve minus a point, the essential Hodge-theoretic information is captured by the j-invariant of the elliptic curve:

$$j(a) = 27\frac{(a^3+216)^3}{(a^3+27)^3}.$$

*Two values a_1, a_2 give analytically equivalent singularities if and only if $j(a_1) = j(a_2)$. Thus the period map faithfully distinguishes all members of this 1-parameter family, demonstrating the **global Torelli theorem** for this case.*

Example 16.2 (Modality and Period Dimension). *Arnold's classification of singularities by modality m (the number of continuous parameters in the normal form) directly corresponds to the dimension of the image of the period map restricted to the μ-constant stratum:*

Type	***Modality***	***Period behavior***
A_k, D_k, E_6, E_7, E_8	*0 (simple)*	*Period map is constant*
$\tilde{E}_6, \tilde{E}_7, \tilde{E}_8, T_{p,q,r}, \dots$	*1 (unimodal)*	*Period map has 1-dim image*
Bimodal singularities	*2 (bimodal)*	*Period map has 2-dim image*

Exercise 16.1. *For the cusp singularity $T_{3,3,3} : f = x^3 + y^3 + z^3 + axyz$, compute the spectral numbers and verify that they are independent of a (confirming μ-constancy of the spectrum).*

Exercise 16.2. *Explain why simple singularities have trivial period maps (i.e., the Hodge filtration is uniquely determined by the topology). Hint: show that for ADE singularities, the MHS on $H^n(F)$ is pure of weight n.*

17 Intersection Forms and Dynkin Diagrams

In §§9–10, we analyzed the entire local moduli space via universal deformations and Kodaira-Spencer maps. But classifying which singular topologies actually appear requires returning to the homology of the Milnor fiber and its rich algebraic structure. By amalgamating the geometric deformations into purely combinatorial data, we arrive at the intersection forms and Dynkin diagrams that exquisitely categorize simple singularities.

17.1 The Intersection Dualities of the Milnor Fiber

Recall that the Milnor fiber F of an isolated hypersurface singularity $(X, 0) \subset (\mathbb{C}^{n+1}, 0)$ defined by $f = 0$ is a $2n$-dimensional real manifold with a smooth boundary $\partial F = K$, the link of the singularity.

Definition 17.1 (Intersection Form)**.** *The **intersection form** on the Milnor fiber is a bilinear pairing defined on the middle homology:*

$$\langle \cdot, \cdot \rangle : H_n(F; \mathbb{Z}) \times H_n(F; \mathbb{Z}) \to \mathbb{Z}$$

Geometrically, for two transverse embedded n-dimensional cycles representing classes $\alpha, \beta \in H_n(F; \mathbb{Z})$, the number $\langle \alpha, \beta \rangle$ is the algebraic sum of intersection points, taking into account their local orientations in the $2n$-dimensional manifold F.

Because F is an oriented manifold of dimension $2n$, the intersection form intimately depends on the parity of n.

Theorem 17.1 (Symmetry)**.** *For any $\alpha, \beta \in H_n(F; \mathbb{Z})$, the intersection form obeys the rule:*

$$\langle \alpha, \beta \rangle = (-1)^n \langle \beta, \alpha \rangle$$

*In particular, the form is **symmetric** when n is even (e.g., surface singularities, $n = 2$), and **skew-symmetric** when n is odd (e.g., plane curve singularities, $n = 1$).*

Proof. This is a standard theorem in differential topology via Poincaré-Lefschetz duality. Let ω_α and ω_β be compactly supported n-forms representing the Poincaré duals of α and β. The intersection product $\langle \alpha, \beta \rangle$ evaluates to the integral $\int_F \omega_\alpha \wedge \omega_\beta$. Because n-forms commute up to a sign governed by $(-1)^{n \times n} = (-1)^n$, the symmetry result directly follows. □

For individual vanishing cycles, the self-intersection is an especially rigid constraint. A vanishing cycle $e \in H_n(F;\mathbb{Z})$ is topologically an n-sphere, and its normal bundle in F is isomorphic to the tangent bundle of S^n. Therefore, its self-intersection equals the Euler characteristic of S^n:

$$\langle e, e \rangle = \chi(S^n) = 1 + (-1)^n.$$

Thus, for even n, $\langle e, e \rangle = 2$, and for odd n, $\langle e, e \rangle = 0$.

17.2 Picard-Lefschetz Formula and Distinguished Bases

We recall from §8 and §13 that under a generic perturbation, a singularity of Milnor number μ splits into exactly μ simple Morse singularities, and to each we associate a vanishing cycle δ_i.

Definition 17.2 (Distinguished Basis)**.** *A **distinguished basis** of $H_n(F;\mathbb{Z})$ is an ordered set of generating vanishing cycles $(\delta_1, \dots, \delta_\mu)$ obtained by choosing a generic non-degenerate deformation f_s and selecting a set of non-self-intersecting paths in the base space linking a regular value exactly to each of the μ critical values in a cyclic order around the boundary of the discriminant.*

Using the homological basis naturally formed by these spheres, we can express the monodromy operator natively via the intersection pairings. The classical Picard-Lefschetz formula dictating how a cycle $\alpha \in H_n(F;\mathbb{Z})$ is transformed by a simple positive loop around the i-th critical point is elegantly expressed as follows:

Theorem 17.2 (Picard-Lefschetz Formula)**.** *Let $h_i : H_n(F;\mathbb{Z}) \to H_n(F;\mathbb{Z})$ be the local algebraic monodromy about the critical value corresponding to the vanishing cycle δ_i. Then for any class $\alpha \in H_n(F;\mathbb{Z})$,*

$$h_i(\alpha) = \alpha + (-1)^{\frac{n(n+1)}{2}} \langle \alpha, \delta_i \rangle \delta_i.$$

The full algebraic monodromy h_* of the singularity around the original central fiber is formed by the product (composition) of these local twists: $h_* = h_\mu \circ h_{\mu-1} \cdots \circ h_1$.

17.3 Dynkin Diagrams of Singularities

Just as Lie groups can be compactly mapped using graph theory, the complexity of isolated singular points can be summarized by plotting how its distinguished vanishing cycles intersect.

Definition 17.3 (Dynkin Diagram of a Singularity)**.** *Let $(\delta_1, \dots, \delta_\mu)$ be a freshly chosen distinguished basis of $H_n(F;\mathbb{Z})$ for an even n (so the intersection is symmetric). The **Dynkin diagram** of the singularity is an undirected graph defined as follows:*

1. *Vertices: Equip the graph with μ vertices, where each vertex v_i corresponds to the vanishing cycle δ_i.*
2. *Edges: The number of edges between vertices v_i and v_j $(i \neq j)$ is given by the absolute value $|\langle \delta_i, \delta_j \rangle|$. If $\langle \delta_i, \delta_j \rangle$ is negative, the edge is usually drawn dashed, and if it is positive, it is drawn solid.*

Let us graph the diagram for the classic A_k singularity $x^2+y^2+z^{k+1} = 0$ $(n = 2)$. The Milnor number is $\mu = k$. We can find a distinguished basis $\delta_1, \dots, \delta_k$ where sequential cycles overlap exactly in one point, giving $\langle \delta_i, \delta_{i+1} \rangle = 1$, and all non-sequential cycles are disjoint (intersection 0).

Dynkin Diagram for A_k **Dynkin Diagram for D_k**

Figure 31: The intersection graphs of the fundamental vanishing cycles precisely recreate the simply-laced Dynkin diagrams (of ADE type) associated with Lie Algebras!

17.4 Gabrielov's Theorem and the ADE Classification

We might ask: are there singularities beyond the ADE types? The key restriction separating simple ADE singularities from the rest of the monstrous space of isolated singularities is the signature of their intersection matrices. Let $I = (\langle \delta_i, \delta_j \rangle)$ be the $\mu \times \mu$ intersection matrix. For isolated surface singularities ($n = 2$), I is always a symmetric integer matrix with 2 along the diagonal.

Theorem 17.3 (Gabrielov's Theorem)**.** *An isolated hypersurface singularity $f = 0$ is a simple singularity (i.e., of type A_k, D_k, E_6, E_7, or E_8) if and only if the intersection form $\langle \cdot, \cdot \rangle$ on its middle homology is strictly* ***positive definite****.*

Proof Sketch. (1) ($\Longleftarrow$) If the intersection form is positive definite, then the symmetric matrix I must correspond to the Cartan matrix of a finite reflection group. A long-standing combinatorial classification in Lie theory proves that connected graphs corresponding to positive definite symmetric integer matrices with diagonal elements 2 can only be the A_k, D_k, and E_6, E_7, E_8 diagrams!

(2) ($\Longrightarrow$) For simple singularities, we can explicitly compute the intersection matrices using a specifically chosen Morsification (such as Brieskorn's resolution) or quiver representations, verifying their positive-definiteness natively. For essentially all neighboring higher-order singularities (such as the unimodal or parabolic singularities like $\widetilde{E}_8, X_9, J_{10}$), the intersection matrix develops a null space, crossing over into being positive semi-definite (where the form is degenerate) exactly at the boundary of simplicity. □

This monumental theorem closes the logical loop: it demonstrates why the classification of generic, non-moduli singularities mysteriously mirrors the classification schemas of completely different mathematical domains—Lie algebras, Coxeter groups, and Quivers. They are all rigorously bound by the arithmetic strictures imposed by positive definite integral quadratic forms!

17.5 Monodromy Groups and Braid Group Actions

The set of reflections generated by the distinguished vanishing cycles δ_i generates a subgroup of the automorphisms of the homology lattice $H_n(F; \mathbb{Z})$. This group is exactly the **Monodromy Group** of the singularity. Because each Picard-Lefschetz transformation acts as a reflection relative to the symmetric intersection form, this monodromy group is inherently a reflection group.

A profound corollary to Gabrielov's theorem dictates the finiteness of this group:

Theorem 17.4 (Finiteness of the Monodromy Group)**.** *The monodromy group of an isolated hypersurface singularity is a finite group if and only if the singularity is simple (ADE). In this case,*

the monodromy group is isomorphic to the finite Weyl group associated with the corresponding ADE Dynkin diagram.

For any singularity more complex than the ADE series (e.g., the unimodal or parabolic singularities), the intersection form is no longer strictly positive definite, and its associated reflection group contains translations, forcing the monodromy group to be strictly infinite.

Furthermore, the set of all possible distinguished bases for a given singularity is not arbitrary; it is governed by the **Artin Braid Group** . If one continuously varies the paths linking the regular value to the critical values within the punctured disk, the distinguished basis undergoes a mutation. The transformation between two distinguished bases corresponds natively to the Hurwitz action of the Braid group B_μ on μ strands, which modifies the ordering and signs of the vanishing cycles but crucially preserves the abstract isomorphism class of the Dynkin diagram.

17.6 Exercises

Exercise 17.1. *Draw the E_6 Dynkin diagram based on the intersection form. Determine how many vertices it has (μ) and outline how one could manually check that its corresponding matrix is positive-definite (for example, using Sylvester's criterion on its principal minors).*

Exercise 17.2. *For a plane curve singularity ($n = 1$), the intersection form is skew-symmetric. If we let μ be the Milnor number, argue why the rank of the intersection form matrix I determines whether the Milnor fiber has boundary components that vanish in homology.*

18 Moduli Spaces and Unimodal Singularities

In the previous chapter, Gabrielov's theorem demonstrated that ADE singularities are characterized by their rigid discrete nature—they are *simple*. A simple singularity has no continuous invariants. No matter how you slightly perturb the function in ways that preserve the Milnor number, you can always transform the new function back into the old one via a biholomorphic change of coordinates.

However, as we move to higher dimensions in the parameter space, this simplicity breaks down. Singularities begin to appear in continuous families, requiring *moduli* to classify them up to Right-equivalence. In this chapter, we step systematically beyond the ADE classification to introduce Arnold's concept of modality and study the most fundamental continuous family: the unimodal (parabolic) singularities.

18.1 The Concept of Modality

When examining the versal deformation $F(x, s)$ of a singularity f, the parameter space $S = \mathbb{C}^\tau$ is partitioned into strata consisting of singularities of the same topological type. For simple singularities, the stratum preserving the exact Milnor number μ is zero-dimensional (just the origin). Thus, they have no moduli.

Definition 18.1 (Modality)**.** *The **modality** m of an isolated singularity f (also known as the inner modality) is the geometric dimension of the stratum of constant Milnor number μ in the base space S of its miniversal unfolding, evaluated near the origin.*

Informally, the modality is the number of *continuousparameters* upon which the Right-equivalence class of the singularity depends.

- $m = 0$: Simple singularities (ADE).

- $m = 1$: Unimodal singularities.
- $m = 2$: Bimodal singularities.

Vladimir Arnold initiated a vast program to classify singularities hierarchically based on their modality.

18.2 The Parabolic (Simply Elliptic) Singularities

The very first singularities encountered that possess moduli (i.e., $m = 1$) lie on the boundary of the simple singularities. Their intersection matrices fail to be positive-definite, becoming exactly positive semi-definite (corank 1).

Definition 18.2 (Parabolic Singularities)**.** *The three **parabolic** (or simply elliptic) singularities are defined by the following germs, characterized by a single continuous complex parameter λ:*

$$\begin{aligned} \widetilde{E}_6 \ (P_8) \quad &: \quad x^3 + y^3 + z^3 + \lambda xyz = 0, \quad \lambda^3 + 27 \neq 0 \\ \widetilde{E}_7 \ (X_9) \quad &: \quad x^4 + y^4 + \lambda x^2 y^2 = 0, \quad \lambda^2 \neq 4 \\ \widetilde{E}_8 \ (J_{10}) \quad &: \quad x^6 + y^3 + z^2 + \lambda xyz = 0, \quad 4\lambda^3 + 27 \neq 0 \end{aligned}$$

The subscript of the alternative Arnold notations (P_8, X_9, J_{10}) indicates their Milnor number μ.

Theorem 18.1 (Arnold)**.** *If an isolated singularity is not simple, it must degenerate to one of the three parabolic singularities $\widetilde{E}_6, \widetilde{E}_7$, or $\widetilde{E}_8$. They form the border of the simple singularities in the deformation space.*

Let us carefully analyze why λ is a true modulus. For $\widetilde{E}_6$, substituting different valid values of λ yields functions that all have Milnor number $\mu = 8$. However, for a generic pair $\lambda_1 \neq \lambda_2$, there is no local analytic change of coordinates that maps $x^3 + y^3 + z^3 + \lambda_1 xyz$ exactly to $x^3 + y^3 + z^3 + \lambda_2 xyz$. The topological type (Milnor fiber, knot type) remains identical, but the analytic geometry differs!

18.3 Elliptic Curves and the j-Invariant

Why are they called *simplyelliptic*?

If we consider the defining equations as homogeneous (or quasi-homogeneous) polynomials and project them into the complex projective plane $\mathbb{P}^2$, the zero locus of each germ defines an **elliptic curve** (a smooth curve of genus 1).

For instance, the projective curve defined by $x^3 + y^3 + z^3 + \lambda xyz = 0$ in $\mathbb{P}^2$ is a well-known family of elliptic curves. In algebraic geometry, elliptic curves are classified up to isomorphism by a single complex number, the absolute j-invariant.

Theorem 18.2. *Two parabolic singularities of the same type with parameters λ_1 and λ_2 are Right-equivalent (analytically isomorphic) if and only if their associated elliptic curves in projective space have the same j-invariant.*

The j-invariant for the $\widetilde{E}_6$ family is given by a specific polynomial ratio in λ:

$$j(\lambda) = \frac{\lambda^3(\lambda^3 - 216)^3}{(\lambda^3 + 27)^3}.$$

Notice that the denominator $\lambda^3 + 27 = 0$ corresponds exactly to the parameter values where the elliptic curve degenerates and the isolated singularity becomes non-isolated!

This establishes a profound connection between the local moduli space of an isolated singularity and the global moduli space of algebraic curves.

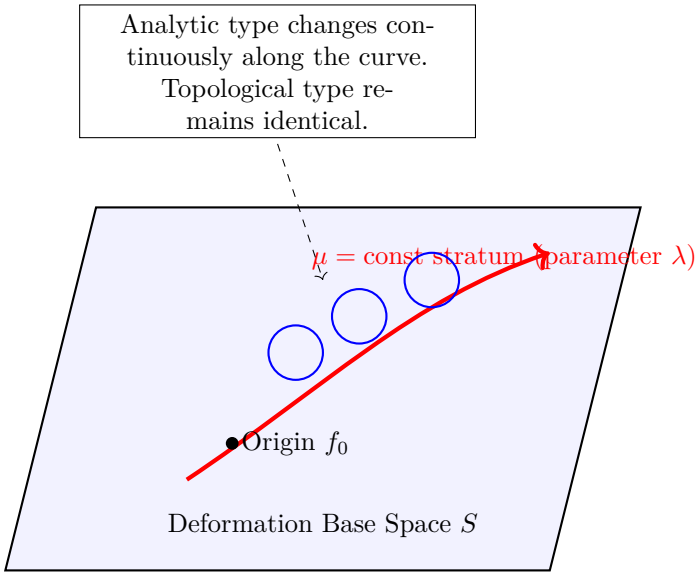

Figure 32: For a unimodal singularity, the miniversal deformation space contains a 1-dimensional μ-constant stratum. Moving along this curve intrinsically alters the complex-analytic structure of the singularity (indexed by the elliptic curve modulus) without fundamentally altering its topology.

18.4 Arnold's Strange Duality

A more spectacular arithmetic symmetry emerges when considering the remaining 14 unimodal singularities mapped out by Arnold in 1974. Following the three parabolic singularities are the hyperbolic and exceptional unimodal singularities.

Arnold noticed that if one computes the Gabrielov intersection diagram for these 14 exceptional singularities, they pair up in an astounding involution, which he termed the **Strange Duality** . An exceptional singularity determined by a quasi-homogeneous polynomial can be characterized by Dolgachev numbers (related to its resolution diagram) and Gabrielov numbers (related to its Dynkin diagram). The duality maps the Dolgachev numbers of one singularity perfectly onto the Gabrielov numbers of its dual partner! This strange local duality was later entirely subsumed and beautifully explained by Mirror Symmetry and K3 surfaces in string theory, revealing that local singularities harbor deep global homological secrets.

18.5 The Hierarchy of Modalities and Adjacency

Arnold's program successfully achieved a complete classification up to modality 2. Following the 3 parabolic (simply elliptic) singularities and the 14 exceptional unimodals, the bimodal singularities ($m = 2$) present an even richer tapestry. Arnold catalogued exactly 14 families of bimodal singularities (including the doubly exceptional and the triangle singularities), which depend on two distinct continuous complex parameters.

A crucial structural feature organizing this vast zoo of polynomials is **adjacency** . We say a singularity X is adjacent to a singularity Y (written $X \to Y$) if Y can be obtained by a small

deformation of X. Geometrically, this means the stratum of singularities of type Y lies strictly in the boundary of the stratum of type X within the universal deformation space.

The concept of modality strictly monotonically decreases (or remains constant) under adjacency. Therefore, every bimodal singularity is adjacent to some unimodal singularity, and every unimodal singularity is inevitably adjacent to one of the simple ADE singularities. This creates a massive directed graph of topological degenerations. For instance, the parabolic $\widetilde{E}_8$ (J_{10}) boundary degenerates natively into the simple E_8 singularity. The classification of singularities thus geometrically rebuilds the stratification of the infinite-dimensional space of all holomorphic functions into a hierarchy of explicitly determined, finite-dimensional orbits.

18.6 Exercises

Exercise 18.1. *Compute the Milnor number μ for the parabolic singularity $\widetilde{E}_6$: $f(x,y,z) = x^3+y^3+z^3+\lambda xyz$. Show that it is equal to 8 independent of the choice of a generic λ.*

Exercise 18.2. *Write down the Jacobian ideal for $f(x,y) = x^4+y^4+\lambda x^2y^2$ (the $\widetilde{E}_7$ singularity, essentially dropping z). Determine the parameter choices of λ for which the origin ceases to be an isolated singularity (i.e., where the surface $f=0$ develops a singular line).*

19 Resolution of Singularities and Dual Graphs

Throughout this course, we have primarily studied isolated hypersurface singularities analytically and topologically via their deformations, Milnor fibrations, and Hodge theoretical invariants. In this final chapter, we introduce the geometric approach: resolving a singular point by blowing it up to a smooth space. This replaces the isolated *badpoint* with a collection of smooth curves or divisors, capturing the singularity's structure within a combinatorial intersection graph known as the dual resolution graph.

19.1 The Blow-up Process

The fundamental operation in resolving singularities is the **blow-up**. Suppose we have an isolated singularity at the origin of $\mathbb{C}^n$. To *unpinch* it, we pull apart the different tangent directions at the origin.

Definition 19.1 (Blow-up of the Origin)**.** *The **blow-up** of $\mathbb{C}^n$ at the origin is a space $\widetilde{\mathbb{C}^n} \subset \mathbb{C}^n \times \mathbb{P}^{n-1}$ defined by:*

$$\widetilde{\mathbb{C}^n} = \{(z,[l]) \in \mathbb{C}^n \times \mathbb{P}^{n-1} \mid z \in l\}$$

where l is a line through the origin in $\mathbb{C}^n$. The natural projection map $\pi : \widetilde{\mathbb{C}^n} \to \mathbb{C}^n$ given by $\pi(z,[l]) = z$ is an isomorphism away from the origin.

The preimage of the origin, $E = \pi^{-1}(0)$, is exactly the projective space $\mathbb{P}^{n-1}$. This is called the **exceptional divisor** . We have effectively replaced the single singular point 0 with the entire space of tangent directions at 0.

If $X \subset \mathbb{C}^n$ is a singular variety passing through the origin, we define its **strict transform** $\widetilde{X}$ as the closure of $\pi^{-1}(X \setminus \{0\})$ in $\widetilde{\mathbb{C}^n}$.

Theorem 19.1 (Hironaka's Resolution Theorem)**.** *For any complex algebraic variety X, there exists a smooth variety $\widetilde{X}$ and a proper birational morphism $\pi : \widetilde{X} \to X$ such that π is an isomorphism over the smooth locus of X, and the exceptional locus $\pi^{-1}(\mathrm{Sing}(X))$ is a union of smooth divisors crossing with normal crossings.*

For curve singularities in $\mathbb{C}^2$, resolving the singularity generally requires a sequence of blow-ups. For surface singularities in $\mathbb{C}^3$, resolving them produces an exceptional divisor composed of a configuration of smooth algebraic curves intersecting one another.

19.2 Resolution of Plane Curve Singularities

For plane curve germs it is natural to use an *embedded resolution*: after finitely many point blow-ups, the total transform becomes a divisor with simple normal crossings.

Definition 19.2 (Embedded Resolution Graph of a Plane Curve)**.** *For a plane curve singularity $C \subset (\mathbb{C}^2, 0)$, the embedded resolution graph is the weighted dual graph of the exceptional divisor together with arrowheads marking the final strict transform. Each exceptional component E_i contributes a vertex weighted by its self-intersection E_i^2, and each branch of the final strict transform contributes an arrow attached to the exceptional component it meets.*

Example 19.1 (Node: $xy = 0$)**.** *The node is already a normal crossings divisor, so the minimal embedded resolution is the identity and the minimal graph has no exceptional vertices. If one nevertheless blows up the origin once, one gets a single exceptional curve $E \cong \mathbb{P}^1$ with $E^2 = -1$, and the two strict transforms meet E transversely at two distinct points. Thus the nonminimal picture consists of one (-1)-vertex with two arrowheads.*

Example 19.2 (Cusp: $y^2 = x^3$)**.** *Start with $C = \{y^2 - x^3 = 0\}$. After the first blow-up in the chart $x = u$, $y = uv$, we obtain*

$$y^2 - x^3 = u^2(v^2 - u),$$

so the strict transform $u = v^2$ is smooth but tangent to the first exceptional curve E_1. A second blow-up resolves the singularity of the strict transform, but the total transform still has a triple point. One further blow-up separates the three tangent directions. The resulting minimal embedded resolution graph is therefore the chain

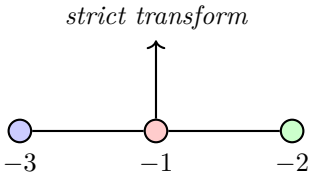

The arrow marks the final strict transform. This is the first nontrivial embedded resolution graph for an irreducible plane branch; see [Wal04, Ch. 3].

Notation 19.1 (Weighted Bamboo Notation)**.** *If an embedded resolution graph is a chain whose exceptional components have self-intersection numbers $-b_1, \dots, -b_r$, we abbreviate the weighted chain by*

$$[b_1, \dots, b_r].$$

The arrowhead specifying the final strict transform is drawn at the vertex it meets. For example, the cusp graph above is the bamboo $[3, 1, 2]$ with the arrow attached to the middle vertex.

Proposition 19.1 (Torus Branches, Euclidean Algorithm, and Continued Fractions)**.** *Let $C_{p,q} = \{x^p - y^q = 0\}$ with $\gcd(p, q) = 1$, and assume $q > p$ (otherwise interchange x and y). If we blow up in the chart $x = uv$, $y = v$, then*

$$x^p - y^q = v^p(u^p - v^{q-p}),$$

so the strict transform has the same form with exponent pair $(p, q-p)$. If $p > q$ and we instead use $x = u$, $y = uv$, then

$$x^p - y^q = u^q(u^{p-q} - v^q),$$

so the exponent pair becomes $(p-q, q)$. Hence the sequence of infinitely near points is controlled by the Euclidean algorithm

$$q = a_1 p + r_1, \qquad p = a_2 r_1 + r_2, \qquad \dots, \qquad r_{s-2} = a_s r_{s-1} + 1,$$

equivalently by the ordinary continued fraction

$$\frac{q}{p} = [a_1, \dots, a_s] = a_1 + \cfrac{1}{a_2 + \cfrac{1}{\ddots + \cfrac{1}{a_s}}}, \qquad a_i \in \mathbb{N},\ a_s \geq 2.$$

The coefficient a_1 records that one performs a_1 consecutive blow-ups before switching charts, then a_2 consecutive blow-ups in the opposite chart, and so on. In particular, the continued fraction $[a_1, \dots, a_s]$ records the block structure of the weighted bamboo. The actual weights are recovered recursively from the blow-up process by the rule that each blow-up decreases by 1 the self-intersection number of every component through the center and creates a new (-1)-curve; see [Wal04, Ch. 3].

Remark 19.1 (Plane Branches versus Hirzebruch–Jung Fractions)**.** *The continued fraction above is the ordinary Euclidean continued fraction attached to the plane branch $x^p - y^q = 0$. It should not be confused with the Hirzebruch–Jung continued fractions used for cyclic quotient* surface *singularities later in this chapter.*

Example 19.3 (A Concrete Torus Branch)**.** *For $x^3 - y^5 = 0$, the Euclidean algorithm gives*

$$(3,5) \rightsquigarrow (3,2) \rightsquigarrow (1,2) \rightsquigarrow (1,1), \qquad \frac{5}{3} = [1,1,2].$$

Thus after the first blow-up the strict transform is already of cusp type $(3,2)$, and the rest of the embedded resolution proceeds exactly as in the cusp calculation above after interchanging coordinates. Carrying out the four successive point blow-ups and keeping track of self-intersection numbers yields the weighted embedded resolution graph

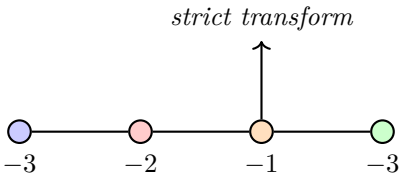

The first (-3)-curve comes from the first exceptional divisor after two further blow-ups above its intersection points; the rightmost (-3)-curve is the transform of the second exceptional divisor; and the central (-1)-curve is created in the last blow-up that separates the remaining triple point. In the bamboo notation just introduced, this graph is the chain $[3,2,1,3]$ with the arrow attached to the third vertex. In particular, this gives a concrete weighted resolution graph for a non-cuspidal torus branch.

19.3 Exceptional Divisors and Dual Graphs

For an isolated surface singularity $X \subset \mathbb{C}^3$ ($n = 2$), the minimal resolution $\pi : \widetilde{X} \to X$ replaces the origin with an exceptional divisor $E = \pi^{-1}(0)$. By Hironaka's theorem, E decomposes into a finite number of irreducible smooth curves $E_1 \cup E_2 \cup \cdots \cup E_r$, intersecting transversally.

Definition 19.3 (Dual Resolution Graph)**.** *The **dual graph** of the resolution is an undirected graph constructed as follows:*

1. *Assign a vertex v_i to each irreducible curve component E_i. Vertices are often decorated with the genus and self-intersection number $E_i^2 = E_i \cdot E_i$ of the curve.*
2. *Draw an edge connecting v_i and v_j for every intersection point between E_i and E_j.*

A miraculous theorem bridges this resolution back to our Dynkin diagram classification from §17.

Theorem 19.2 (Du Val)**.** *An isolated surface singularity is an ADE singularity (a simple singularity) if and only if the curves E_i in its minimal resolution are all smooth rational curves ($\mathbb{P}^1$, genus 0) with self-intersection -2, and their dual resolution graph is precisely the corresponding ADE Dynkin diagram!*

Remark 19.2 (ADE Resolution Graphs)**.** *For every ADE surface singularity, every vertex in the minimal resolution graph carries the weight -2. Thus:*

- *A_k is a chain of k vertices;*
- *D_k is a fork with one trivalent vertex;*
- *E_6, E_7, and E_8 are the corresponding exceptional trees with 6, 7, and 8 vertices.*

Equivalently, the ADE resolution graph is obtained by taking the ADE Dynkin diagram and decorating each vertex by -2; see [Dim92, Ch. 4].

Let us visualize the dual geometry of an A_3 surface singularity's resolution. The exceptional divisor consists of three spheres (E_1, E_2, E_3), each with self-intersection -2, intersecting in a chain.

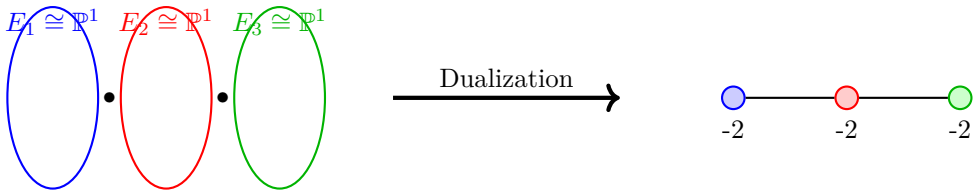

Geometric curves intersecting transversally — Dual Graph (Dynkin A_3)

Figure 33: The resolution of an A_3 surface singularity replaces the singular point with a chain of three $\mathbb{P}^1$ components. The dual resolution graph perfectly reconstructs the A_3 Dynkin diagram, visually cementing the equivalence between algebraic geometry, deformation intersection theory, and Lie algebra combinatorics.

Example 19.4 (Resolution of D_4: $f(x,y,z) = x^2 + y^2z + z^3$)**.** *The minimal resolution of the D_4 surface singularity produces an exceptional divisor $E = E_1 \cup E_2 \cup E_3 \cup E_4$, where E_1 is a central $\mathbb{P}^1$ (with multiplicity 2 in the exceptional set) intersecting three other $\mathbb{P}^1$'s E_2, E_3, E_4, each meeting E_1 at a single point. All components have self-intersection -2. The dual graph is the D_4 Dynkin diagram:*

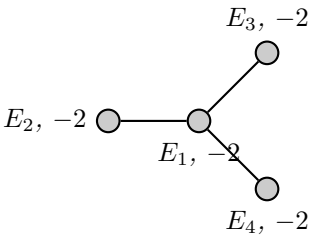

This is the unique Dynkin diagram with a triple branch point, reflecting the trimodal symmetry of D_4 (the S_3 symmetry permuting the three branches).

Example 19.5 (Resolution of a Non-Simple Singularity: the Cusp $T_{2,3,7}$)**.** *Consider the singularity $f = x^2 + y^3 + z^7$ with Milnor number $\mu = 12$. This is a* unimodal *singularity (one continuous modulus). Its minimal resolution has exceptional divisor with self-intersection numbers $-2, -3, -7$ along a chain, producing the* Gabrielov graph*:*

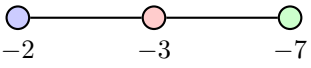

Note that the self-intersection numbers are no longer all -2: this deviation from the ADE pattern characterizes non-simple singularities. The intersection matrix determined by these self-intersection numbers is negative semi-definite *(but not negative definite), consistent with Gabrielov's theorem.*

19.4 The Plumbing Construction

The dual resolution graph encodes not only the combinatorial intersection pattern, but also the full topology of the resolution. The key construction is **plumbing**: given the weighted graph, one can reconstruct the boundary of a regular neighborhood of the exceptional divisor, which is precisely the **link** K of the singularity.

Definition 19.4 (Plumbing)**.** *Let Γ be a resolution graph with vertices $v_1, \ldots, v_r$, edge set E, genus decorations $g_i = g(E_i)$, and self-intersection decorations $e_i = E_i^2$. The* ***plumbed 4-manifold*** *$P(\Gamma)$ is constructed as follows:*

1. *To each vertex v_i, associate the disk bundle D_i over a Riemann surface Σ_{g_i} of genus g_i, with Euler number e_i.*
2. *For each edge $(v_i, v_j) \in E$, choose a small disk $\Delta_i \subset \Sigma_{g_i}$ and $\Delta_j \subset \Sigma_{g_j}$, and glue $D_i|_{\Delta_i}$ to $D_j|_{\Delta_j}$ by identifying the fiber direction of one with the base direction of the other (and vice versa).*

The boundary $\partial P(\Gamma)$ is a closed oriented 3-manifold, naturally identified with the link K of the singularity.

Theorem 19.3 (Mumford, Grauert)**.** *For a normal surface singularity, the intersection matrix $(E_i \cdot E_j)$ of the exceptional divisor is* ***negative definite****. Conversely, any negative definite weighted graph can be realized as the resolution graph of some normal surface singularity.*

This negative definiteness is the algebraic manifestation of the contractibility of the exceptional divisor: the exceptional curves can be blown down precisely because the intersection form is negative definite. The plumbing construction then recovers the link K from the graph, closing the circle between resolution, topology, and combinatorics.

Example 19.6 (Lens Spaces from Cyclic Singularities)**.** *The cyclic quotient singularity $\mathbb{C}^2/\mathbb{Z}_n$ (where $\mathbb{Z}_n$ acts by $(x, y) \mapsto (\zeta x, \zeta^{-1} y)$ with $\zeta = e^{2\pi i/n}$) has its minimal resolution described by a chain of $\mathbb{P}^1$'s with self-intersection numbers determined by the continued fraction expansion of $n/1 = [a_1, a_2, \ldots, a_k]$. The link is the lens space $L(n, 1)$, and the plumbing reproduces it exactly from the chain graph with decorations $-a_1, -a_2, \ldots, -a_k$.*

19.5 The Relationship Between Resolution and the Milnor Fiber

A beautiful theorem connects the resolution of singularities with the Milnor fiber topology studied throughout this course.

Theorem 19.4 (A'Campo's Formula)**.** *Let $\pi : \widetilde{X} \to X$ be an embedded resolution of the hypersurface $\{f = 0\} \subset \mathbb{C}^{n+1}$, and let $E = \sum m_i E_i$ be the exceptional divisor where m_i are the multiplicities. The Euler characteristic of the Milnor fiber is:*

$$\chi(F) = \sum_i (-1)^{n-1} m_i \chi(E_i^\circ)$$

where $E_i^\circ = E_i \setminus \bigcup_{j \neq i} E_j$ is the open stratum of E_i.

Moreover, A'Campo gave a formula for the **zeta function of the monodromy** in terms of the resolution:

$$\zeta_f(t) = \prod_i (1 - t^{m_i})^{-\chi(E_i^\circ)}.$$

This provides a purely algebro-geometric computation of the monodromy eigenvalues, complementing the Hodge-theoretic approach via the spectrum.

Exercise 19.1. *Compute the monodromy zeta function $\zeta_f(t)$ for the A_2 surface singularity $f(x, y, z) = x^2 + y^2 + z^3$ using A'Campo's formula and a single blow-up resolution. Verify that the eigenvalues match those predicted by the spectrum.*

Exercise 19.2. *Show that for a simple singularity of type $\Gamma \in \{A_k, D_k, E_6, E_7, E_8\}$, the Milnor number μ equals the number of vertices of the corresponding Dynkin diagram, by using either the intersection form or the resolution graph.*

Exercise 19.3. *Let $f(x, y) = x^p + y^q$ with $\gcd(p, q) = 1$. Use the iterated blow-up process to resolve the curve singularity $\{f = 0\} \subset \mathbb{C}^2$, and show that the number of blow-ups required equals $p + q - 1 - \gcd(p, q)$. Relate the resolution to the continued fraction expansion of p/q.*

19.6 Conclusion to the Course

As we conclude these lecture notes, we reflect on the unity of mathematics revealed by Singularities. What began in §1 as the study of algebraically *pinched* points gradually expanded to

map out local Milnor fibers via topological tools like braids and vanishing cycles. Armed with complex Hodge theory and Brieskorn lattices, we transitioned into deformation theory, witnessing how singular isolated features dictate global structural landscapes (Moduli spaces). Finally, via the resolution dual graphs and intersection forms, we uncovered deep reflections of Lie algebras safely resting at the heart of algebraic geometry. The study of singularities mathematically embodies that locally singular *imperfections* intrinsically govern, and dynamically unfold into, the universe's most beautifully symmetrical macrostructures.

References

[ACa75] Norbert A'Campo. "La fonction zêta d'une monodromie". In: *Commentarii Mathematici Helvetici* 50 (1975), pp. 233–248.

[AGV85] Vladimir I. Arnold, S. M. Gusein-Zade, and A. N. Varchenko. *Singularities of Differentiable Maps: Volume I*. Birkhäuser, 1985 (cit. on pp. 6, 7, 15).

[Bri70] Egbert Brieskorn. "Die Monodromie der isolierten Singularitäten von Hyperflächen". In: *Manuscripta Mathematica* 2.2 (1970), pp. 103–161 (cit. on pp. 5–7, 84).

[CMS16] Paul Cadman, David Mond, and Duco van Straten. "Logarithmic vector fields and the Severi strata in the discriminant". In: *arXiv preprint arXiv:1609.09305* (2016). arXiv: 1609.09305 [math.AG] (cit. on pp. 68, 70).

[Dim92] Alexandru Dimca. *Singularities and Topology of Hypersurfaces*. Springer, 1992 (cit. on pp. 6, 118).

[Ebe87] Wolfgang Ebeling. *The Monodromy Groups of Isolated Singularities of Complete Intersections*. Vol. 1293. Lecture Notes in Mathematics. Springer, 1987 (cit. on p. 6).

[GLS07] Gert-Martin Greuel, Christoph Lossen, and Eugenii Shustin. *Introduction to Singularities and Deformations*. Springer Monographs in Mathematics. Springer, 2007 (cit. on pp. 5–7, 19, 68).

[Ham71] Helmut A. Hamm. "Lokale topologische Eigenschaften komplexer Räume". In: *Mathematische Annalen* 191 (1971), pp. 235–252.

[Her02] Claus Hertling. *Frobenius Manifolds and Moduli Spaces for Singularities*. Vol. 151. Cambridge Tracts in Mathematics. Cambridge University Press, 2002 (cit. on p. 6).

[HR15] Michael B. Henry and Dan Rutherford. "Ruling polynomials and augmentations over finite fields". In: *Journal of Topology* 8.1 (2015), pp. 1–37. DOI: 10.1112/jtopol/jtu013 (cit. on p. 43).

[Kas83] Masaki Kashiwara. "Vanishing cycle sheaves and holonomic systems of differential equations". In: *Algebraic Geometry (Tokyo/Kyoto, 1982)* (1983), pp. 134–142.

[Kou76] Anatoli G. Kouchnirenko. "Polyèdres de Newton et nombres de Milnor". In: *Inventiones Mathematicae* 32.1 (1976), pp. 1–31.

[Kul98] Valentine S. Kulikov. *Mixed Hodge Structures and Singularities*. Vol. 132. Cambridge Tracts in Mathematics. Cambridge University Press, 1998 (cit. on pp. 5–7, 84).

[LG76] Dũng Tráng Lê and Gert-Martin Greuel. "Spitzen, Doppelpunkte und vertikale Tangenten in der Diskriminante verseller Deformationen von vollständigen Durchschnitten". In: *Mathematische Annalen* 222 (1976), pp. 71–88.

[Loo84] Eduard J. N. Looijenga. *Isolated Singular Points on Complete Intersections*. Vol. 77. London Mathematical Society Lecture Note Series. Cambridge University Press, 1984 (cit. on pp. 5–7, 15, 17, 22, 26, 27, 29, 34, 35, 45, 46, 51, 56, 64, 65, 73, 74, 76, 79, 81–83).

[Mal74] Bernard Malgrange. "Intégrales asymptotiques et monodromie". In: *Annales Scientifiques de l'École Normale Supérieure* 7.3 (1974), pp. 405–430.

[Mil68] John W. Milnor. *Singular Points of Complex Hypersurfaces*. Vol. 61. Annals of Mathematics Studies. Princeton University Press, 1968 (cit. on pp. 6, 7, 58).

[MS13] Luca Migliorini and Vivek Shende. "A support theorem for Hilbert schemes of planar curves". In: *Journal of the European Mathematical Society* 15.6 (2013), pp. 2353–2367. DOI: 10.4171/JEMS/423 (cit. on p. 71).

[NS06] Lenhard Ng and Joshua Sabloff. "The correspondence between augmentations and rulings for Legendrian knots". In: *Pacific Journal of Mathematics* 224.1 (2006), pp. 141–150. DOI: 10.2140/pjm.2006.224.141 (cit. on p. 43).

[ORS18] Alexei Oblomkov, Jacob Rasmussen, and Vivek Shende. "The Hilbert scheme of a plane curve singularity and the HOMFLY homology of its link". In: *Geometry & Topology* 22 (2018), pp. 645–691. DOI: 10.2140/gt.2018.22.645 (cit. on pp. 43, 71).

[OS12] Alexei Oblomkov and Vivek Shende. "The Hilbert scheme of a plane curve singularity and the HOMFLY polynomial of its link". In: *Duke Mathematical Journal* 161.7 (2012), pp. 1277–1303. DOI: 10.1215/00127094-1593281 (cit. on pp. 43, 71).

[Pio06] Jens Piontkowski. "Topology of the compactified Jacobians of singular curves". In: *Mathematische Zeitschrift* 255.1 (2006), pp. 195–226. DOI: 10.1007/s00209-006-0021-3 (cit. on p. 71).

[Rut06] Dan Rutherford. "The Thurston-Bennequin number, Kauffman polynomial, and ruling invariants of a Legendrian link: The Fuchs conjecture and beyond". In: *International Mathematics Research Notices* 2006 (2006), Art. ID 78591, 1–15. DOI: 10.1155/IMRN/2006/78591 (cit. on p. 43).

[Sai88] Morihiko Saito. "Modules de Hodge polarisables". In: *Publications of the Research Institute for Mathematical Sciences* 24.6 (1988), pp. 849–995.

[She12] Vivek Shende. "Hilbert schemes of points on a locally planar curve and the Severi strata of its versal deformation". In: *Compositio Mathematica* 148 (2012), pp. 531–547. DOI: 10.1112/S0010437X11007378 (cit. on p. 71).

[SS85] John Scherk and Joseph H. M. Steenbrink. "On the mixed Hodge structure on the cohomology of the Milnor fibre". In: *Mathematische Annalen* 271.4 (1985), pp. 641–665 (cit. on p. 104).

[Ste77] Joseph H. M. Steenbrink. "Mixed Hodge structure on the vanishing cohomology". In: *Real and Complex Singularities (Proc. Ninth Nordic Summer School/NAVF Sympos. Math., Oslo, 1976)* (1977), pp. 525–563 (cit. on pp. 5–7, 13, 104).

[STZ17] Vivek Shende, David Treumann, and Eric Zaslow. "Legendrian knots and constructible sheaves". In: *Inventiones Mathematicae* 207.3 (2017), pp. 1031–1133. DOI: 10.1007/s00222-016-0681-5 (cit. on p. 43).

[Var81] Alexander N. Varchenko. "Asymptotic Hodge structure on the cohomology of the vanishing cycles". In: *Izvestiya Akademii Nauk SSSR. Seriya Matematicheskaya* 45.3 (1981), pp. 540–591 (cit. on pp. 5, 14, 105).

[Wal04] Charles T. C. Wall. *Singular Points of Plane Curves*. Vol. 63. London Mathematical Society Student Texts. Cambridge University Press, 2004 (cit. on pp. 6, 20, 68, 116, 117).

Index